Performance of Silver-Exchanged Mordenite and Silver-functionalized Silica-Aerogel under Vessel Off-gas Conditions

Nuclear Technology Research and Development

Approved for public release. Distribution is unlimited

Prepared for
U.S. Department of Energy
Material Recovery and Waste Form Development Campaign
R. T. Jubin, J. A. Jordan, and S. H. Bruffey
Oak Ridge National Laboratory

August 21, 2017
NTRD-MRWFD-2017-000034
NTRD-MRWFD-2017-000211
ORNL/SR-2017/477

SUMMARY

US regulations 40 CFR 61, 40 CFR 190, and 10 CFR 20 govern release limits for volatile radionuclides contained in the gaseous effluents of used nuclear fuel (UNF) reprocessing facilities. Of the four volatile radionuclides that are restricted by the release limits (^{3}H, ^{14}C, ^{85}Kr, and ^{129}I) ^{129}I will require the greatest degree of abatement. Previous studies have shown that overall plant decontamination factor (DF) for ^{129}I must, at minimum, exceed 1,000 to meet regulatory requirements. Iodine-containing off-gas will be present in the dissolver off-gas, the cell off-gas, the vessel off-gas (VOG), the waste off-gas, and the shear off-gas. The VOG will most likely contain 1%–5% of the total iodine at part per billion (ppb) concentrations. A number of studies have examined iodine abatement from the dissolver off-gas, which contains greater than 95% of the iodine inventory of the plant, but very few have examined the recovery of iodine from the VOG stream.

Reduced silver-exchanged mordenite (Ag^0Z) has been considered a promising iodine sorbent for use in UNF reprocessing plants, but recent efforts have identified silver-functionalized silica-aerogel (AgAerogel) as a potential alternative. The testing reported here reflects a substantial increase in the body of work available on iodine adsorption by both silver sorbents under prototypical VOG conditions. Both I_2 and methyl iodide (CH_3I) adsorption tests have been conducted with Ag^0Z and AgAerogel at a range of concentrations up to 1,000 ppb. These experiments were performed with two specific aims: (1) to assess the effect of iodine concentration on its adsorption by the sorbent and (2) to compare the performance of Ag^0Z and AgAerogel in the removal of iodine from a prototypical VOG stream.

Results show that the concentration of CH_3I within the range studied (40–1,000 ppb CH_3I) does not affect either the maximum observed iodine loading for the sorbent or the penetration of CH_3I into the Ag^0Z sorbent bed. Similar testing performed on the adsorption of CH_3I by AgAerogel showed the same lack of dependence on CH_3I feed concentration. The lack of dependence on feed concentration can also provide a technical basis for the type of accelerated testing that was conducted in this effort. Early testing on the adsorption of iodine under VOG conditions was performed through extended duration testing using very low iodine feed concentrations (7–40 ppb). The tests were required to run for 3–4 months to obtain an iodine adsorption profile through the sorbent deep bed.

An examination of the penetration depth for each test indicates that CH_3I does not necessarily penetrate the sorbent bed to a depth greater than that of I_2, which had been assumed to date. However, a visual examination of the iodine loading profiles reveals a greater fraction of recovered iodine present in the tails of the penetration curves for CH_3I tests versus I_2. The percent of iodine retained in the first 2 cm of sorbent in the test system showed an inverse relationship to the penetration depth in the AgAerogel.

The second aim of this report was to compare the performance of Ag^0Z and AgAerogel in VOG conditions. Ag^0Z and AgAerogel iodine adsorption performance was examined for two I_2 concentrations (7 and 500 ppb) and three CH_3I concentrations (40, 400, and 1,000). The most notable difference between the two sorbents is that in all cases for both sorbates, the maximum observed iodine loadings are higher for AgAerogel. This has also been observed in thin-bed testing performed at higher concentrations. However, if the iodine loading data is normalized to account for the higher silver content in the AgAerogel, then no clearly discernable differences exist between the two sorbents.

Although the loading data are similar, the mechanical performance for the two sorbents is notably different. Little or no mechanical degradation is observed for the Ag^0Z. During the course of each test a notable amount of fines were created from the AgAerogel material. Density measurements performed show that the posttest bulk density of the AgAerogel is ~15% greater than that of the initial material. This increase in bulk density can be attributed to the breakdown of the larger aerogel structure into finer particles, resulting in bed compaction.

Throughout these tests, and particularly in the case of CH_3I adsorption tests, there was a significant discrepancy in the iodine material balances. This discrepancy does not appear to result from leaks or from concentration effects on the adsorption process. Future work in this area should be focused on resolving the outstanding questions about the closure of the material balance. The first step here will be to determine the extent of physisorption of CH_3I and the extent that it is easily removed. The second objective should be the determination of the length of the mass transfer zone and saturation loadings under VOG conditions. This avenue of research appears more promising based on the data on concentration effects and the potential to conduct accelerated testing. However, the results of accelerated tests may not account for any detrimental sorbent aging effects that could occur during longer duration testing.

CONTENTS

FIGURES

This page is intentionally left blank.

TABLES

This page is intentionally left blank.

ACRONYMS

AgAerogel	silver-functionalized silica-aerogel
AgZ	silver-exchanged mordenite
Ag^0Z	reduced silver-exchanged mordenite
DF	decontamination factor
FY	fiscal year
DOG	dissolver off-gas
MFC	mass flow controller
NAA	neutron activation analysis
ORNL	Oak Ridge National Laboratory
SOG	shear off-gas
UNF	used nuclear fuel
VOG	vessel off-gas
WOG	waste off-gas

This page is intentionally left blank.

PERFORMANCE OF SILVER-EXCHANGED MORDENITE AND SILVER-FUNCTIONALIZED SILICA-AEROGEL UNDER VESSEL OFF-GAS CONDITIONS

1. INTRODUCTION

US regulations 40 CFR 61, 40 CFR 190, and 10 CFR 20 govern release limits for volatile radionuclides contained in the gaseous effluents of used nuclear fuel (UNF) reprocessing facilities. Of the four volatile radionuclides that are restricted by the release limits (^{3}H, ^{14}C, ^{85}Kr, and ^{129}I) ^{129}I will require the greatest degree of abatement. Previous studies have shown that overall plant decontamination factor[a] (DF) for ^{129}I must, at minimum, exceed 1,000 to meet regulatory requirements (Jubin 2012).

A DF of 1,000 for ^{129}I translates to 99.9% abatement or sequestration of iodine across the plant. In a traditional aqueous-based UNF reprocessing facility, iodine will distribute through multiple unit operations, and the release from each of those operations must be such that the total release across the plant is less than 0.1% of iodine entering the plant within the UNF. This is a challenging requirement and recent research funded by the US Department of Energy has focused on the development and characterization of iodine abatement technologies that would facilitate compliance with regulations.

Iodine will be present in the dissolver off-gas (DOG), the cell off-gas, the vessel off-gas (VOG), the waste off-gas, and the shear off-gas. A number of studies have examined iodine abatement from the DOG, which contains greater than 95% of the iodine inventory of the plant (Jubin et al. 2013). This stream primarily contains elemental iodine (I_2) at part per million concentrations.

The VOG will most likely contain iodine at part per billion[b] concentrations. VOG refers to the gas venting from all chemical process tanks and equipment in the primary (non-waste) process line downstream of dissolver operations, including the solvent extraction operations that occur during aqueous UNF reprocessing. Volatile components and their degradation products present in the solvent extraction vessels can transfer to these gas streams, react with the iodine present in liquid or gas phases, or both. The VOG will most likely contain iodine at parts per billion concentrations. The VOG is also the stream most likely to contain organic iodides, which have been considered more difficult to remove (or more penetrating) than I_2 when using with traditional sorbents (Bruffey et al. 2015a).

Silver-exchanged mordenite (AgZ) has been considered a promising iodine sorbent for use in UNF reprocessing plants, but recent efforts have identified silver-functionalized silica-aerogel (AgAerogel) as an alternative iodine sorbent. In testing under simulated DOG stream conditions, AgAerogel demonstrates a resistance to degradation from NO_x gases present within the plant, has high iodine loadings by weight, and is easily converted to a condensed waste form through hot isostatic pressing (Bruffey et al. 2015a; Matyas et al. 2016). However, the mechanism for iodine adsorption and immobilization by AgAerogel is not yet understood, and it is not currently available in an engineered form with a large particle size and resistance to mechanical and thermal degradation.

Several years ago, Oak Ridge National Laboratory (ORNL) initiated an effort to evaluate both hydrogen-reduced AgZ ($Ag^{0}Z$) and AgAerogel under simulated VOG conditions. Initial tests were performed to evaluate the adsorption of elemental and organic iodine (Jubin et al. 2015; Bruffey et al. 2016). These tests were typically 3–4 months in duration, because at the low iodine concentrations in the prototypical

[a] The decontamination factor is defined as the concentration of the species of interest in the inlet stream divided by the concentration in the outlet stream. For an entire plant it would be the amount of the species in the feed streams to the plant divided by the amount exiting the plant in the off-gas streams.
[b] Throughout this report parts per billion or parts per million concentrations will be used on a molar basis.

VOG stream, considerable time was required to even begin to achieve significant iodine loading on the sorbent materials as compared to loading with prototypic DOG streams. Previous reports have characterized the results from adsorption of 7 ppb I_2 by Ag^0Z, 40 ppb methyl iodide (CH_3I) by Ag^0Z, and 40 ppb CH_3I by AgAerogel.

The testing reported here reflects a substantial increase in the body of work available on iodine adsorption by both silver sorbents under prototypical VOG conditions. Both I_2 and CH_3I have been tested on Ag^0Z and AgAerogel at a range of concentrations up to 1,000 ppb. These experiments were performed with two specific aims: (1) to assess the effect of iodine concentration on its adsorption by the sorbent and (2) to compare the performance of Ag^0Z and AgAerogel in the removal of iodine from a prototypical VOG stream. Results from the new tests were combined with previously reported testing to achieve these objectives.

2. MOTIVATION

Many scientific questions motivated the testing of iodine adsorption by both Ag^0Z and AgAerogel in VOG conditions. A previous literature review by Jubin and Bruffey (2015) indicated that dilute organic iodides present in the VOG stream would be more difficult to remove (i.e., more penetrating) than I_2. However, the data supporting this was relatively sparse, and no reported testing has examined either elemental or organic iodine adsorption from dilute streams by silver-based sorbents. As a result, this effort sought to answer the following questions of interest:

1. What is the saturation concentration for I_2, CH_3I, and other organic iodides on silver-based sorbents in VOG conditions?
2. What is the length and shape of the mass transfer zone, and how does this vary or change for I_2, CH_3I, and other organic iodides on silver-based sorbents in VOG conditions?
3. What is the iodine DF for I_2, CH_3I, and other organic iodides on silver-based sorbents in VOG conditions?
4. What is the effect of the gas velocity on the properties determined in questions 1–3?
5. What is the effect of iodine concentration on the properties determined in questions 1–3?
6. Is there an iodine concentration below which the sorbent becomes ineffective?
7. What is the effect of sorbent surface area on the properties determined in questions 1–3?

A report written in 2017 identified the highest priority knowledge gaps for iodine adsorption in the VOG system as the DF and the length of the mass transfer zone (Jubin et al. 2017). Fundamental adsorption data such as the iodine saturation capacity on the sorbent and the rate of iodine adsorption were also gauged to be of high priority.

There is inherent difficulty in investigating these particular questions because of the nature of the VOG system. Providing (and measuring) extremely low concentrations of iodine presents a challenge. Ensuring reliable delivery of iodine to the test system is complicated by the corrosive nature of iodine, which can foul gas regulators and generate deliquescent metal iodides in moist environments. Most important, very low iodine concentrations mean that it can take years to saturate even small amounts of sorbent. If the sorbent cannot be saturated, the mass transfer zone of the bed cannot be determined. The VOG testing performed at ORNL to date has not saturated the silver sorbent with iodine (though a test designed to saturate part of a deep bed is underway and is expected to last at least 1 year). In an effort to provide an indication of the iodine distribution through the bed, previous studies have compared the depth of penetration of iodine into the sorbent bed.

Determination of another key engineering parameter, DF, is also very difficult in this system. First, to determine a DF of 1,000 in a VOG system with 40 ppb CH_3I in the feed stream, iodine detection on the effluent would require quantification to parts-per-trillion levels. Analytical methodology for this type of

effort requires a high degree of expertise. Second, the analytical methodology should be able to analyze all possible iodine species present in the effluent gas. It is known that the decomposition of organic iodine species to I_2 or HI can be catalyzed by some sorbents (Nenoff et al. 2014). Thus, any measurement of iodine DF will be skewed if the analysis method is incapable of measuring all iodine-bearing species present in the effluent.

Given the limitations in our ability to fully quantify the effluent from the test system at VOG feed conditions, the testing of iodine adsorption by silver sorbents at ORNL has focused on the determining the extent of the penetration of iodine into the sorbent material as a function of the sorbate species and concentration. This parameter is then used to compare the performance of both silver-containing sorbents.

2.1 Previously Reported Testing

As a starting point, a single test system was built in 2015 to test I_2 adsorption on Ag^0Z at 7 ppb. This system is fully described in Section 3. The first test identified that residual iodine from previous tests was present in the delivery lines that resulted in a higher concentration of iodine being delivered to the test beds than was planned. Refinements of the delivery system to alleviate this issue were completed before advancing further. This testing was reported in Jubin, Bruffey, and Spencer (2015) and is referred to "2015-VOG1" in this report.

2.1.1 Adsorption of Iodine by Ag^0Z

2.1.1.1 Adsorption of 40 ppb CH_3I by Ag^0Z (2015-VOG2)

After the modification of the delivery system, a test examining the adsorption of CH_3I on Ag^0Z at 40 ppb was completed (referred to as "2015-VOG2"). This testing is summarized here and fully detailed in Bruffey et al. (2016). The sorbent bed was held at 150°C. The feed stream contained 40 ppb CH_3I in a moist feed stream with an inlet dew point of 0°C. The gas velocity through the bed was 10 m/min. The CH_3I feed stream was generated by dilution of a 1,000 ppm CH_3I (bal. N_2) blended gas cylinder.

The iodine adsorption on the initial thin bed (Bed 1) of Ag^0Z from a CH_3I stream was reported. It was observed that total adsorbed iodine increased linearly with respect to time over the 16-week test (Figure 1) to a maximum iodine loading of ~ 6 mg I/g Ag^0Z.

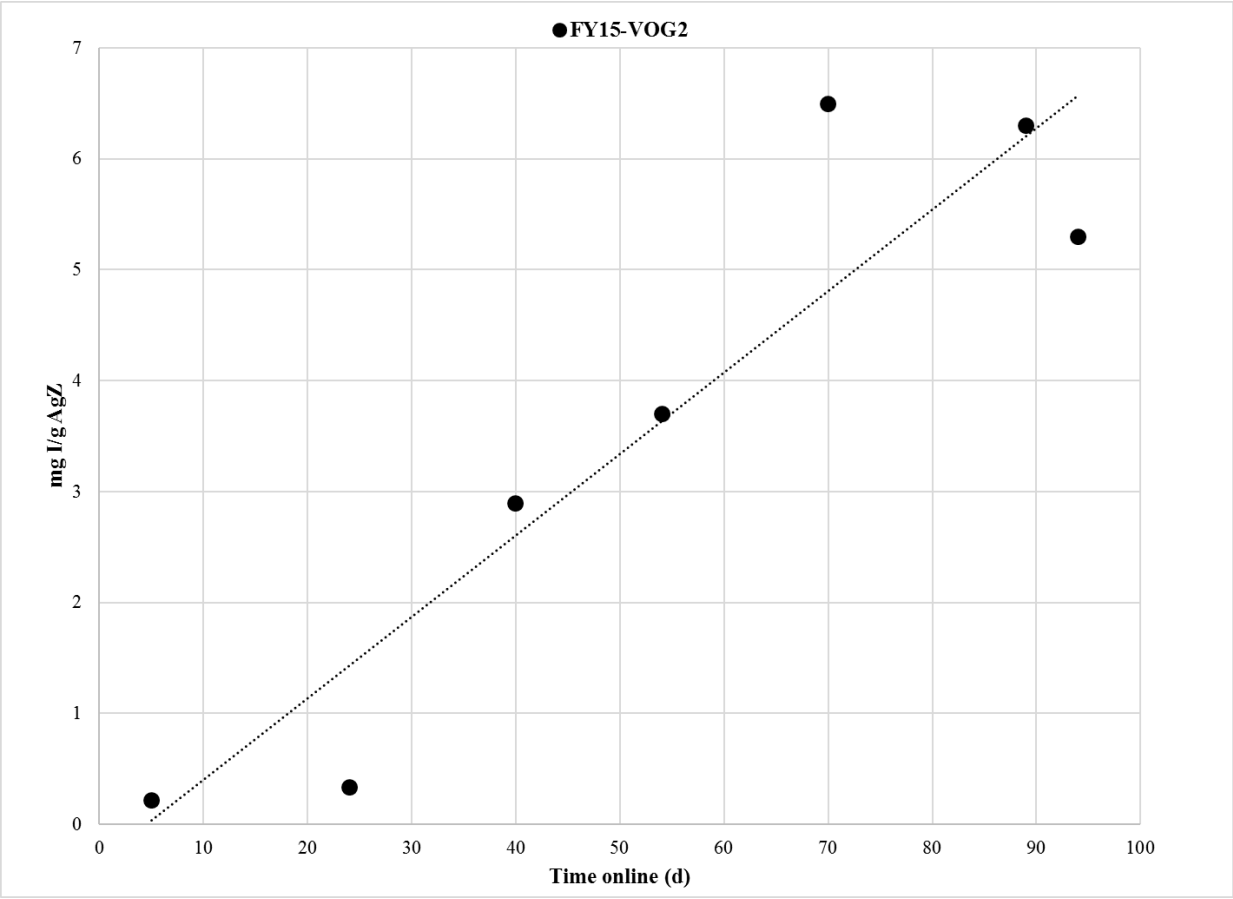

Figure 1. Bed 1 iodine loading on Ag^0Z as a function of time on line for 40 ppb CH_3I feed stream (Test ID: 2015-VOG2).

Bed 2 was removed in sections by vacuum. The sections were each homogenized, and then a small portion from each section was sub-sampled for iodine analysis by neutron activation analysis (NAA). The results from the NAA for each sub-sample are considered to be the average loading for that section. As shown in Figure 2, CH_3I was observed to penetrate 4.2 cm into the sorbent bed, with 84% of the recovered iodine located in the first 2 cm of the bed. For the purposes of this analysis, the penetration depth is defined as the cumulative length of all bed segments with a reported concentration greater than the detection limit provided by NAA. The black bars represent the length of sorbent bed that was removed and homogenized before analysis and the average loading of that section. The dotted line is plotted through the midpoint of the section length.

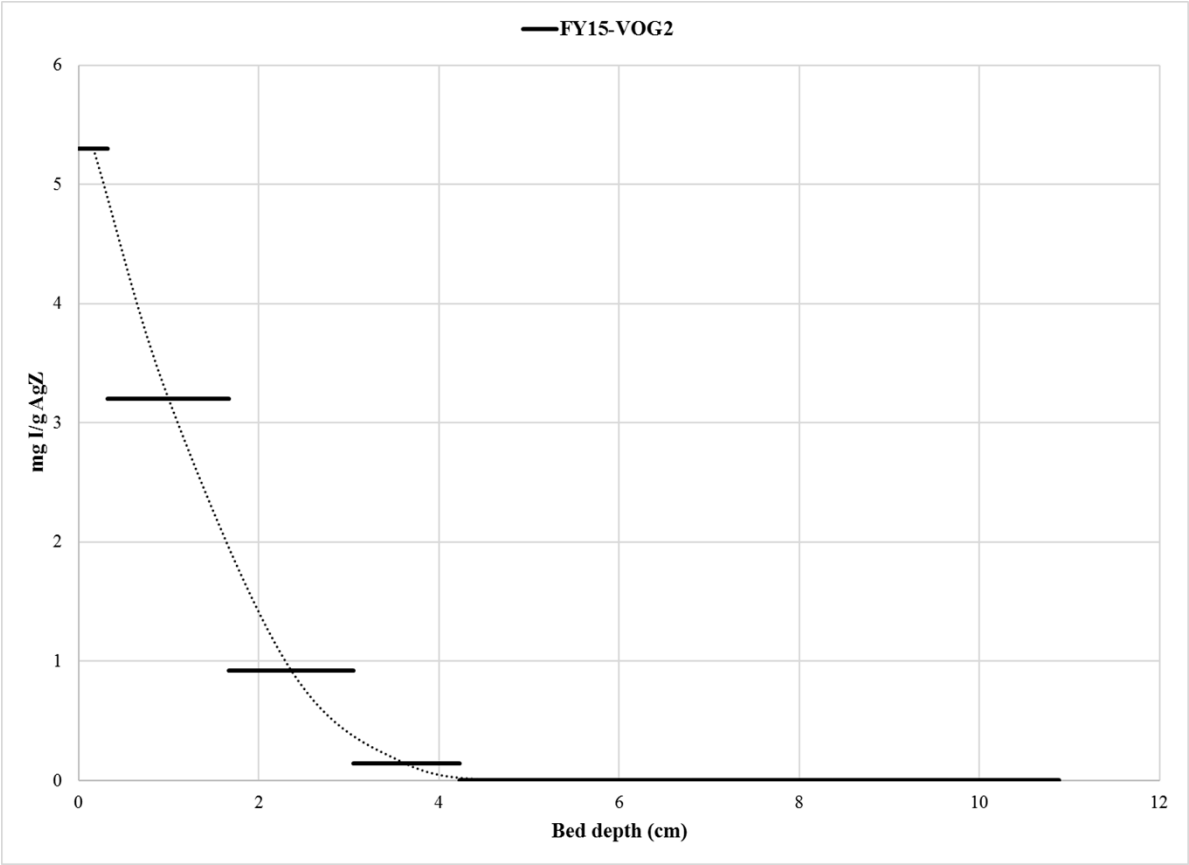

Figure 2. Iodine loading profile on Ag^0Z with a feed of 40 ppb CH_3I (Test ID: 2015-VOG2).

The analysis indicated that the amount of iodine recovered on the sorbent beds was 33% of the total amount delivered. The following potential causes were considered:

1. The CH_3I source was not delivering the mass of CH_3I expected.
2. The CH_3I feed system had a leak.
3. A portion of the feed gas was leaking from the test bed.
4. The low CH_3I concentration resulted in very low mass transfer and reaction rates in the sorbent, so much of the CH_3I was not reacted and not retained.
5. A significant fraction of the CH_3I was only physisorbed on the sorbent, and the method to remove the iodine-loaded sorbent material from the columns desorbed the physisorbed iodine from the sorbent during the vacuum removal of the bed.

At the conclusion of this test, it was judged that small, undetected leaks in the feed system or test bed could have contributed to the inability to close the mass balance, and further system modifications and extensive leak checking was implemented for future testing in an attempt to eliminate potential causes 2 and 3 from further consideration.

2.1.1.2 Adsorption of 7 ppb I_2 by Ag^0Z (2016-VOG-002)

The adsorption of 7 ppb I_2 by Ag^0Z was also reported in Bruffey et al. (2016). The iodine loading of the sorbent as a function of time is shown in Figure 3 to reach a maximum loading of 11 mg I/g Ag^0Z after 16.28 weeks. Unlike the adsorption of CH_3I by Ag^0Z reported in Section 2.1.1.1, the rate of loading is not linear throughout the test duration. As the sorbent time on line increases, the rate of loading decreases

(Figure 4). This observation is consistent with previous studies that quantified the effect of sorbent aging on the adsorption of I_2 by Ag^0Z. Previous thin-bed tests have shown that there is up to 40% loss in I_2 capacity after static aging in a dry air stream for 4 months and to 60% loss in iodine capacity after static aging in a moist air stream for the same period (Bruffey et al. 2013; and Jubin 2011).

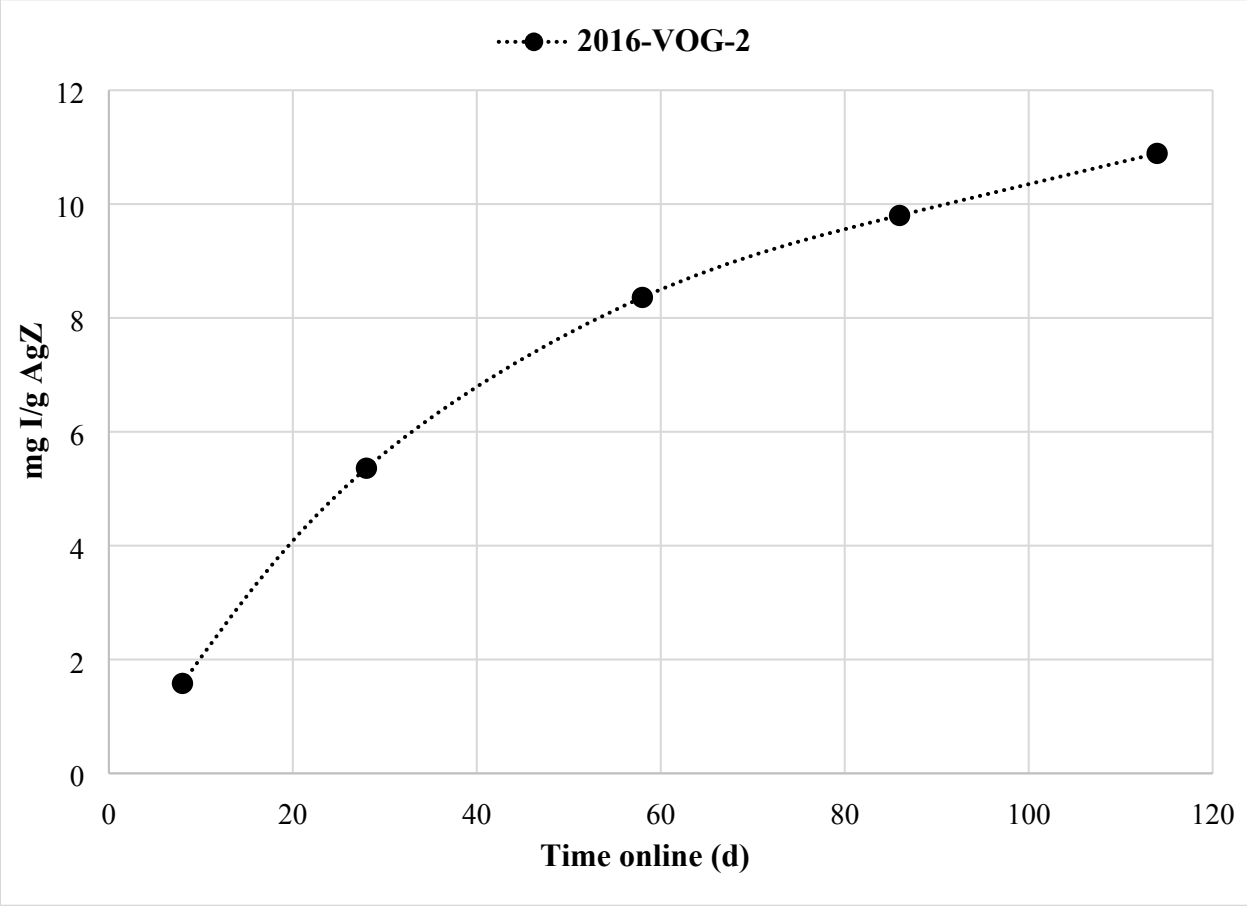

Figure 3. Bed 1 iodine loading on Ag^0Z as a function of time on line for 7 ppb I_2 feed stream (Test ID: 2016-VOG-002).

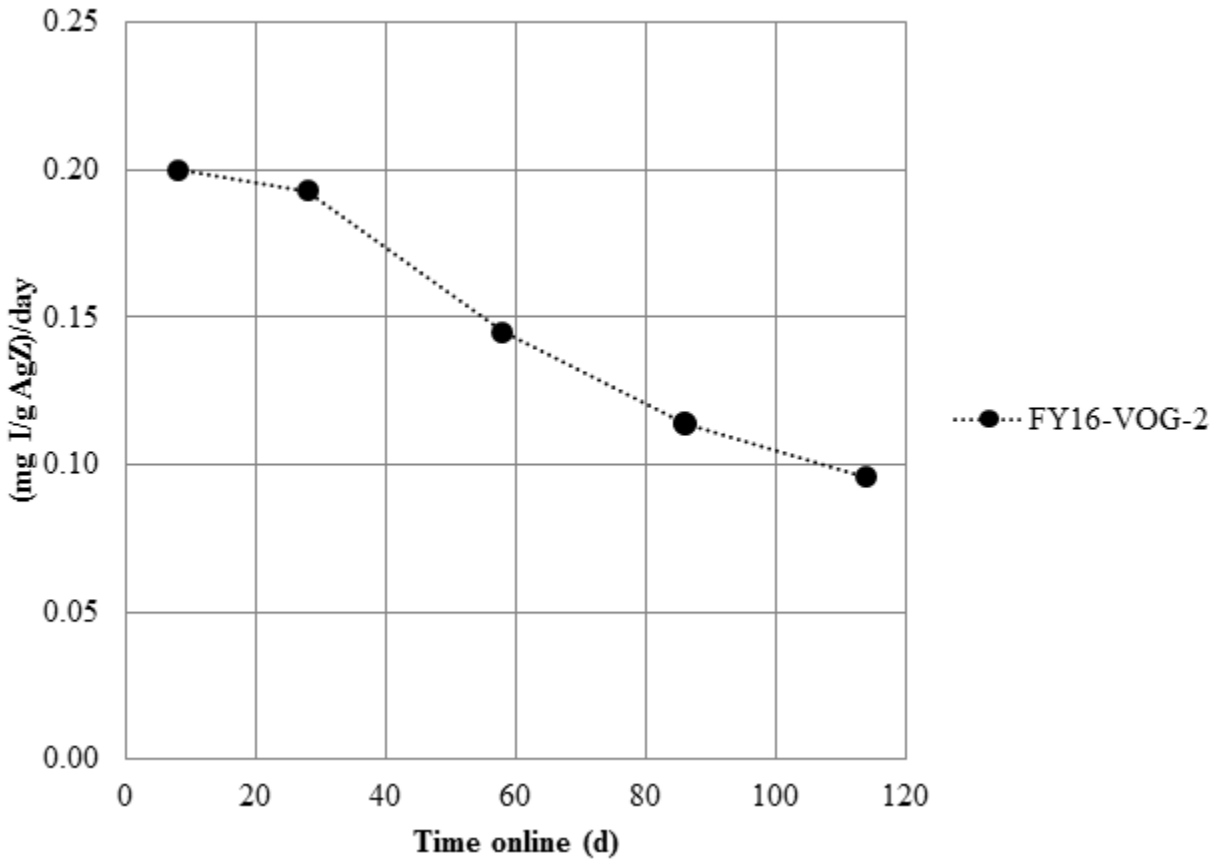

Figure 4. Effect of time on line on the iodine loading on Bed 1 quadrants for 7 ppb I_2 feed on Ag^0Z (Test ID: 2016-VOG-002).

Figure 5 shows the iodine content determined by NAA for the sub-samples for segments of Bed 2 as well as the sum of the Bed 1 quadrants. As before, these are considered the average iodine content for the segment. I_2 was observed to penetrate the Ag^0Z bed to a depth of 2.7 cm, with 87% of recovered iodine located in the first 2 cm. The mass balance for this testing indicated that 84% of the iodine fed to the system was recovered on the sorbent bed.

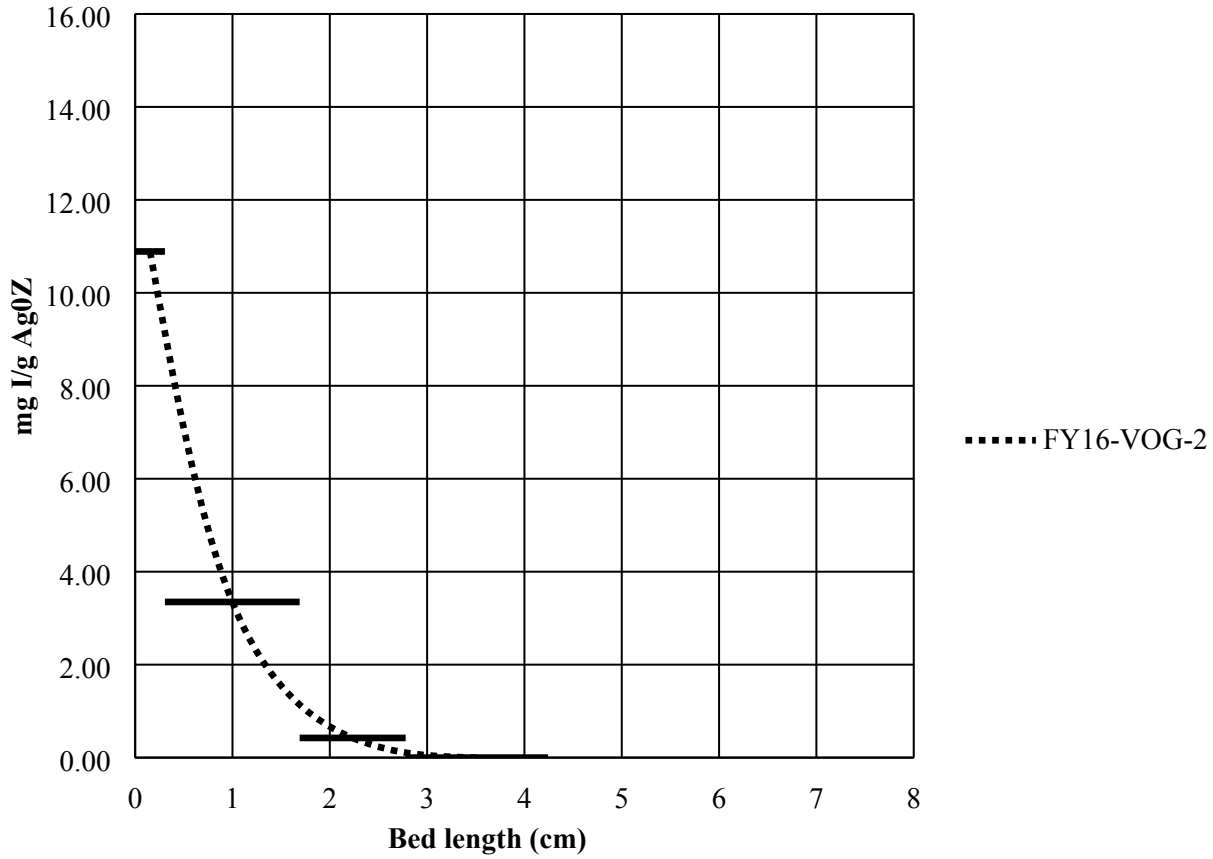

Figure 5. Iodine loading on Ag^0Z with a feed of 7 ppb I_2 (Test ID: 2016-VOG-002).

2.1.2 Adsorption of Iodine by AgAerogel

2.1.2.1 Adsorption of 40 ppb CH_3I by AgAerogel (2016-VOG-T3)

The adsorption of CH_3I by AgAerogel under VOG conditions is reported in Bruffey et al. (2016). Upon exposure to a feed stream of 40 ppb CH_3I, AgAerogel was found to load to a maximum of 21 mg I/g AgAerogel after 4 months of testing. This was intended to be a duplicate of 2015-VOG2 using AgAerogel instead of Ag^0Z. The rate of iodine loading based on analysis of the Bed 1 quadrants is shown in Figure 6.

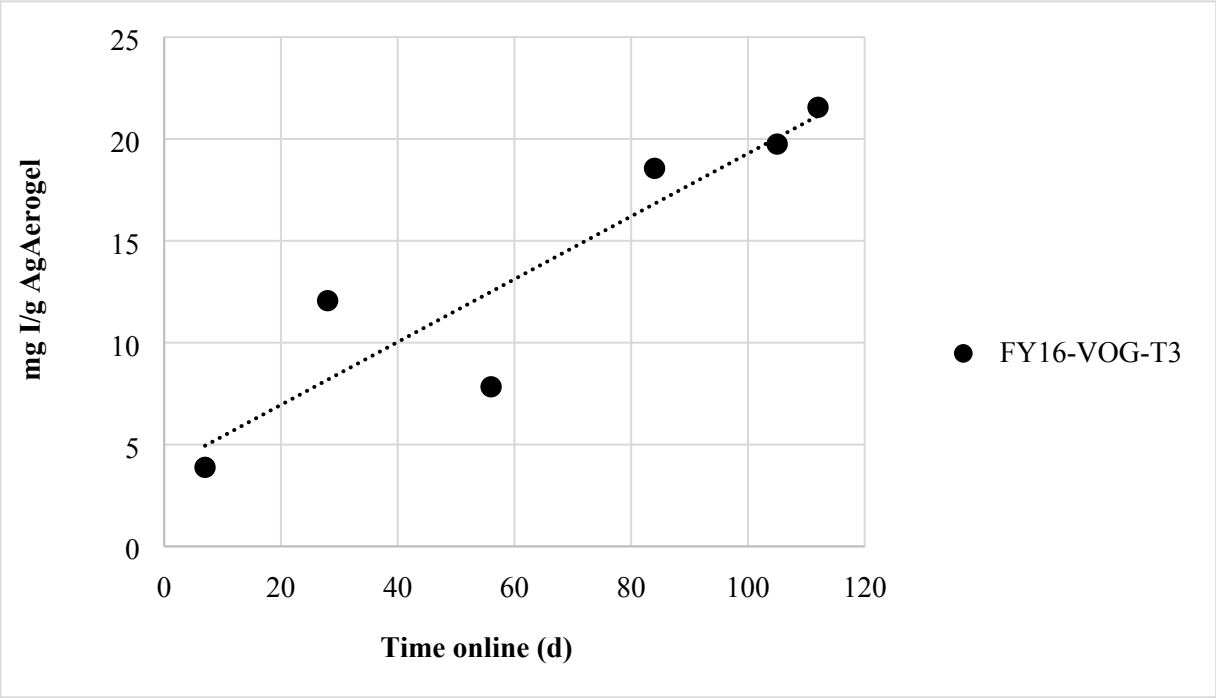

Figure 6. Bed 1 iodine loading on AgAerogel as a function of time on line for 40 ppb CH_3I feed stream (Test ID: 2016-VOG-T3).

Figure 7 shows the iodine content as determined by NAA for the sub-samples for segments of Bed 1 and Bed 2. As before, these are considered the average iodine content for the segment. CH_3I was observed to penetrate the AgAerogel bed to a depth of 5.6 cm, with 77% of recovered iodine located in the first 2 cm. The mass balance for this testing indicated that 50% of the CH_3I fed to the system was recovered on the sorbent bed.

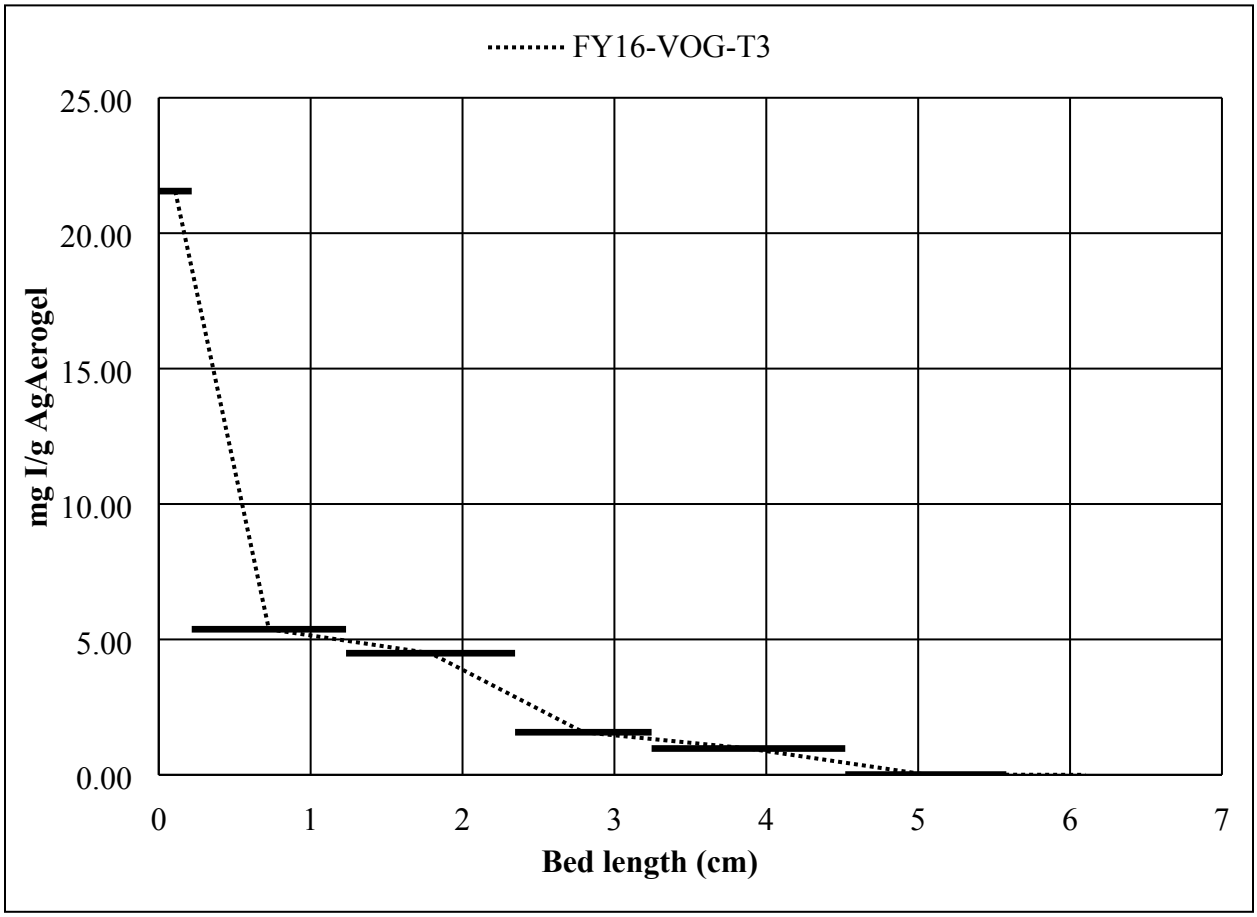

Figure 7. Iodine loading on AgAerogel with a feed of 40 ppb CH_3I (Test ID: 2016-VOG-T3).

2.2 Resolution of the Mass Balance

As referenced in Section 2.1.1.1, testing of 40 ppb CH_3I on Ag^0Z (2015-VOG2) identified concerns regarding a failure to close the mass balance, so additional leak tests were performed before each subsequent test to ensure there were no feed system leaks that would alter the total amount of iodine fed to the test beds. However, analysis of each test described in Section 2.1 showed that the concerns surrounding the mass balance persisted despite these leak check measures. A summary of the mass balances for the testing described above is provided in Table 1.

Table 1. Mass balances for previous VOG testing

Test description	Species	Concentration (ppb)	Mass balance (%)
Ag^0Z			
2016-VOG-002	I_2	7	84
2015-VOG2	CH_3I	40	33
AgAerogel			
2016-VOG-T3	CH_3I	40	50

The iodine mass balance for the test with I_2 was found to be higher than those of the two CH_3I tests. Organic iodide mass balances were 33% and 50%. The potential causes of incomplete mass balances listed in Section 2.1.1.1 were revisited, and it was determined that incomplete mass balances were most likely to be arising as a result of cause 1 (i.e., a failure of the CH_3I test gas generation system) or cause 4 (i.e., a fundamental adsorption problem at low concentrations of CH_3I).

2.3 Scope of Fiscal Year (FY) 2017 VOG Test Program

The test program completed in FY 2017 and described in the remainder of this document was designed to achieve two main goals. The first aim was to determine the effects of CH_3I concentration on CH_3I adsorption by Ag^0Z. This test series was undertaken to provide insight into whether the incomplete mass balance was because of low CH_3I concentration resulting in very low mass transfer rates (cause 4). The second aim was to compare the adsorption of CH_3I by Ag^0Z and AgAerogel. These two sorbents have very different physical properties and iodine capture behavior at high iodine concentrations, and it was unknown how these differences would manifest at low iodine concentrations. This testing is shown in Table 2, along with whether each test was used to satisfy aim 1 (concentration), aim 2 (comparison), or both. Throughout this report, this data is plotted with previously reported data, as relevant.

Table 2. VOG testing completed in late FY 2016 and FY 2017

Test ID	Species	Concentration (ppb)	Mass balance (%)	Data uses
Ag^0Z				
2017-VOG-T4	I_2	500	100	Comparison
2017-VOG-T5(4)	CH_3I	400	39	Both
2017-VOG-T7(4)	CH_3I	1,000	50	
AgAerogel				
2016-VOG-T4	I_2	7	165	Comparison
2017 T5-Aerogel	CH_3I	400	114	
2017 T7-Aerogel	CH_3I	1,000	80	
2017 T4-Aerogel	I_2	500	67	

Before these tests, substantial changes were enacted in the VOG test system and test protocols. First, the test systems were duplicated to enable the simultaneous testing of up to four test beds, each with individual gas feed systems. Second, upon discovery that a CH_3I gas cylinder used in the CH_3I feed system did not deliver the CH_3I concentration detailed on the cylinder certification, the decision was made to use permeation tubes for both I_2 and CH_3I delivery, except at high I_2 concentrations. The third adjustment, and most marked of the three, was that of iodine concentration in the feed stream. Iodine concentrations in the feed stream were increased, and testing ranged from 400 to 1,000 ppb for both I_2 and CH_3I. These higher concentrations enabled the completion of multiple tests throughout the year with durations of 1–3 weeks, rather than months. Although these concentrations are higher than expected in the VOG stream of an operating reprocessing plant, they are still two orders of magnitude lower than the majority of testing that has been performed on iodine adsorption by silver-based sorbents. Testing was completed so that the concentration was varied but the total amount of iodine delivered to the bed remained the same by adjusting the test duration. This approach allows any observed variation in iodine distribution in the beds to be attributed primarily to the variation in feed concentration.

3. EXPERIMENTAL

3.1 Materials and Methods

This section describes the approach used for all VOG testing completed thus far, including previously reported testing.

3.1.1 Experimental Materials

Testing was conducted by flowing a gas stream containing I_2 or CH_3I through a sorbent bed containing either Ag^0Z or AgAerogel for 1–16 weeks. The silver mordenite (AgZ) was obtained from Molecular Products in an engineered 1/16-in. pellet form (Ionex-Type Ag 900 E16) containing 9.5% silver by weight. The material was reduced before testing by 10-day exposure to a H_2/N_2 gas stream at 270°C as described in Anderson et al. (2012). The reduced AgZ (Ag^0Z) had a measured bulk density of 0.84 g/cm^3.

Silver-functionalized silica-aerogel was provided by Pacific Northwest National Laboratory in 100 g batches from 2014 through 2017. A description provided with the 2017 shipment reports an iodine sorption capacity of 394 mg/g. Assuming 100% silver utilization, this corresponds to a silver content of 33.5 wt%. AgAerogel, as provided, was a granular, primarily black material of nonuniform particle size with heterogeneously distributed flecks of yellow color. After extended exposure to the gas streams used in these experiments, the material converted to a purer black color. The measured bulk density was 0.54 g/cm^3 for the as-received material and was 0.62 g/cm^3 for the post-run material.

3.1.2 Test Systems and General Protocol

Because iodine can be corrosive, especially in the presence of water, the materials of construction for the system were carefully selected to minimize iodine retention to system components and piping. The sorbent beds were contained within glass columns (internal diameter = 3.45 cm) and separated by glass frits. Iodine was carried into the system by flexible stainless-steel tubing. Stainless steel was chosen instead of a flexible fluoropolymer, such as PFA, because prior experience has indicated that iodine adsorbs onto PFA at room temperature. These iodine generation streams were dry (−70°C dew point), limiting the potential for corrosion of the metal. The humid air and iodine (I_2 or CH_3I) supply streams were piped through separate lines of 316 stainless-steel tubing. The two streams were blended together at high temperature (150°C) in a glass tee directly before introduction into the sorbent bed.

Although an all-glass system would be preferable, ensuring that glass connections are leak-tight at high temperatures and in a positive-pressure system is difficult. Previously reported work used ground glass ball joints to connect adjacent units, but small perturbations in the system alignment could misalign the joints. In late 2016, the ground glass joints were changed to Swagelok Ultra-Torr fittings, which are stainless steel with FKM O-rings, and have a certified helium leak rate of 4×10^{-9} std cm^3/s at ambient temperature. The system was leak checked via vacuum, pressure or water displacement as appropriate.

Three sorbent beds were placed in series. The first, Bed 1, was a thin bed with a depth of ~0.25 cm segmented azimuthally into quadrants. Bed 2 was a ~10 cm long deep bed intended to be longer than the length of the mass transfer zone and to capture the bulk of the iodine in the stream. The final bed was ~0.75 cm in depth and was intended to serve as a breakthrough detector. A schematic of this system is shown in Figure 8. Figure 9 shows the assembled bed system before installation in the oven. Figure 10 is a photograph of the oven and permeation tube feed system as installed in the hood.

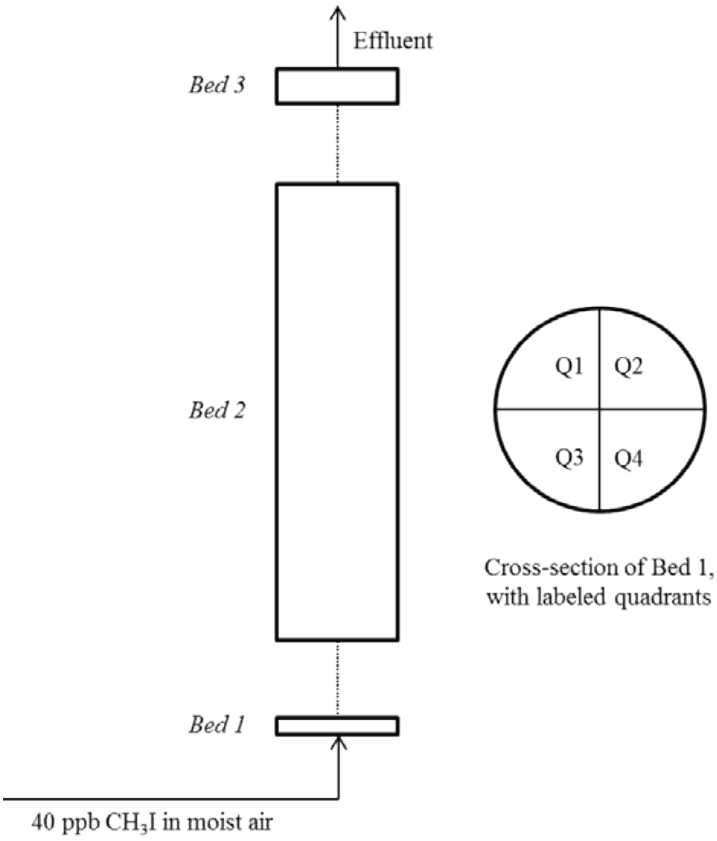

Figure 8. Schematic of test system. Feed concentration and gas can vary from 10 to 1,000 ppb and can be either CH_3I or I_2.

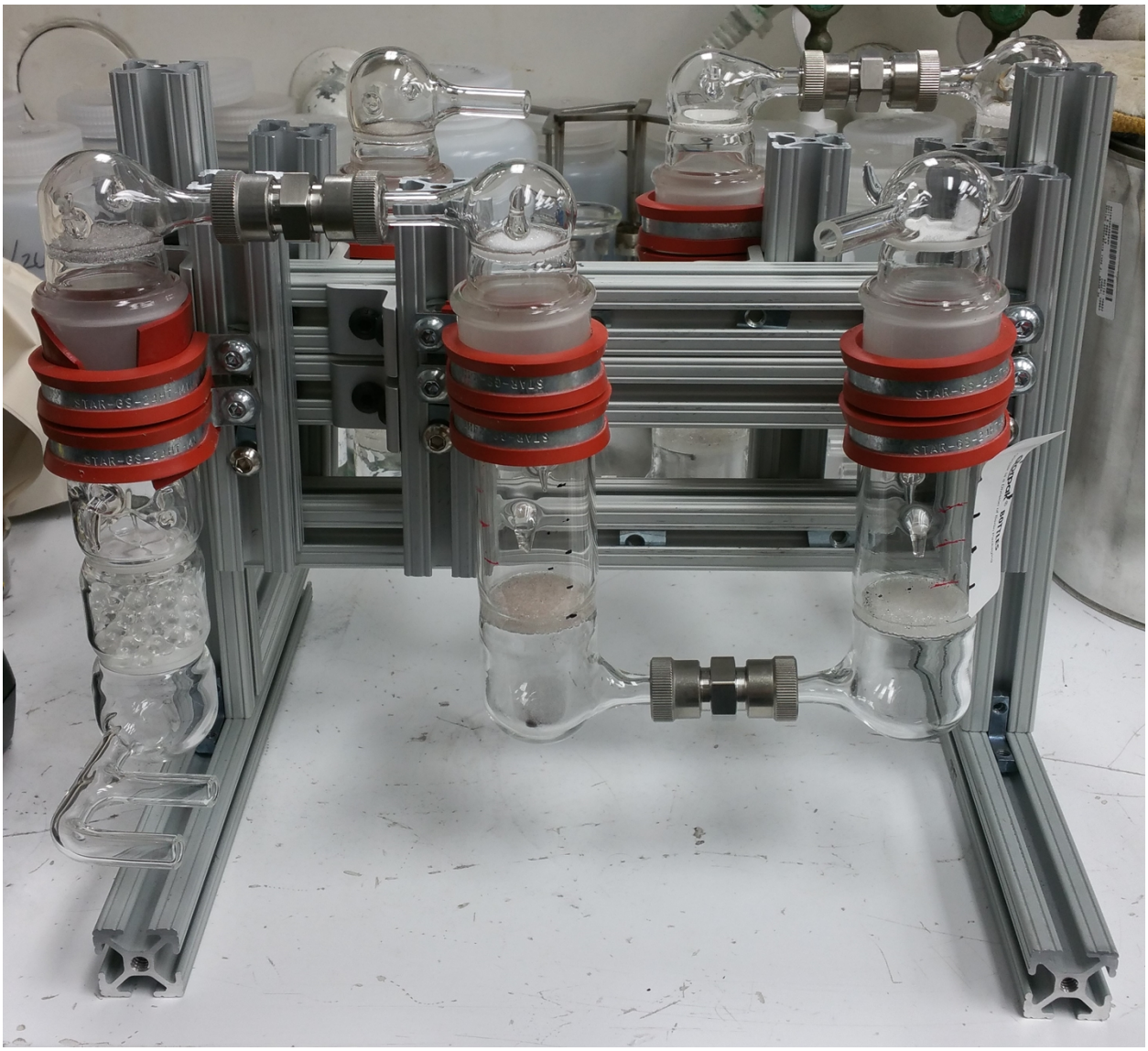

Figure 9. VOG test beds.

Figure 10. VOG test system.

The system was designed to capture multiple pieces of information in a single test. The quadrant bed could provide adsorption rate data because individual quadrants could be sampled at various times, allowing comparisons between sorbent material capture performance after times such as 1 day and 1 week. Prior experience at higher iodine concentrations (~50 ppm as opposed to 10–1,000 ppb) in a thermogravimetric analyzer with beds of similar length has demonstrated that the capture performance of thin beds at parts per million concentrations is not effective enough to sufficiently deplete the inlet stream, meaning that the concentration profile of the feed stream does not change significantly throughout the bed. For example, 2 g of sorbent exposed to 50 ppm I_2 at 10 m/min total gas velocity would be expected to saturate with iodine in ~30 min., but a similar amount of sorbent can take up to 1–2 weeks to fully saturate at parts per billion concentrations. At parts per billion concentrations, the presence of even a short initial bed could deplete the feed gas stream enough to significantly alter the makeup of the stream entering the deep bed.

Bed 2 was split into two nearly equal halves across two glass columns. Upon completion of the tests, Bed 2 could be selectively removed by vacuum into sections (typically eight) and analyzed to determine

iodine distribution through the bed. Finally, the gas passes through Bed 3, which can be sampled intermittently and replaced on line during the test to determine iodine breakthrough.

Certain engineering parameters within an adsorption system, particularly the length of the mass transfer zone, may be functions of the gas velocity. The gas velocity for VOG testing was set to 10 m/min in a glass column of 3.45 cm diameter held at 150°C. This did not result in a turbulent flow regime, and the velocity profile could be radially uneven. This did not affect the total iodine delivery to the system, but it could have the effect of preferentially distributing iodine toward the center of the column. To minimize this concern, the inlet portion of the Bed 1 was modified to include a mixing zone consisting of glass bead packing before the sorbent bed to ensure that the water and iodine-bearing streams mixed thoroughly and were evenly distributed to the sorbent bed. FY 2017 testing included this modification.

3.1.3 Test Series and Conditions

The general conditions of for all VOG testing were similar. The face velocity calculated based on the total flow rate and the system cross-sectional area was 10 m/min at 150°C. Each experiment was conducted at a temperature of 150°C, and the humid air feed stream was directed through a 10 ft length of tubing within the oven to allow the gas to heat to process temperature. Iodine concentrations ranged from ~10 to ~1,000 ppb of either I_2 or CH_3I.

3.1.4 Generation Methods for Test Gases

There were three methods used to generate iodine-bearing streams: gas cylinders (for CH_3I), crystalline generator (I_2), and permeation tube within a gas generator (both CH_3I and I_2).

CH_3I was delivered using 1,000 ppm CH_3I/N_2 blended pressurized cylinders provided by Air Liquide/AirGas. These cylinders were heated slightly to limit settling of the heavier CH_3I to the bottom of the cylinder, which could result in uneven delivery of CH_3I. The gas from these cylinders was delivered to the process through a Sierra mass flow controller (MFC). This method was not used after the completion of test FY16-VOG-2.

A crystalline iodine generator was used to generate high-concentration I_2 streams (500 ppb I_2 for a total atomic iodine content of 1,000 ppb). The dry air to the column containing crystalline iodine maintained at 18°C was controlled by a separate MFC. Based on the vapor pressure of iodine at this temperature the total iodine content in the feed stream could be determined. Based on prior work, this method is known to reliably generate iodine at high concentrations.

The final method of generation was the use of permeation tubes provided by Kin-Tek Analytical. Nitrogen was passed through a glass chamber containing a permeation tube that released either iodine or CH_3I at a predetermined rate. This was then fed to the process and diluted with the humid air stream. The permeation tubes were certified by gravimetric analysis by the manufacturer before delivery; delivery rates were known to within 1 ng/min. All FY 2017 CH_3I testing used this generation method, as well as earlier testing conducted at 7 ppb I_2.

3.2 Results Presentation

There are two types of data obtained from this testing. The first is that of the intermittently sampled quadrants, which can provide the rate of iodine loading onto the sorbent. The second is that of the iodine loading progression through the deep-bed segments. This data can be presented in multiple ways.

The most intuitive is the representation of iodine loading as a function of column depth (Figure 11). In this case, segment length or column depth is calculated based on the mass of the sample and the density of the sorbent. The length of the bar represents the length of the individual segment and the area under the bar is proportional to the total amount of iodine retained in that segment.

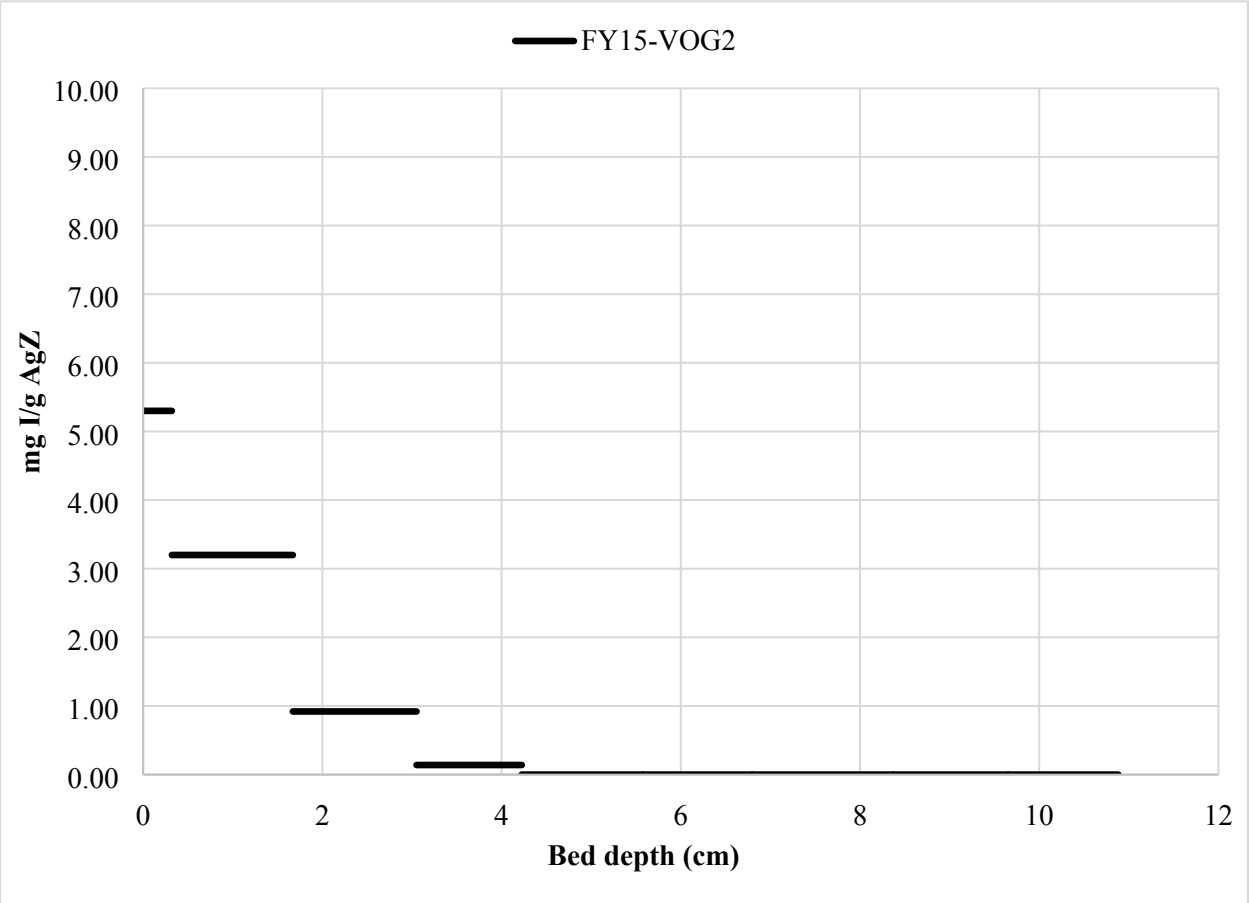

Figure 11. Direct presentation of the column loading data where the concentration of iodine on sorbent is shown as a function of bed depth (Test ID: 2015-VOG-2).

This representation does not account for the different silver content of the two sorbents, which is likely to be an important factor in total capacity. It also does not directly account for any change in sorbent density that occurs during testing. For example, AgAerogel was shown to increase in density by 15% over the course of a typical VOG test. This is believed to be a result of mechanical degradation of the bulk structure and the production of material fines that compacted the sorbent bed. Evaluation of the iodine loading on the AgAerogel in Bed 2 of all tests ranged from ~0 to ~17 mg I/g or ~1.7 wt% and thus to not appear to account for the increase in bulk density.

While the bar representation is effective in accurately portraying the data collected it is difficult to provide clear overlays to compare multiple runs on a single graph. This data can be simplified for graphing purposes by plotting as a continuous curve using the midpoint of the segment and the average concentration, as shown in Figure 12. It is recognized that the average loading may not actually occur at the midpoint in the segment if the shape of the adsorption front is curved.

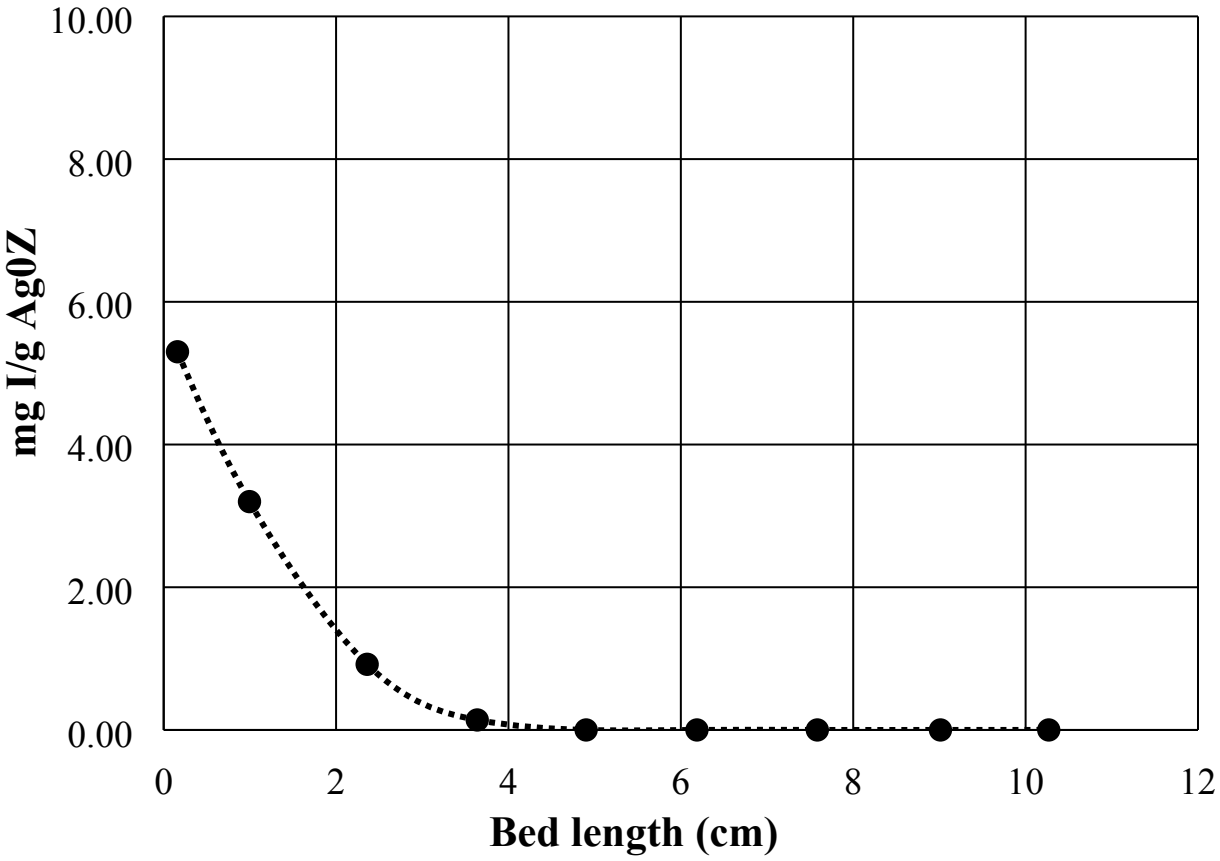

Figure 12. Single curve presentation of the column loading profile using the midpoint of each segment and average segment loading to display the concentration profile of iodine on sorbent as a function of bed depth (Test ID: 2015-VOG-2).

These two approaches, while providing a good indication of the loading on the sorbent, do not provide an indication if there is a portion of the iodine that is not being retained on the sorbent. The discrepancy between amount of iodine delivered and recovered can be represented as shown in Figure 13. This figure shows the cumulative amount of iodine recovered as a function of bed depth, rather than showing the loading of individual bed segments. The total amount of iodine delivered can be shown for easy comparison to the amount recovered as indicated by the dashed line at 60.8 mg. However, this method becomes cumbersome when plotting multiple runs on a single graph. Also, the overall material balances can be more easily presented in tabular form.

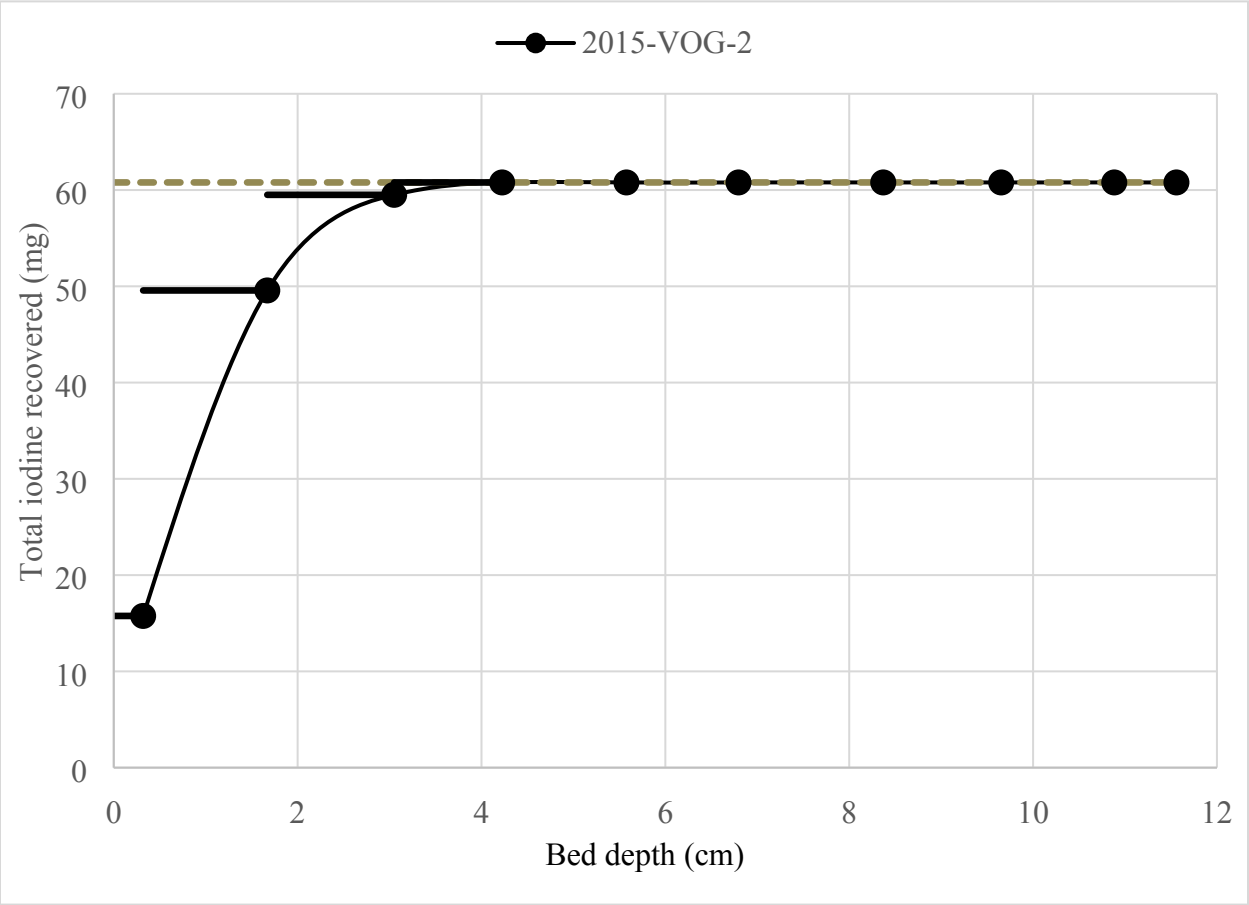

Figure 13. Presentation of the total iodine recovered on sorbent columns as a function of bed depth (Test ID: 2015-VOG-2).

A fourth representation can account for the different silver contents of the two sorbents (Figure 14). Here the iodine loading for each bed segment is provided in mg I/g silver, as opposed to mg I/g sorbent.

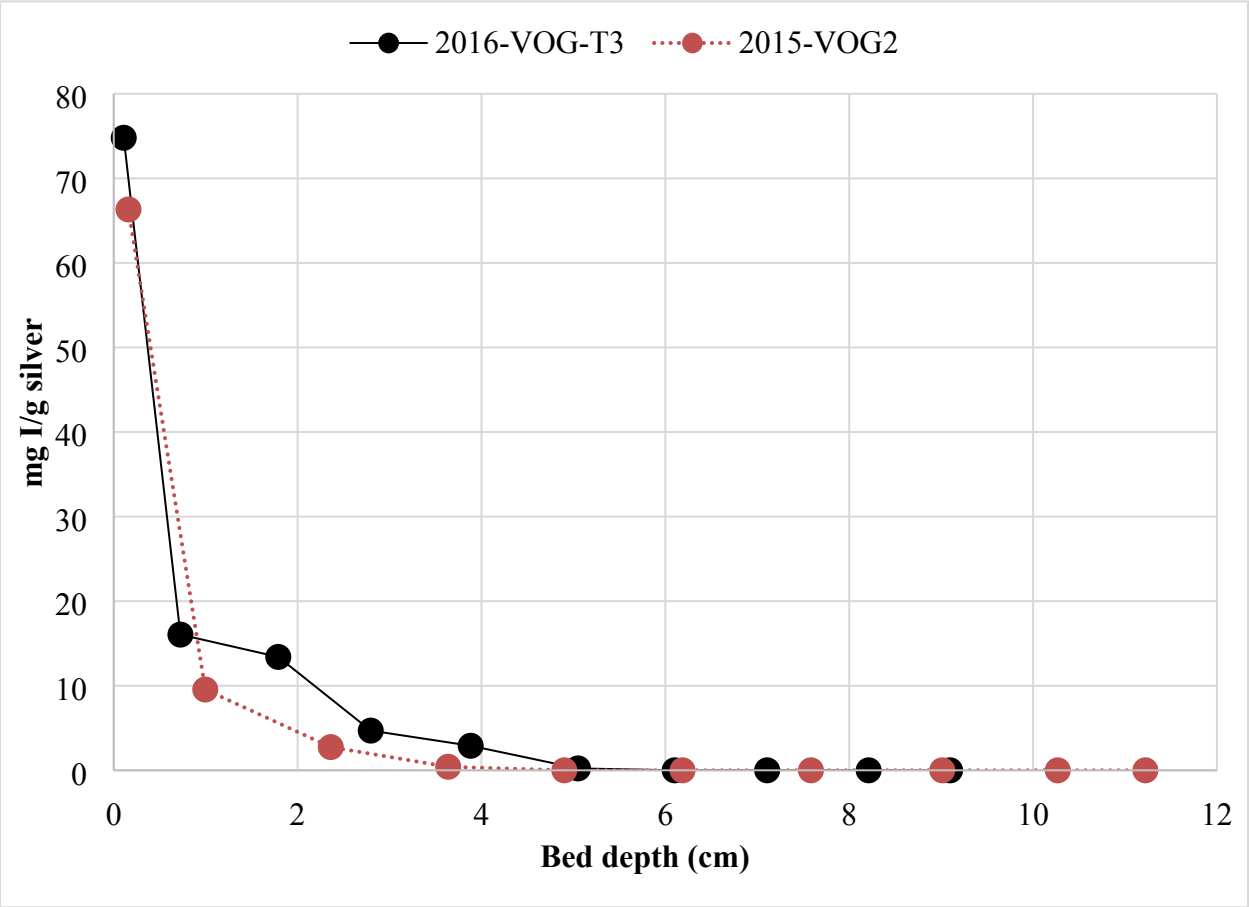

Figure 14. Presentation of the column loading data normalized for silver content of sorbent where the concentration of iodine per gram of silver in sorbent is shown as a function of bed depth.

In this report, the iodine loading profile across the sorbent bed will be primarily represented as shown in Figure 12. Plots of each individual test showing the actual segment length and average segment loading are presented in Appendix A along with a table showing the segment lengths, quadrant masses, and iodine loadings. This discussion is provided to illustrate that a single graph cannot convey all aspects of adsorption testing for these two different silver-based sorbents.

3.3 Discussion of Experimental Variability

Several sources of variability may exist within the VOG test system. As previously mentioned, difficulty generating consistent iodine feed streams has resulted in modifications to the iodine generator system (e.g., permeation tubes versus blended gas cylinders). Other possible sources of variations include loss of iodine through reaction before reaching the sorbent bed (i.e., iodine reacting with metal in the feed lines), loss of physisorbed material, and sub-sampling variability present upon analysis with neutron activation analysis. Quantification of the extent of the variability has proven difficult to measure directly. Discussion of these sources of variability, their likely effects on the system, and their relative magnitudes follows.

3.3.1 Sorbent Sampling and Analysis

Upon completion of each test, samples were removed from the test bed by vacuum. Sorbent samples removed from the system range in mass from 0.3–10 g. Each sample was homogenized by manual mixing, sub-sampled and a portion sent to ORNL's High Flux Isotope Reactor for neutron activation analysis (NAA) of iodine content. These sub-samples are typically on the order of 0.2 g, and there will be

some variability associated with sub-sampling. To quantify this variability for thin bed sampling and for the associated NAA analysis, in which the sub-sample is 33%–66% of the total mass of the thin bed quadrant, three VOG tests were examined in which the quadrants were not removed at intermittent points. Thus the variation was determined by analyzing quadrant samples that had been exposed under identical conditions for identical durations. These tests yielded percent deviations across the four quadrants of 8.0%, 6.4%, and 16% (calculated as standard deviation of the sample divided by the mean of the sample).

The variability associated with deep-bed sampling, in which the sub-sample is 2%–3% of the total mass of the deep-bed segment, has also been assessed. Two separate tests were run with ~10 g of Ag^0Z (corresponding to ~1.5 cm bed length) exposed to equal concentrations of CH_3I. Three sub-samples of ~0.2–0.35 g were taken from each of these larger 10 g samples and analyzed by NAA for iodine content. These two tests resulted in standard deviations of iodine content that were 12% and 27% of the mean iodine content. Further testing will be required to provide a quantitative variability estimation on the deep-bed sub-sampling method.

Applying these margins to the data could serve to bound the likely mass balances. It should be noted that this variability estimation was limited to Ag^0Z because of the limited availability of AgAerogel material.

4. EFFECTS OF CH_3I CONCENTRATION ON ADSORPTION BY Ag^0Z

As noted above, the results arising from the initial series of VOG tests indicated there was a discrepancy between the amount of CH_3I that was thought to have been fed into the test systems and the amount of iodine that was determined by NAA to be present on the sorbent material at the termination of the run. One of the theories proposed was that there may be a *de minimus* concentration at which the adsorption rate was too low to be effective. If this hypothesis is correct, then increasing the feed concentration would result in higher recovery. This was evaluated by conducting a series of tests at higher CH_3I feed concentrations over a shorter time period such that the total amount of CH_3I fed was the same for all runs.

A total of three tests were conducted at CH_3I concentrations ranging from 40 ppb to 1,000 ppb (Table 3). The iodine loading versus time on line of the thin beds is shown in Figure 15.

Table 3. Comparison of CH_3I recovery on Ag^0Z as a function of feed concentration

Test	CH_3I concentration (ppb)	Time on line (d)	Iodine delivered (g)	Iodine recovered (g)	Maximum sorbent loading (mg I/g Ag^0Z)	Recovery (%)	CH_3I source
FY15-VOG2	40	93.94	0.179	0.060	6	34	Blended gas cylinder
FY17-VOG-T5(4)	400	9.985	0.155	0.061	9	39	Certified permeation tubes
FY17-VOG-T7(4)	1,000	3.980	0.155	0.077	8	50	

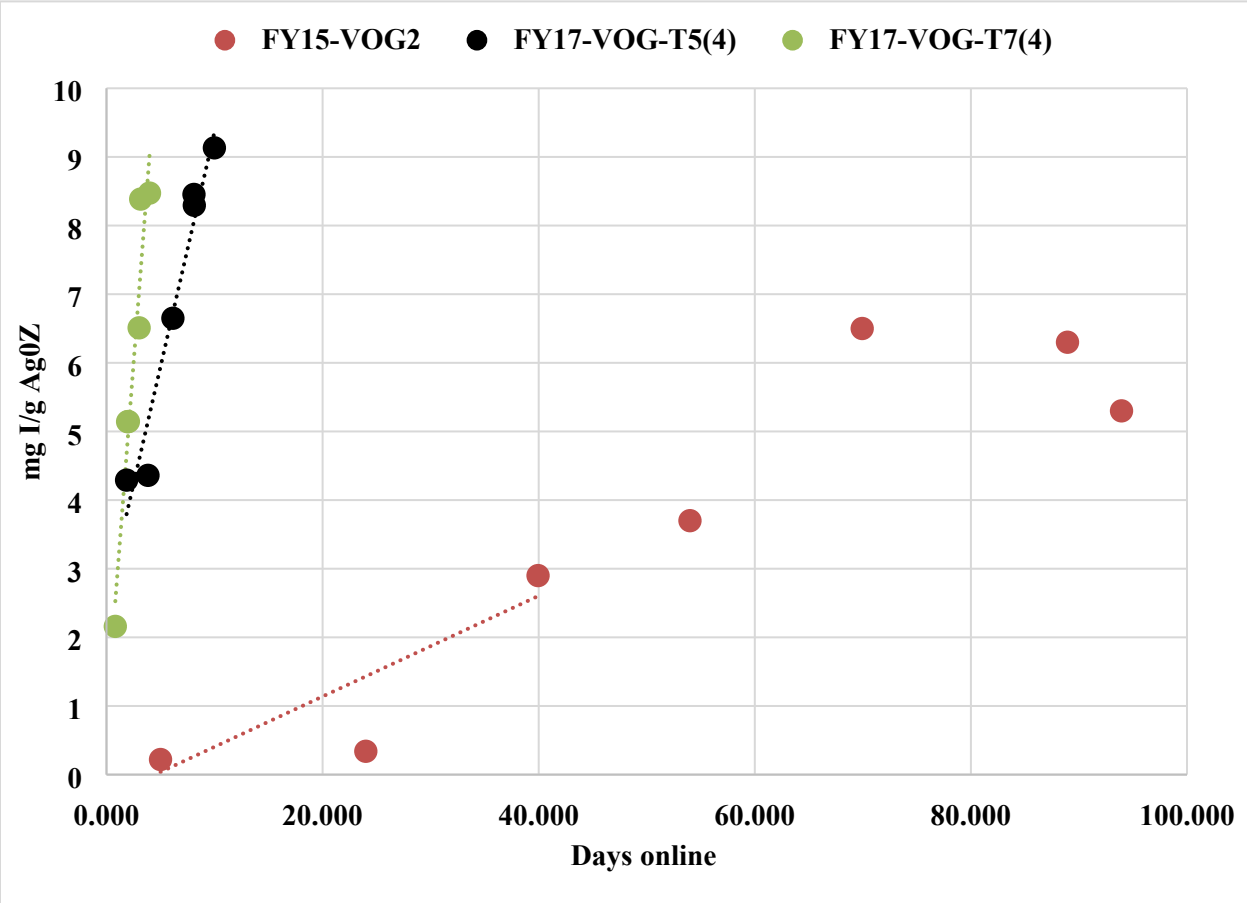

Figure 15. Comparison of Bed 1 iodine loading on Ag^0Z for various CH_3I concentrations as a function of time on line (Test ID: 2015-VOG2, 40 ppb CH_3I; 2017-VOG-T5(4), 400 ppb CH_3I; 2017-VOG-T7(4), 1,000 ppb CH_3I).

Iodine loading is linear even at the longer durations associated with the 40 ppb run, which would indicate that there was little or no significant aging of the sorbent at this sorbent saturation level as was noted for Test 2016-VOG-002 in Section 2.1.1.2.

This data was then recast to examine the loading as a function of total amount to CH_3I that had fed into the test bed (Figure 15). Increasing the concentration of CH_3I resulted in significantly higher iodine retention on the first quadrant segments at a constant amount of delivered iodine. Because the mass of the thin bed is 2% of the total sorbent bed mass, this only represents 1%–3% of the total iodine recovered by the sorbent bed, with the bulk of the iodine captured by the deep sorbent bed.

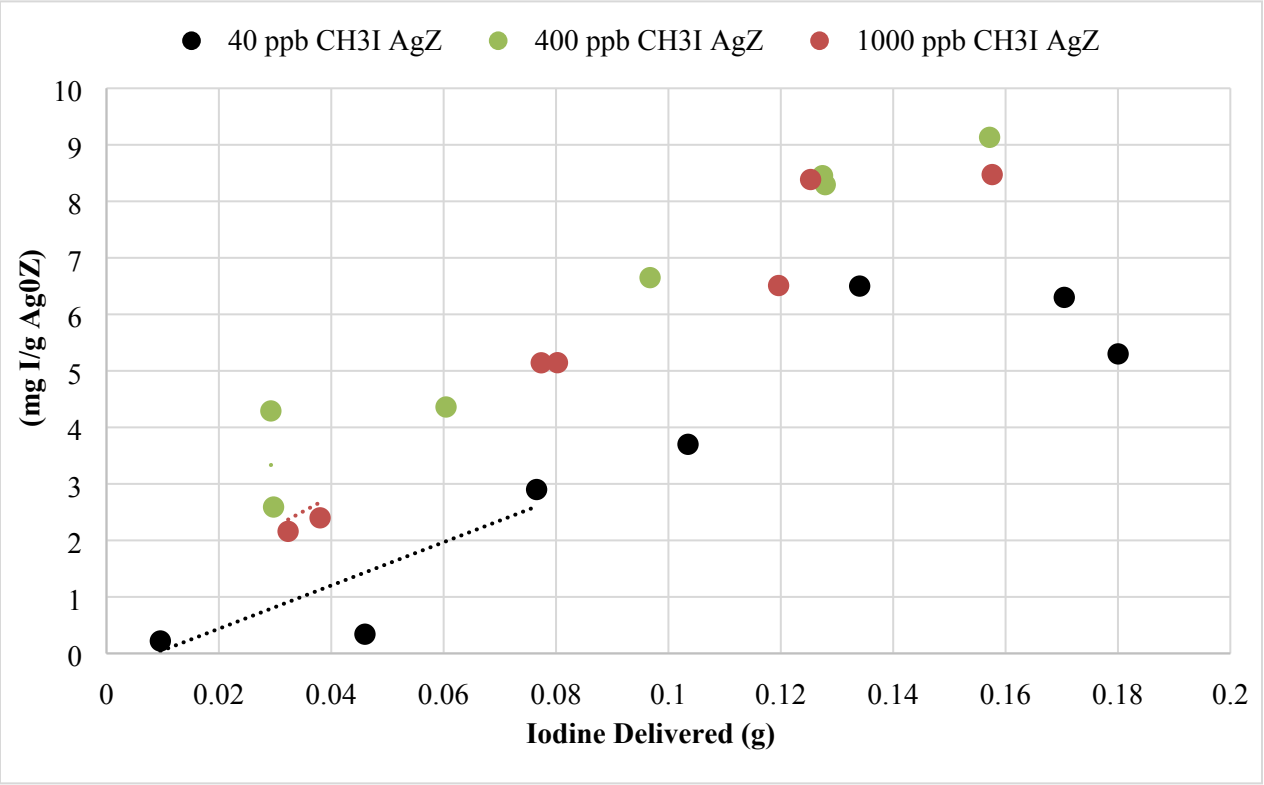

Figure 16. Bed 1 iodine loading of Ag^0Z as a function of iodine delivered as CH_3I (Test ID: 2015-VOG2, 40 ppb CH_3I; 2017-VOG-T5(4), 400 ppb CH_3I; 2017-VOG-T7(4), 1,000 ppb CH_3I).

The loading of Ag^0Z by CH_3I appears to increase at the same rate for all three concentrations examined, but a linear regression provides a different *y*-intercept for each data set. This may reflect that the intermittent sampling method does not fully capture the early loading behavior of CH_3I onto the sorbent bed. For example, the sorbent beds are not presaturated with water, and water will not fully saturate the sorbent bed until hour 2–3 of testing. Prior to water saturation, iodine loading may proceed at a different rate than can be observed through intermittent sampling.

The penetration of CH_3I into the Ag^0Z test bed at varying CH_3I concentrations is shown in Figure 17. With the exception of the quadrant portion of the test beds (the data point to the far left of each curve) the loading across the length of beds appears virtually identical with the exception of one portion of the 1,000 ppb bed that has a slightly elevated iodine level at about 40% of the bed depth. This minor anomaly could be the result of sub-sampling variability. This series of tests would indicate that neither the total amount of iodine removed nor the total penetration depth is impacted over the concentration range of 40–1,000 ppb CH_3I.

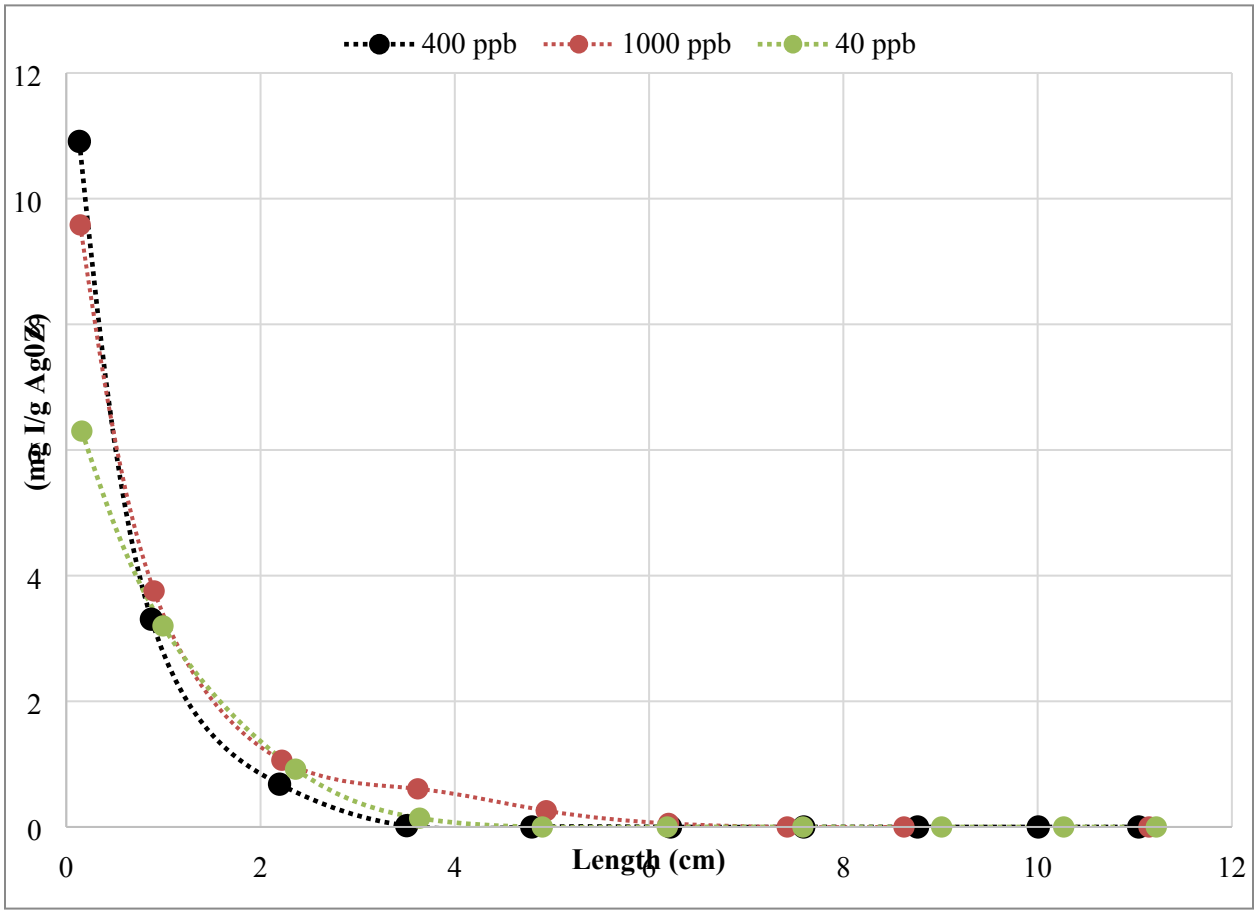

Figure 17. Iodine loading profile on Ag^0Z as a function of bed depth and CH_3I feed concentrations from 40 to 1,000 ppb CH_3I. (Test ID: 2015-VOG2, 40 ppb CH_3I; 2017-VOG-T5(4), 400 ppb CH_3I; 2017-VOG-T7(4), 1,000 ppb CH_3I).

The fractional recovery of iodine on the column increased slightly with increasing feed concentrations (from 33% at 40 ppb to 50% at 1,000 ppb CH_3I), which could support the original hypotheses that the sorbent may become less effective as the iodine feed concentration decreases. However, assuming feed system integrity, this would imply that a significant fraction of CH_3I was passing through the bed unreacted in all cases. In the case of the 1,000 ppb CH_3I fed gas and 50% recovery, this would imply that the average effluent concentration should be ~500 ppb. The tests conducted at a lower concentration clearly show that the sorbent is capable of adsorbing at the 400 ppb and even 40 ppb levels. Thus, increased iodine recovery at higher CH_3I concentrations is not reflective of a fundamental relationship between concentration and total iodine recovery. Further, the results also provide an indication that the loading and penetration is not a function of the iodine concentration and that the modest increase in iodine recovery does not fully explain the discrepancy between the amount of CH_3I fed and the amount of iodine retained on the bed

4.1 Potential Loss of Physisorbed Material

As noted in Section 3.3.1 at the completion of each test, samples were removed from the test bed by vacuum. The assumption is that all of the iodine captured during the test remains on the samples through vacuum removal and NAA analysis. Iodine that is physisorbed on the sorbent could be released upon vacuuming or other physical handling. A preliminary test was performed to assess the magnitude of

iodine that could be removed from the sorbent during vacuuming. Two identical systems were prepared. Silver mordenite (20 g) was placed into one bed for each test. CH_3I was generated using a blended gas cylinder and was passed through the bed at 600 ppb. Other experimental conditions were set to typical VOG test conditions, which are described in Section 3.1.3. At the conclusion of iodine exposure, one bed was removed by vacuum, and the second removed by pouring. These tests revealed that the iodine loading on the bed that was vacuumed was lower than iodine loading on the bed that was not vacuumed (0.0352 mg I/g versus 0.0187 mg I/g). However, the mass balance for these tests was very low (only 0.37% and 0.20% recovery, respectively). The results indicate that vacuuming could have a significant impact on the total iodine retained (by as much as 33%), but these results will require additional confirmation.

Additional testing is planned in which a single bed will be loaded. The loaded bed will first be poured out, mixed and sub-sampled, and then it will be returned to the column and removed a second time by vacuum. This approach will eliminate differences that could have occurred between the two independent test columns used in the initial test. In addition, an iodine trap should be placed in the vacuum line to recover physisorbed iodine that is removed during the vacuum process.

If additional testing confirms that there is a significant amount of physisorbed iodine on the sorbent at VOG conditions that is easily removed by vacuuming, this is an important finding and will impact the post-loading treatment of the beds. This removable iodine could be concentrated because of the relative volume of gas streams involved in the loading process (~6 L/min × 7 days) and the vacuum process (~30 L/min × 10 min). For, example, a total of ~60,000 L will pass the bed in the loading phase but only 300 L in the vacuum phase. Assuming the feed gas was 600 ppb and all of it was captured on the bed initially, only 50% was chemisorbed under VOG conditions and the other 50% was physisorbed and subject to potential vacuum removal. Under these conditions, the vacuum effluent could contain ~60 ppm iodine on average.

5. RESULTS: COMPARISON OF AGAEROGEL AND AG^{0}Z PERFORMANCE

The major aim of this testing was to compare the performance of both AgAerogel and Ag^{0}Z as penetrating iodine sorbents in a VOG iodine abatement system. These sorbents have different iodine-loading behavior in thin beds at DOG conditions. First, total iodine loading capacity of these sorbents in prototypical DOG streams is ~100 mg I/g sorbent for Ag^{0}Z and >250 mg I/g sorbent for AgAerogel. These capacities are dependent on the total silver content of the sorbent. Second, AgAerogel does not have measurable capacity for water, and Ag^{0}Z has a water loading capacity of ~10 mg H_2O/g sorbent. Third, the resistance of AgAerogel to corrosive components such as NO_x gases appears to be higher than that of Ag^{0}Z (Bruffey et al. 2015b). Fourth, the mechanical stability of AgAerogel is lower than that of Ag^{0}Z. Ag^{0}Z, which is supplied in an engineered form, does not appear to degrade even when held at elevated temperatures for months. AgAerogel is friable, and material fines are generated even in the pouring of material into the column. The bulk density of AgAerogel increases 15% over the course of a VOG test because of fines generation during exposure to the gas stream.

The tests performed that support this objective are listed in Table 4. There are five test conditions used for each sorbent, resulting in a total of 10 tests. I_2 was the sorbate for two test conditions at concentrations of 7 and 500 ppb. CH_3I was the sorbate for three test conditions at concentrations of 40, 400, and 1,000 ppb.

Table 4. Testing in support of comparison objective

Designation	Species	Concentration (ppb)	Mass balance (%)
Ag^0Z			
2016-VOG-002	I_2	7	84
2017-VOG-T4	I_2	500	100
2015-VOG2	CH_3I	40	34
2017-VOG-T5(4)	CH_3I	400	39
2017-VOG-T7(4)	CH_3I	1,000	50
AgAerogel			
2016-VOG-T4	I_2	7	165
2017 T4-Aerogel	I_2	500	67
2016-VOG-T3	CH_3I	40	50
2017 T5-Aerogel	CH_3I	400	114
2017 T7-Aerogel	CH_3I	1,000	80

5.1 Data on AgAerogel

Bruffey et al. (2016) presented data on the adsorption of CH_3I by AgAerogel in VOG conditions with a CH_3I concentration of 40 ppb, and that test is summarized in Section 2. The four additional tests completed using AgAerogel sorbent during FY 2017 substantially increased understanding of AgAerogel capture behavior in VOG streams.

5.1.1 Elemental Iodine Adsorption on AgAerogel

Figure 17 shows the I_2 loading of AgAerogel as a function of total iodine delivered. This can be also viewed as an initial iodine capture rate by accounting for the iodine delivery rate concentration or the flow rate of the feed gas and time on line to achieve that total amount of iodine delivered (i.e., taking the slope of the line through the origin). Iodine loading per milligram of I_2 delivered is linear for both concentrations examined, with a maximum loading of 63 mg I/g sorbent for the 500 ppb and 73 mg I/g sorbent at 7 ppb. Note this is not an iodine saturation value but only the maximum value achieved during the loading period. Further, the linear behavior may reflect that all of the Bed 1 loadings are far from saturation values. As stated previously, measured iodine loadings on the initial thin bed were found to have 10% variability. This variability means that the final loadings of both the 500 and 7 ppb tests are not distinguishable. In these tests, the sorbents were not loaded to saturation, and the effect of I_2 concentration on the saturation capacity of the sorbent is unknown.

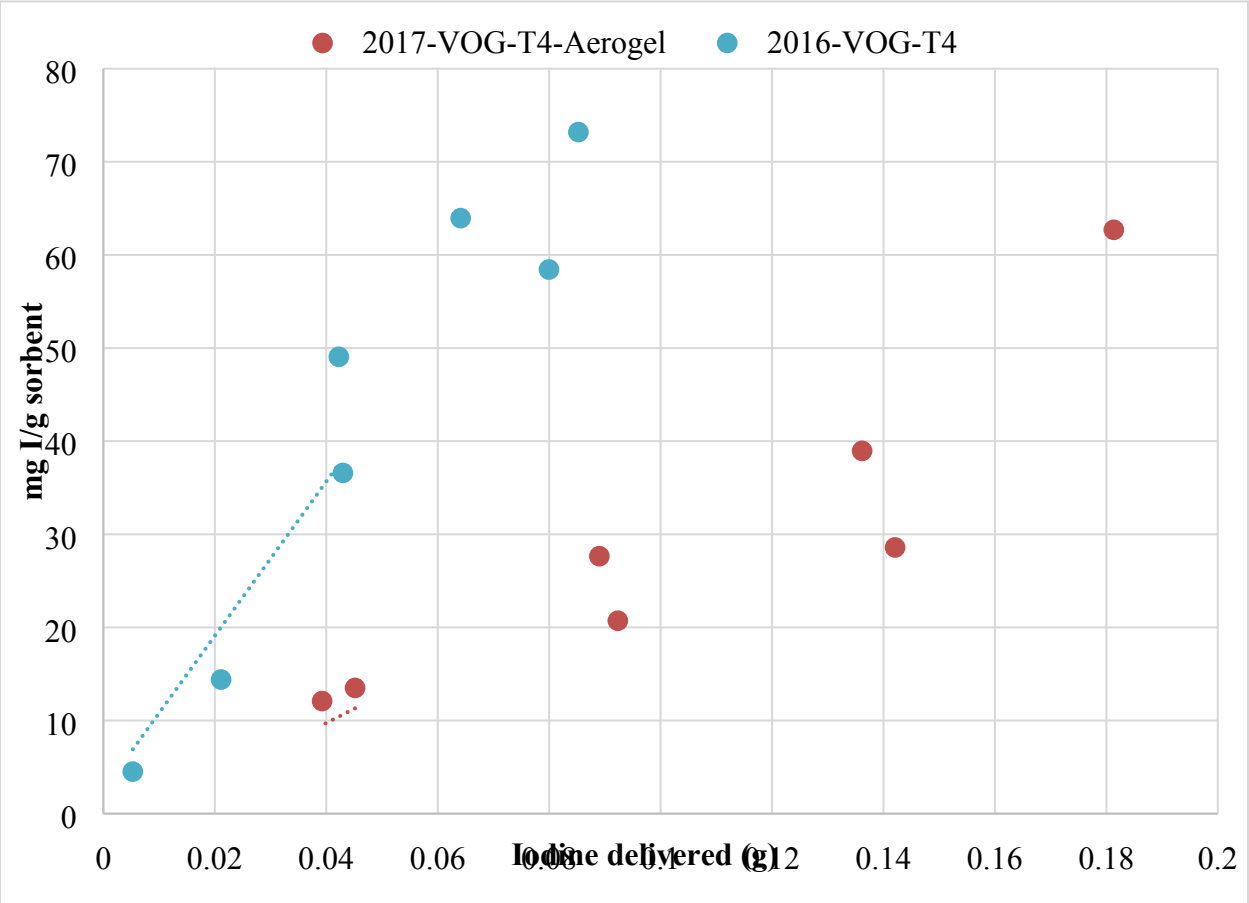

Figure 18. Iodine loading on AgAerogel as a function of I_2 delivered for two I_2 concentrations (Test ID: 2016-VOG-T4, 7 ppb I_2; 2017 T4-Aerogel, 500 ppb I_2).

The penetration of I_2 through a deep bed of AgAerogel is shown in Figure 19. I_2 loading in the bed decreases from the maximum loading of 63–73 mg I/g sorbent to below detection by 4.4 cm for both 500 and 7 ppb concentrations. One potential complication in comparing these two runs is that based on feed stream calculations, the total quantity of iodine fed to Test 2016-VOG-T4 at 7 ppb I_2; was about 50% of that fed to Test 2017 T4-Aerogel at 500 ppb I_2. The iodine material balance for Test 2016-VOG-T4 was 165% while for 2017 T4-Aerogel it was only 67%. This results in the 7 ppb I_2 data points displaying higher loadings than that of data points for 500 ppb I_2.

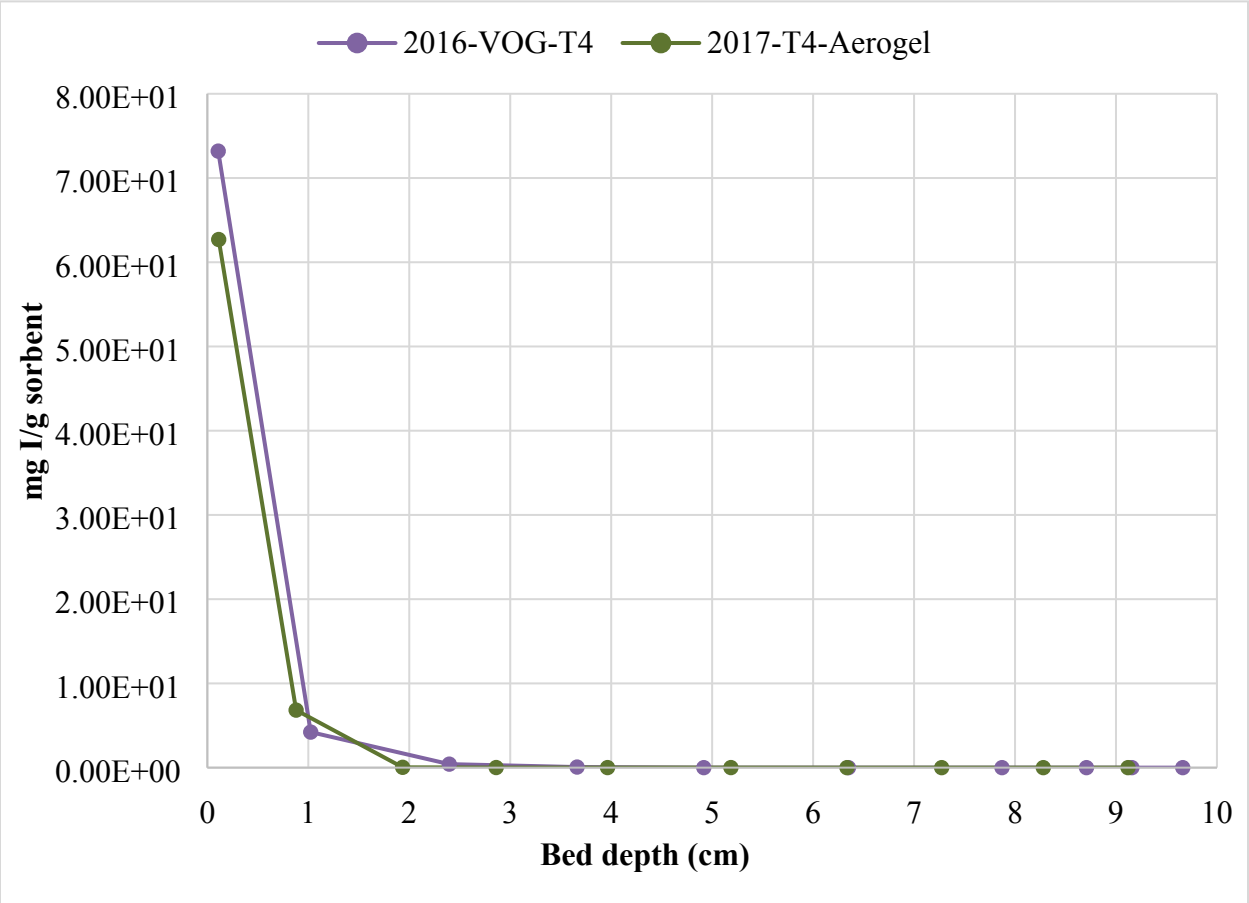

Figure 19. Iodine loading on AgAerogel as a function of bed depth and I_2 feed concentration (Test ID: 2016-VOG-T4, 7 ppb I_2; 2017 T4-Aerogel, 500 ppb I_2).

5.1.2 CH_3I Loading on AgAerogel

Figure 20 shows the iodine (CH_3I) loading of AgAerogel for Bed 1 as a function of total iodine delivered. CH_3I loading is linear at all three concentrations examined in this sorbent saturation range. The total iodine loadings for CH_3I are shown in Table 5. The maximum iodine loading for the 400 and 1,000 ppb tests are indistinguishable from each other but resolved from the maximum loading of the 40 ppb test assuming that the AgAerogel sorbent has a similar standard deviation for Bed 1 materials as does the Ag^0Z. Although the 40 ppb test had the most total iodine delivered of all three tests, its maximum loading was 21 mg I/g sorbent, only 70% of the maximum iodine loading observed for the 400 ppb test. The iodine loading for CH_3I adsorption at 40 ppb is measurably lower than that of the 400 and 1,000 ppb tests for the same amount of CH_3I delivered to the system. It was observed that the maximum total loadings for CH_3I were less than 50% of those observed for I_2 adsorption by AgAerogel.

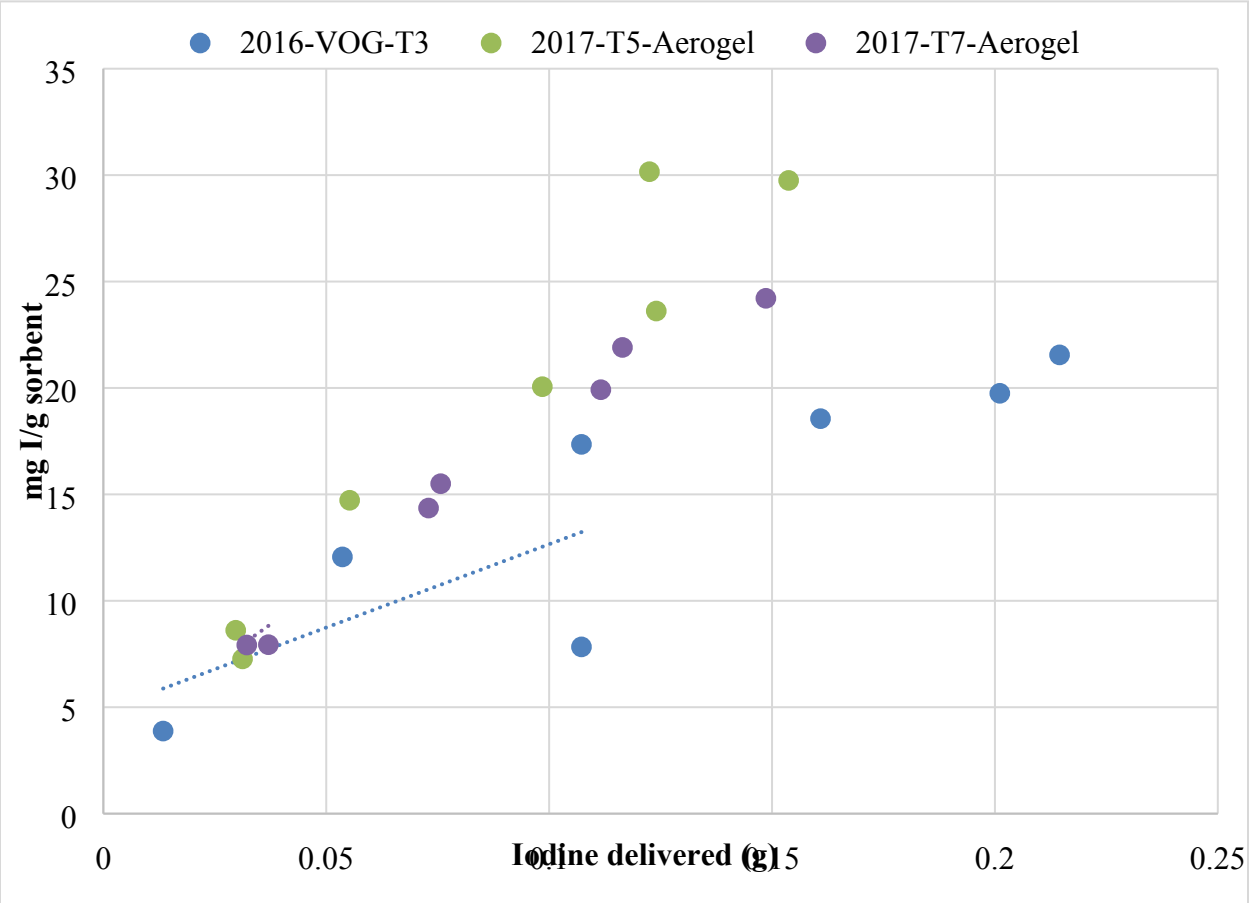

Figure 20. Bed 1 iodine loading on AgAerogel as a function of iodine delivered for three CH_3I concentrations (Test ID: 2016-VOG-T3, 40 ppb CH_3I; 2017 T5-Aerogel, 400 ppb CH_3I; 2017 T7-Aerogel, 1,000 ppb CH_3I).

Table 5. Maximum Bed 1 iodine loading on AgAerogel for three CH_3I concentrations

Test ID	CH_3I concentration (ppb)	Maximum iodine loading (mg I/g sorbent)
2016-VOG-T3	40	21
2017 T5-Aerogel	400	30
2017 T7-Aerogel	1,000	24

The penetration of CH_3I through the AgAerogel sorbent bed is shown in Figure 21. Although the sorbent loading decreases to <5 mg I/g sorbent at 1.5 to 1.8 cm, the curves show a long tail that is a result of the beds containing measurable iodine to ~5.5 cm of the bed. The first 2 cm of each bed contains 77%, 92.8% and 90.1% of the total iodine retained on the beds for the 40, 400 and 1,000 ppb CH_3I feed conditions respectively.

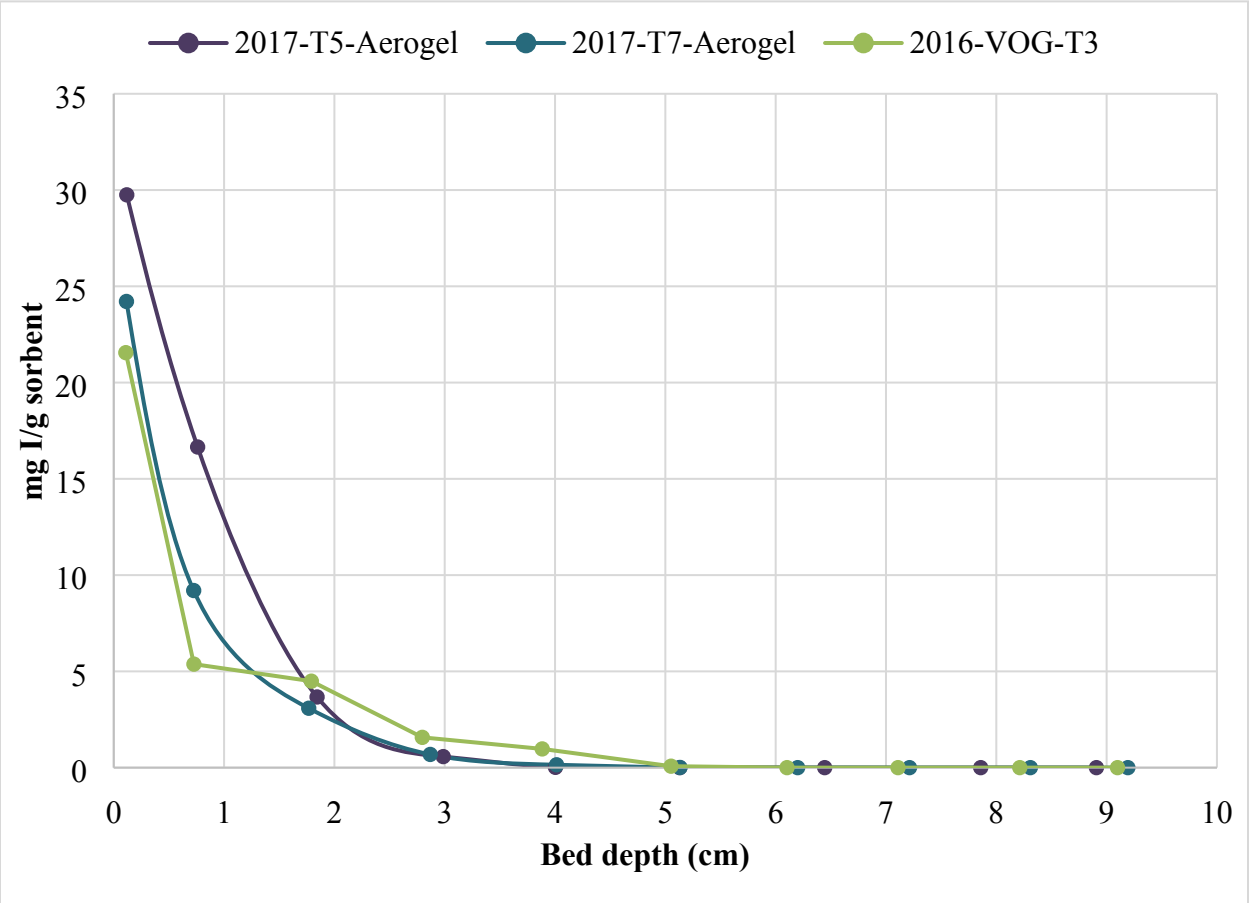

Figure 21. Iodine loading profile on AgAerogel as a function of bed depth and CH_3I feed concentration (Test ID: 2016-VOG-T3, 40 ppb CH_3I; 2017 T5-Aerogel, 400 ppb CH_3I; 2017 T5-Aerogel, 1,000 ppb CH_3I).

5.1.3 Comparison of I_2 and CH_3I Adsorption on AgAerogel

Figure 22 shows the Bed 1 iodine loading of AgAerogel as a function of total iodine delivered as either I_2 or CH_3I over a range of feed concentrations. Loading with I_2 at either 7 ppb or 500 ppb showed a higher concentration of iodine on the Bed 1 sorbent for all amounts of iodine delivered than for comparable amounts of CH_3I delivered. In addition, the maximum iodine loading was higher for I_2 loading than for the CH_3I feed gas tests.

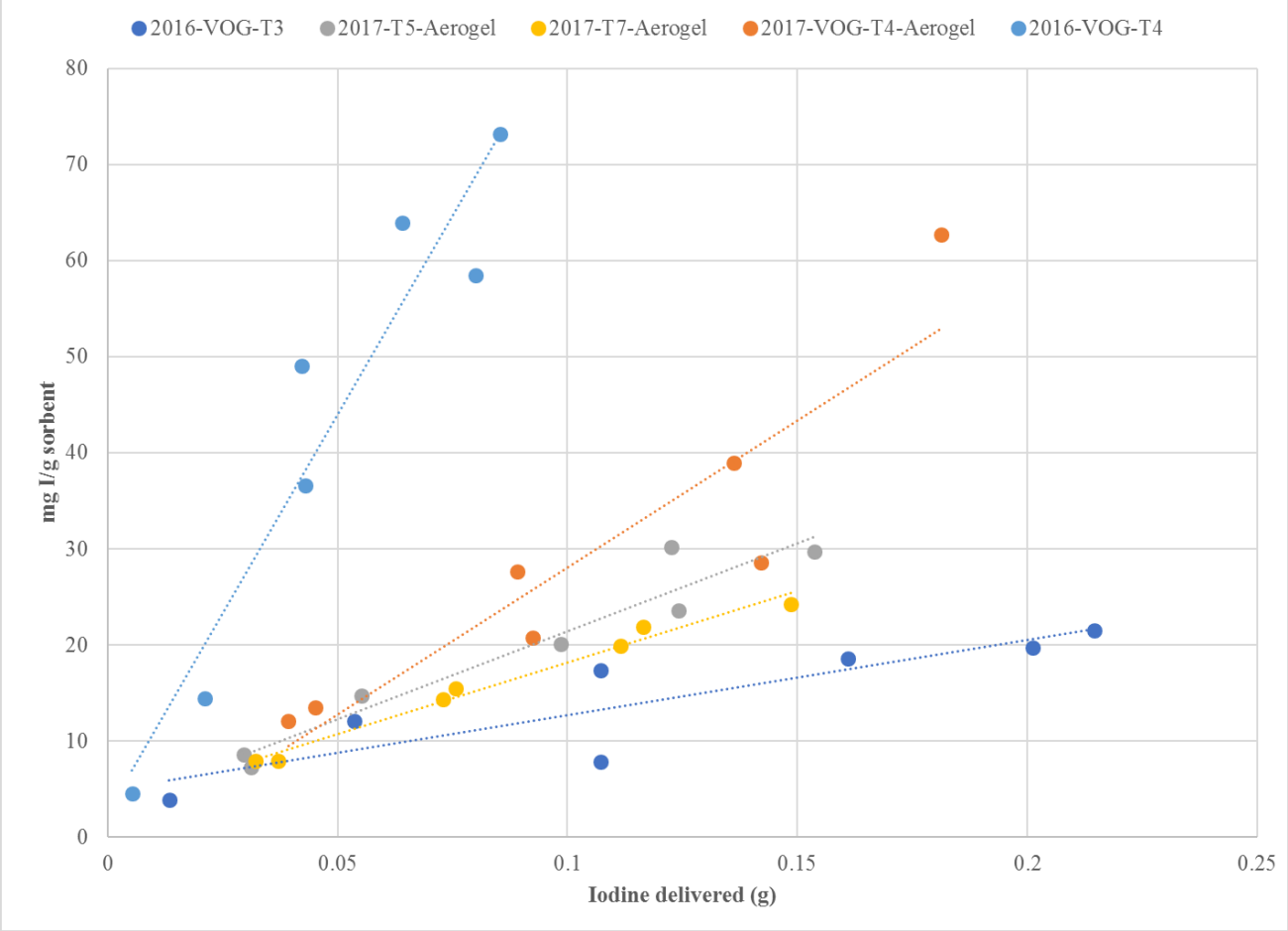

Figure 22. Bed 1 iodine loading on AgAerogel as a function of iodine delivered for a range of I_2 or CH_3I concentrations. (Test ID: 2016-VOG-T3, 40 ppb CH_3I; 2017 T5-Aerogel, 400 ppb CH_3I; 2017 T5-Aerogel, 1,000 ppb CH_3I; 2016-VOG-T4, 7 ppb I_2; 2017 T4-Aerogel, 500 ppb I_2).

A comparison of the iodine loading profile for both I_2 and CH_3I on an AgAerogel bed is shown in Figure 23. I_2 is observed to penetrate ~35% less into the sorbent bed than CH_3I does. Both sorbents have iodine loadings below detection at 6 cm. A summary of the completed tests to support the comparison are shown in Table 6.

The data on I_2 and CH_3I adsorption show that in the first thin layer of the sorbent bed, there is 2× more iodine adsorbed as I_2. However, as the iodine progresses through the bed, the data sets are not resolvable in the range from 1 to 2 cm. The bulk of the iodine removal for both species is occurring within the first 1.5–2.0 cm, with 85%–99.8% of the iodine captured in the first 2 cm from I_2 gas streams and 77%–92.8% captured from CH_3I streams in first 2 cm.

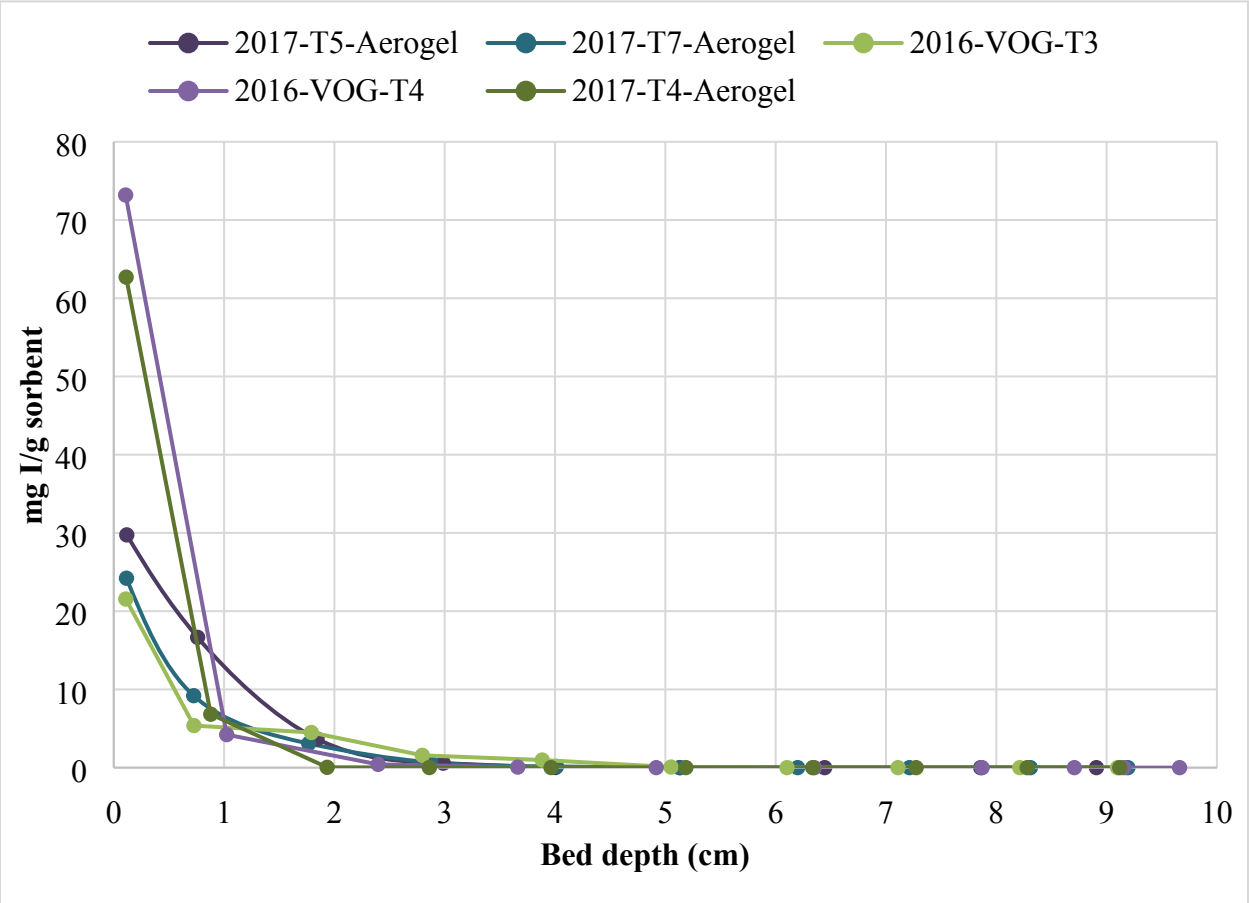

Figure 23. Iodine loading profile on AgAerogel as a function of bed depth and iodine feed concentrations from 40 to 1,000 ppb CH_3I and 7 and 500 ppb I_2. (Test ID: 2016-VOG-T3, 40 ppb CH_3I; 2017 T5-Aerogel, 400 ppb CH_3I; 2017 T7-Aerogel, 1,000 ppb CH_3I; 2016-VOG-T4, 7 ppb I_2; 2017 T4-Aerogel, 500 ppb I_2).

Table 6. Summary of tests completed in support of Ag^0Z and AgAerogel comparison objective

Designation	Species	Concentration (ppb)	Mass balance (%)	Bed 1 max loading (mg I/gm sorbent)	Adsorbed iodine retained in first 2 cm (%)
Ag^0Z					
2016-VOG-002	I_2	7	84	11	96.4
2017-VOG-T4	I_2	500	100	17	85.8
2015-VOG2	CH_3I	40	34	6	84.4
2017-VOG-T5(4)	CH_3I	400	39	9	91.9
2017-VOG-T7(4)	CH_3I	1,000	50	8	77.9
AgAerogel					
2016-VOG-T4	I_2	7	165	73	98.0
2017 T4-Aerogel	I_2	500	67	63	99.8
2016-VOG-T3	CH_3I	40	50	21	77.0
2017 T5-Aerogel	CH_3I	400	114	30	92.8
2017 T7-Aerogel	CH_3I	1,000	80	24	90.1

5.2 Iodine Loading on Ag^0Z

To provide a basis for comparison of Ag^0Z and AgAerogel, testing investigating I_2 adsorption by Ag^0Z is presented here, and data investigating CH_3I adsorption by Ag^0Z is presented in Section 4. The completed tests are shown in Table 7.

Table 7. Summary of tests completed on iodine adsorption on Ag^0Z

Test designation	Species	Concentration (ppb)
2016-VOG-002	I_2	7
2017-VOG-T4	I_2	500
2015-VOG2	CH_3I	40
2017-VOG-T5(4)	CH_3I	400
2017-VOG-T7(4)	CH_3I	1,000

5.2.1 I_2 Loading on Ag^0Z

As reported in Section 2, I_2 adsorption by Ag^0Z at an I_2 concentration of 7 ppb appeared to indicate some potential aging effects (2016-VOG-002). A second test investigating I_2 adsorption by Ag^0Z was performed at an I_2 concentration of 500 ppb (2017-VOG-T4). Because of the much shorter duration of this test (1 week versus 16 weeks), periodic sampling of the initial thin bed was not performed during for this test.

The maximum iodine loadings found for I_2 testing were 11 and 17 mg I/g sorbent for the 7 ppb and 500 ppb I_2 concentrations respectively. As shown in Figure 24, the iodine loading profile of I_2 within the bed is slightly different for the two concentrations examined, with the 7 ppb test showing measurable iodine loadings on Ag^0Z to 2.8 cm, and the 500 ppb test showing measurable iodine to 5.5 cm. The first

2 cm of each bed contains 96.4% and 85.8% of the total iodine retained on the beds for the 7 and 500 ppb I_2 feed conditions respectively. One potential complication in comparing these two runs is that the total quantity of iodine fed to Test 2016-VOG-002 at 7 ppb I_2 was about 50% of that fed to Test 2017-VOG-T4 at 500 ppb I_2 based on feed stream calculations. The iodine material balances for both runs were 84.3%–99.6%. This increase in total iodine captured is reflected in the 500 ppb I_2 curve being higher than the curve for 7 ppb I_2. Although the adsorption behavior at these two concentrations does display some differences, these observations should be confirmed by additional testing.

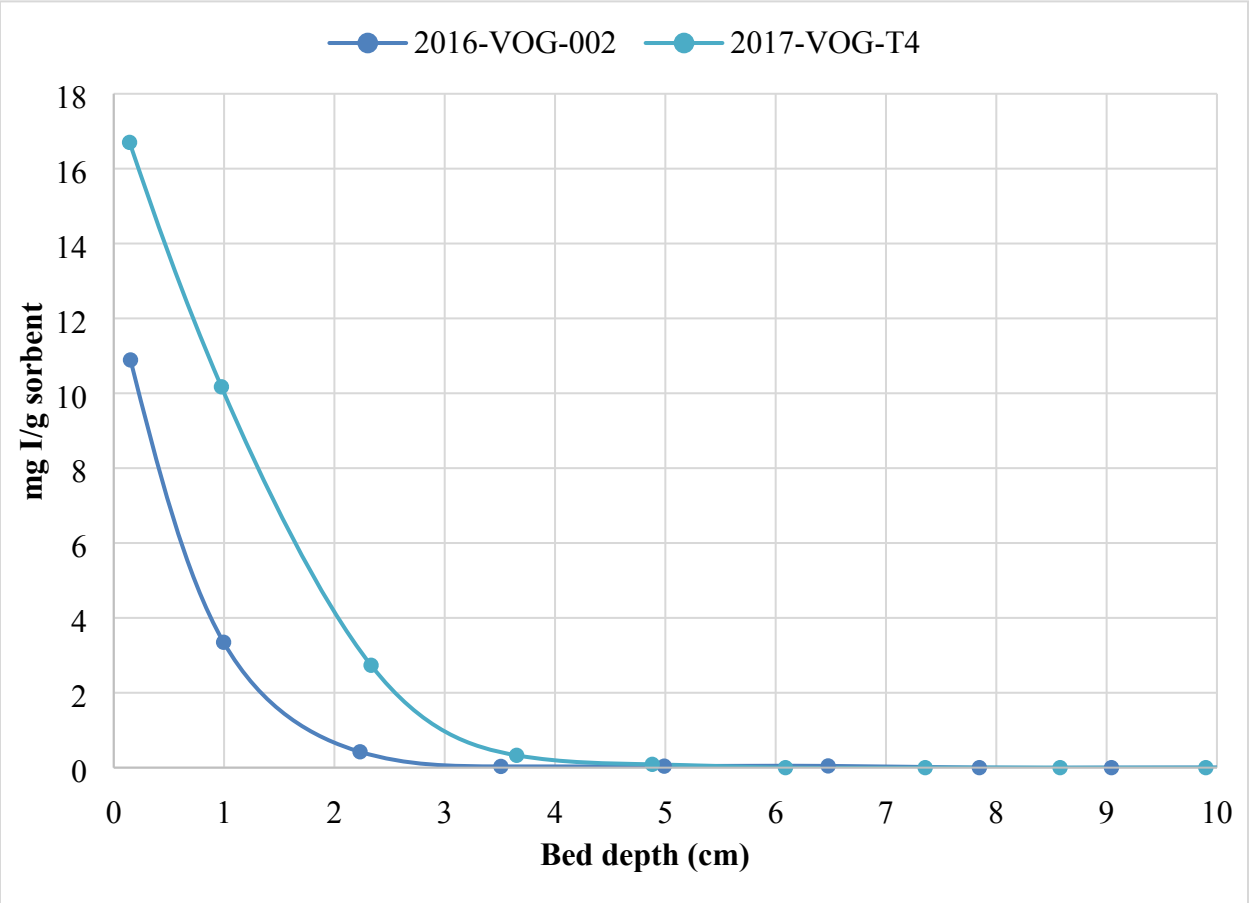

Figure 24. Iodine loading profile on Ag^0Z as a function of bed depth and iodine feed concentrations from 40 to 1,000 ppb CH_3I and 7 and 500 ppb I_2 (Test ID: 2016-VOG-002, 7 ppb I_2; 2017-VOG-T4, 500 ppb I_2).

5.2.2 CH_3I Loading on Ag^0Z

Results from CH_3I loading on Ag^0Z are provided in Section 4.

5.2.3 Comparison of I_2 and CH_3I Adsorption by Ag^0Z

Figure 25 compares the iodine loading on Ag^0Z as a function of the total amount of iodine delivered as either I_2 or CH_3I. For the same amount of iodine delivered the sorbent loadings are higher for 7 ppb I_2 than for even the 1,000 ppb CH_3I. Figure 26 shows the penetration of both I_2 and CH_3I into an Ag^0Z bed. It was observed that, with the exception of the 500 ppb I_2 test, each test displayed similar penetration curves. The list of penetration depths as a function of sorbate and concentration are shown in Table 8.

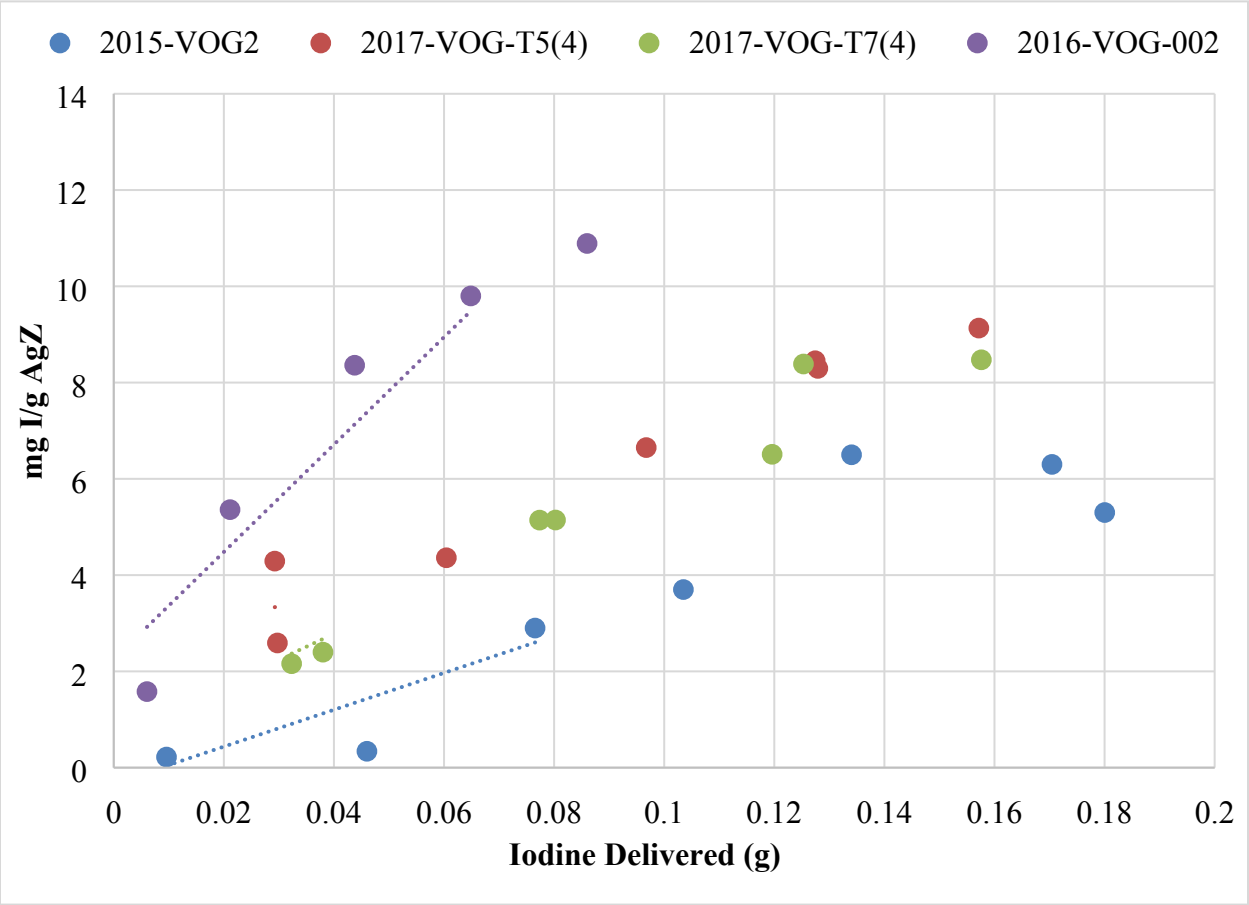

Figure 25. Bed 1 iodine loading on Ag^0Z as a function of iodine delivered for a range of I_2 or CH_3I concentrations (Test ID: 2015-VOG2, 40 ppb CH_3I; 2017-VOG-T5(4), 400 ppb CH_3I; 2017-VOG-T7(4), 1,000 ppb CH_3I; 2016-VOG-002, 7 ppb I_2).

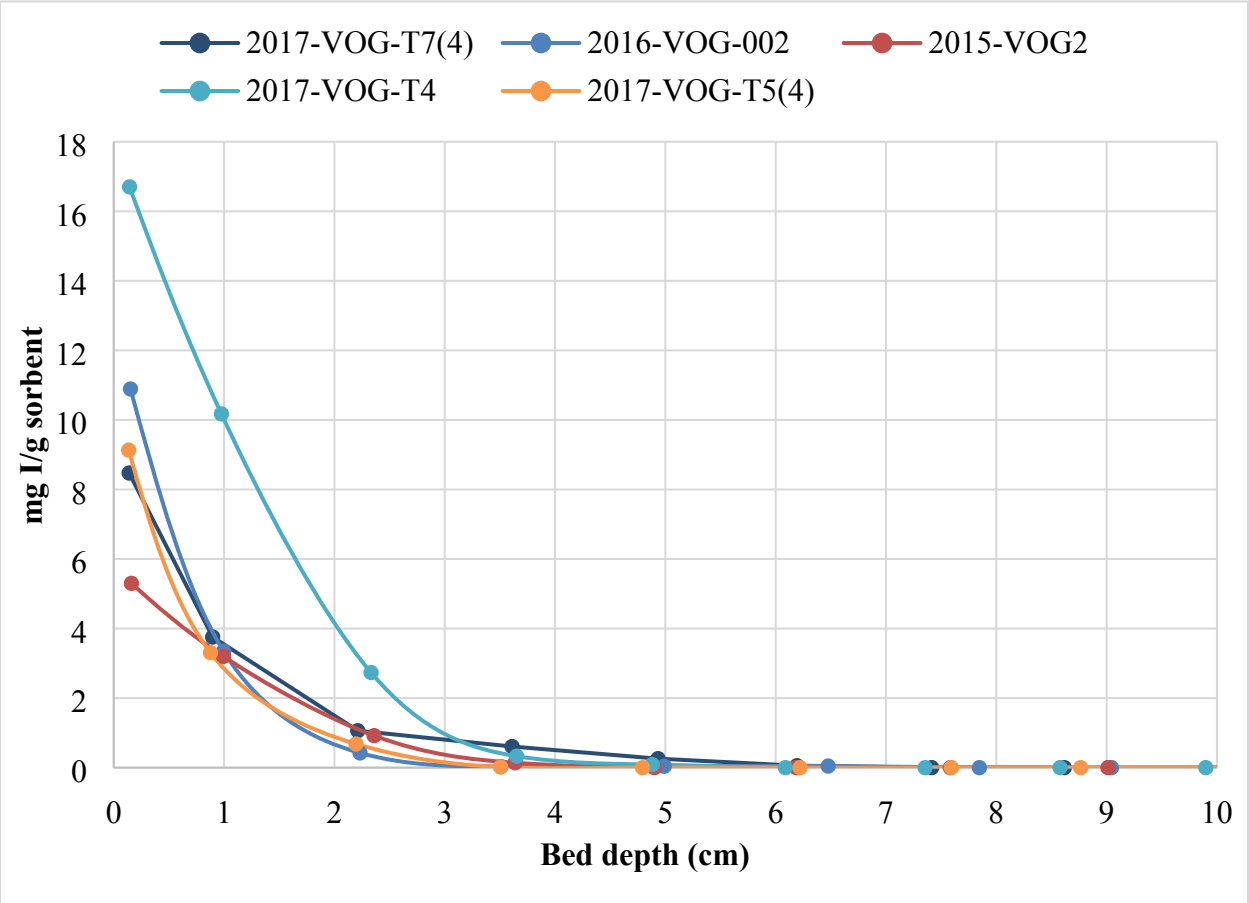

Figure 26. Iodine loading profile on Ag^0Z for I_2 and CH_3I feed concentrations (Test ID: 2015-VOG2, 40 ppb CH_3I; 2017-VOG-T5(4), 400 ppb CH_3I; 2017-VOG-T7(4), 1,000 ppb CH_3I; 2016-VOG-002, 7 ppb I_2; 2017-VOG-T4, 500 ppb I_2).

Table 8. Penetration depth of CH_3I and I_2 into an Ag^0Z sorbent bed

Test	Sorbate	Concentration (ppb)	Maximum iodine loading (mg/g sorbent)	Penetration depth (cm)	Adsorbed iodine captured in initial 2 cm (%)
2016-VOG-002	I_2	7	11	2.8	96.4
2017-VOG-T4	I_2	500	17	5.5	85.8
2015-VOG2	CH_3I	40	6	4.2	84.4
2017-VOG-T5(4)	CH_3I	400	9	4.1	91.9
2017-VOG-T7(4)	CH_3I	1,000	8	6.8	77.9

5.3 Comparison of Iodine Adsorption by Ag^0Z and AgAerogel under VOG Conditions

5.3.1 Iodine Adsorption by Ag^0Z and AgAerogel

The loading of I_2 onto both Ag^0Z and AgAerogel as a function of the total iodine delivered is shown in Figure 27. It is observed that adsorption of 7 ppb I_2 by Ag^0Z occurs at a markedly lower loading than that of 7 ppb AgAerogel, and the maximum loading of Ag^0Z (11 mg I/g Ag^0Z) is 17% of the maximum loading for AgAerogel at 7 ppb I_2 (63 mg I/g AgAerogel).

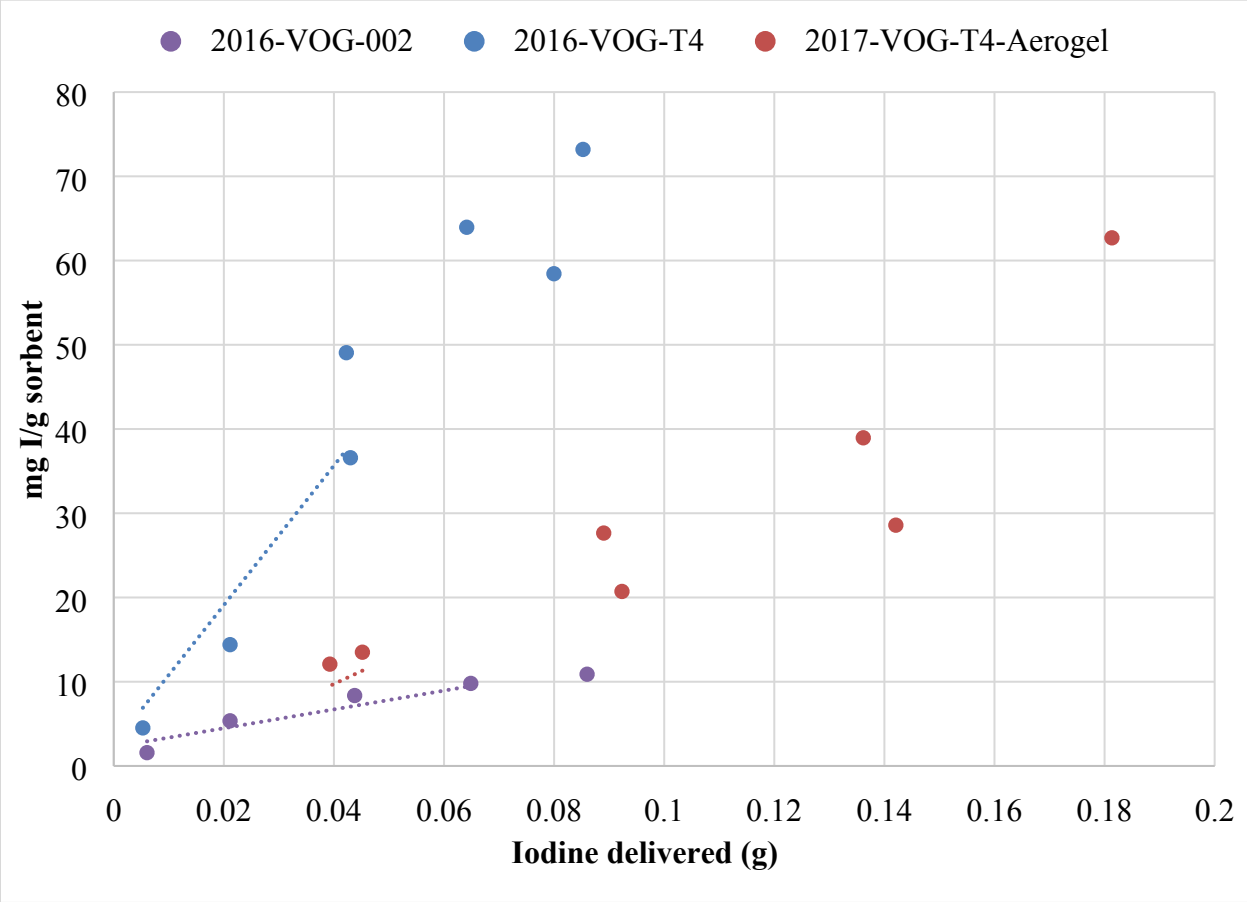

Figure 27. Bed 1 iodine loading on AgAerogel and Ag^0Z as a function of iodine delivered for a range of I_2 concentrations (Test ID: 2016-VOG-T4, 7 ppb I_2; 2017 T4-Aerogel, 500 ppb I_2; 2016-VOG-002, 7 ppb I_2).

The penetration of I_2 into both Ag^0Z and AgAerogel beds is shown in Figure 28, and the total penetration depths are reported in Table 9. There are two notable observations from the table. First, the maximum iodine loading appears to correspond to the total iodine loaded on the sorbent beds. Second, the penetration depth also corresponds to the amount of iodine loaded on the sorbent beds.

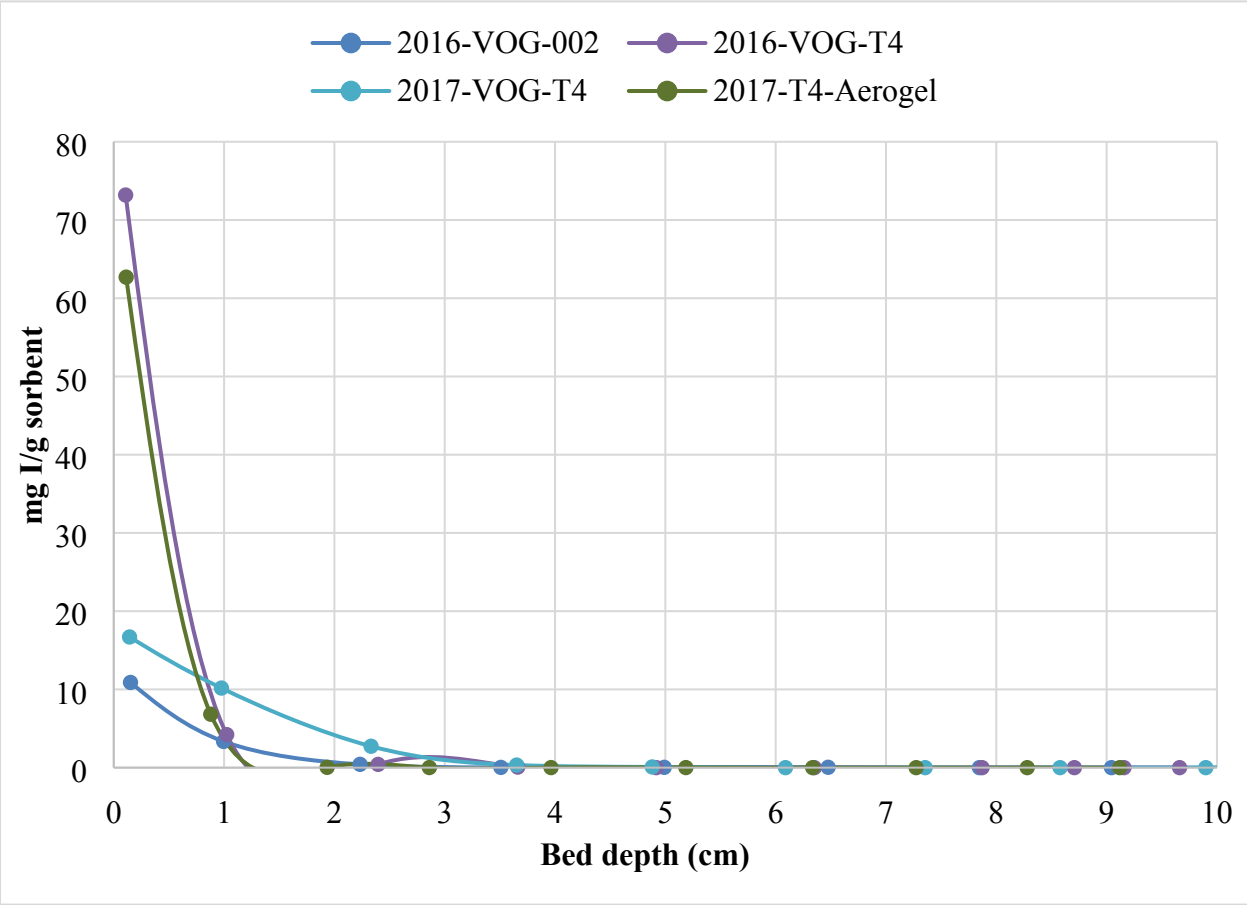

Figure 28. Iodine loading profile for I_2 adsorption by Ag^0Z and AgAerogel sorbent beds (Test ID: 2016-VOG-T4, 7 ppb I_2; 2017 T4-Aerogel, 500 ppb I_2; 2016-VOG-002, 7 ppb I_2; 2017-VOG-T4, 500 ppb I_2).

Table 9. Penetration depths for I_2 into Ag^0Z and AgAerogel sorbent beds

Test	Sorbent	Concentration (ppb)	Total iodine recovered (g)	Maximum iodine loading (mg/g sorbent)	Penetration Depth (cm)	Adsorbed iodine retained in first 2 cm (%)
2016-VOG-002	Ag^0Z	7	0.0725	11	2.8	93.7
2017-VOG-T4	Ag^0Z	500	0.1806	17	5.5	85.8
2016-VOG-T4	AgAerogel	7	0.1407	73	4.4	98
2017-VOG-T4-Aerogel	AgAerogel	500	0.1177	63	2.4	99.8

5.3.2 CH_3I Adsorption by Ag^0Z and AgAerogel

The iodine loading on Bed 1 as a function of the total CH_3I delivered to the test systems for both Ag^0Z and AgAerogel are shown in Figure 29. More iodine is captured in this segment by the AgAerogel than by the Ag^0Z for the same total amount of CH_3I fed at all CH_3I concentrations. The 400 ppb CH_3I and 1,000 ppb CH_3I feed concentrations that appeared to result is the highest iodine loading on Bed 1 as a function of the total CH_3I delivered, and the loading for 40 ppb on AgAerogel was greater than that of

1,000 ppb CH_3I onto Ag^0Z. The maximum iodine loadings of AgAerogel in each case are larger than the maximum iodine loadings on Ag^0Z observed at any of the three concentrations, with the maximum iodine loadings of Ag^0Z in Bed 1 ranging between 22% and 33% of those observed for AgAerogel (Table 10).

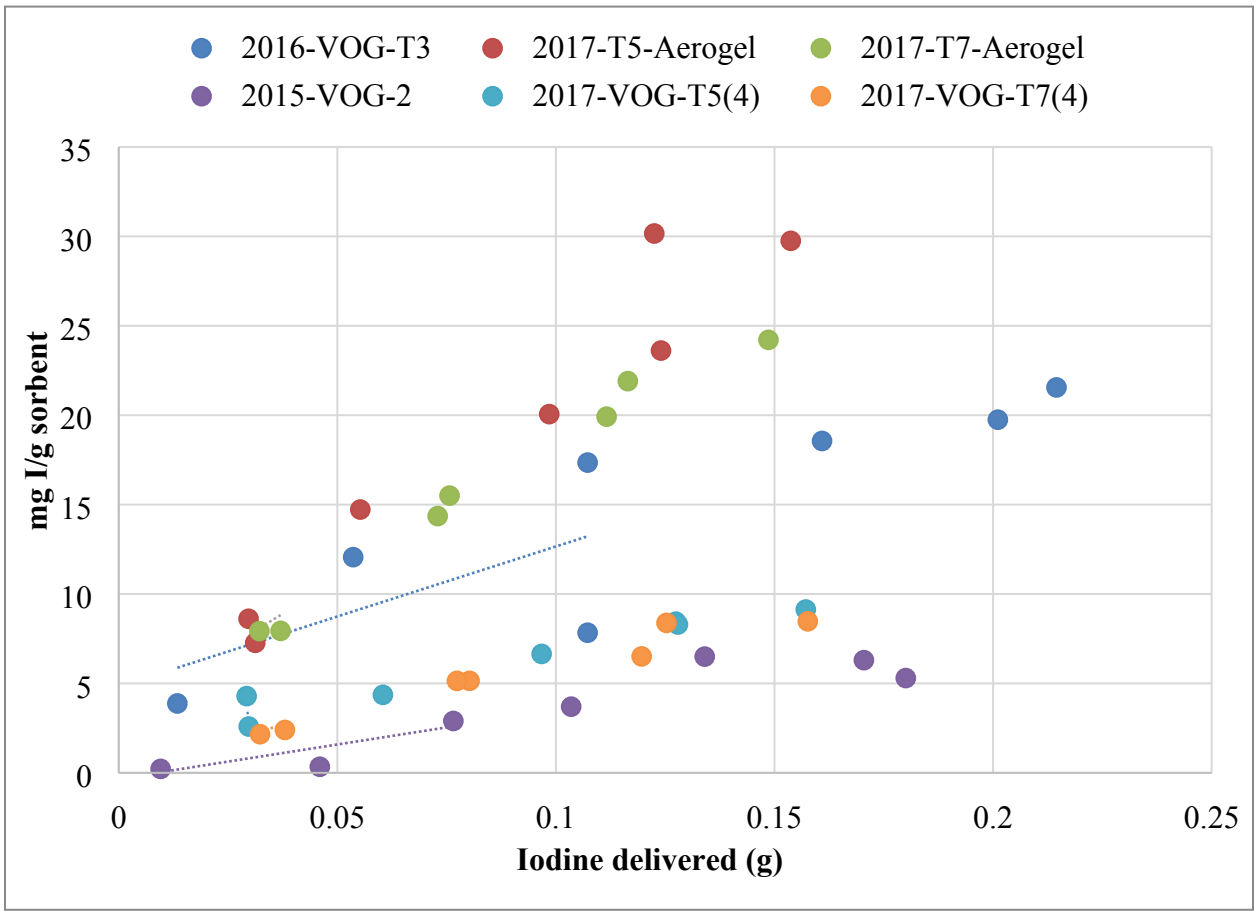

Figure 29. Bed 1 iodine loading on Ag^0Z and AgAerogel as a function of iodine delivered for a range of CH_3I concentrations. (Test ID for AgAerogel: 2016-VOG-T3, 40 ppb CH_3I; 2017 T5-Aerogel, 400 ppb CH_3I; 2017 T7-Aerogel, 1,000 ppb CH_3I; and for Ag^0Z: 2015-VOG2, 40 ppb CH_3I; 2017-VOG-T5(4), 400 ppb CH_3I; 2017-VOG-T7(4), 1,000 ppb CH_3I).

The penetration of CH_3I onto both Ag^0Z and AgAerogel is shown in Figure 30. The penetration depth for each test is also provided in Table 10. With the exception of the higher initial loadings in the first 0.3 cm of the AgAerogel beds, the penetration curves appear very similar for both sorbents. In five of the six tests, iodine loading on the sorbent bed was below detection by 6 cm. The exception was the 1,000 ppb CH_3I test on Ag^0Z, which showed penetration to 6.8 cm.

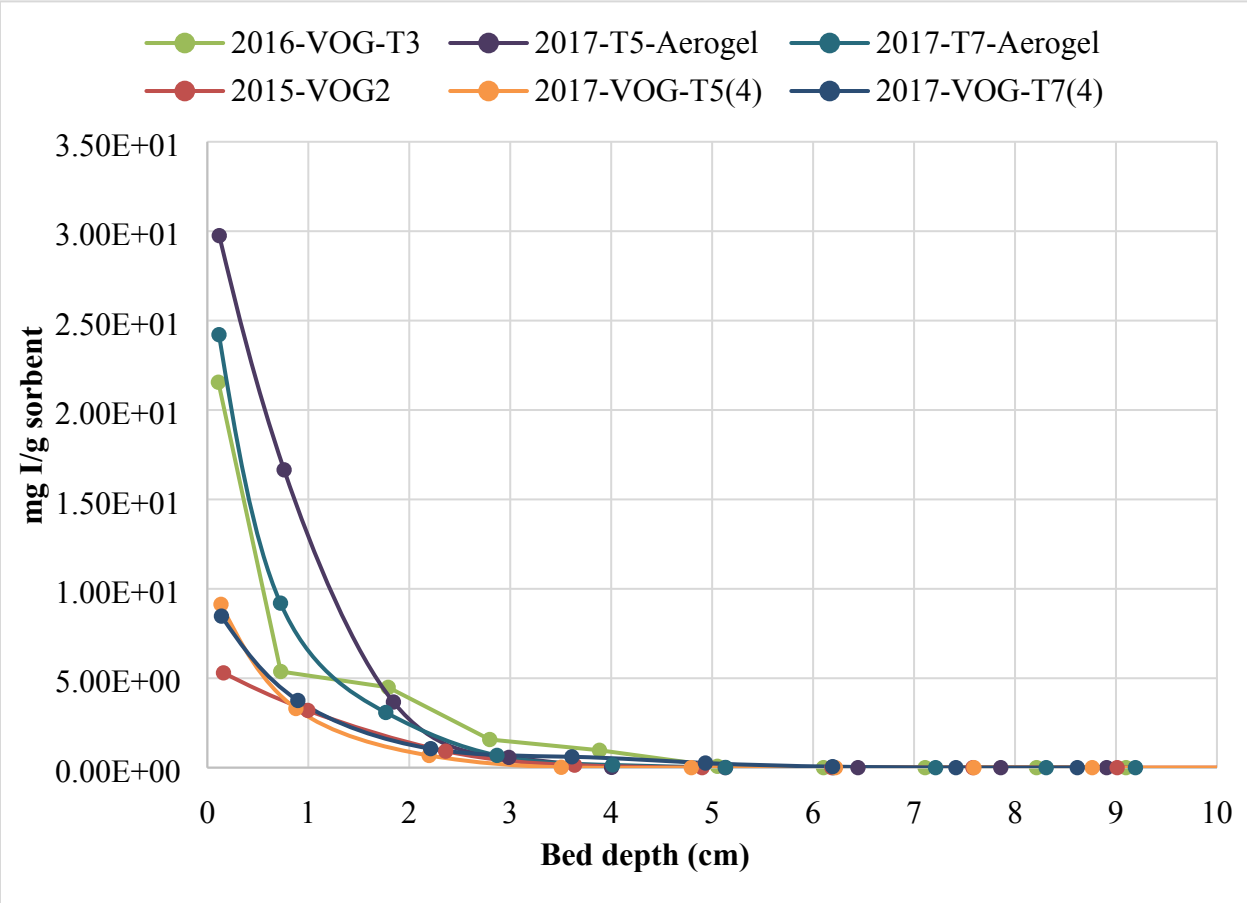

Figure 30. Iodine loading profile on for CH_3I on Ag^0Z and AgAerogel sorbent beds. (Test ID for AgAerogel: 2016-VOG-T3, 40 ppb CH_3I; 2017 T5-Aerogel, 400 ppb CH_3I; 2017 T7-Aerogel 1,000 ppb CH_3I; and for Ag^0Z: 2015-VOG2, 40 ppb CH_3I; 2017-VOG-T5(4), 400 ppb CH_3I; 2017-VOG-T7(4), 1,000 ppb CH_3I).

Table 10. Penetration depths for CH_3I into Ag^0Z and AgAerogel sorbent beds

Test	Sorbent	Concentration (ppb)	Maximum iodine loading (mg/g sorbent)	Penetration depth (cm)	Adsorbed iodine retained in first 2 cm (%)
2015-VOG2	Ag^0Z	40	6	4.2	84.4
2017-VOG-T5(4)	Ag^0Z	400	9	4.1	91.9
2017-VOG-T7(4)	Ag^0Z	1,000	8	6.8	77.9
2016-VOG-T3	AgAerogel	40	21	5.6	77
2017 T5-Aerogel	AgAerogel	400	30	4.4	92.8
2017 T7-Aerogel	AgAerogel	1,000	24	5.7	90.1

5.3.3 Impact of Sorbent Silver Content on Iodine Adsorption

To this point, all penetration results have been represented as the iodine loading for bed segments as a function of total bed depth. However, as discussed in Section 3, another way to represent the data is to

present the iodine loading as a function of sorbent silver content (Figure 12). This is a useful way to assess the performance for two sorbents in which the silver content varies significantly. Figure 31 presents the adsorption of 400 ppb CH_3I onto both Ag^0Z and AgAerogel in terms of iodine loaded on the sorbent as a function of bed depth, and Figure 32 presents the same data but normalizes the iodine loading to the amount of silver contained in the sorbent.

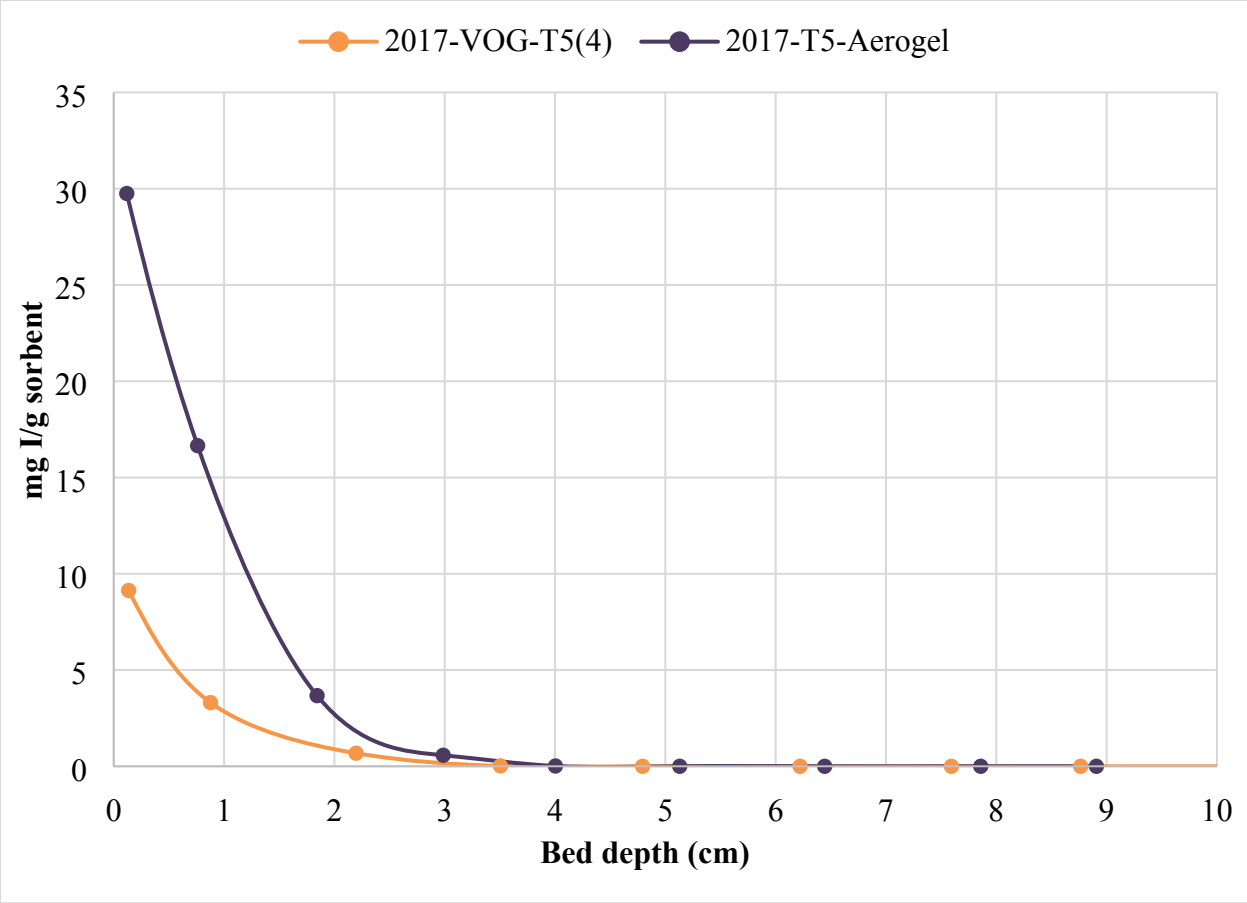

Figure 31. Adsorption of 400 ppb CH_3I on Ag^0Z and AgAerogel shown with iodine loading per mass sorbent (Test ID for AgAerogel: 2017 T5-Aerogel; and for Ag^0Z: 2017-VOG-T5(4)).

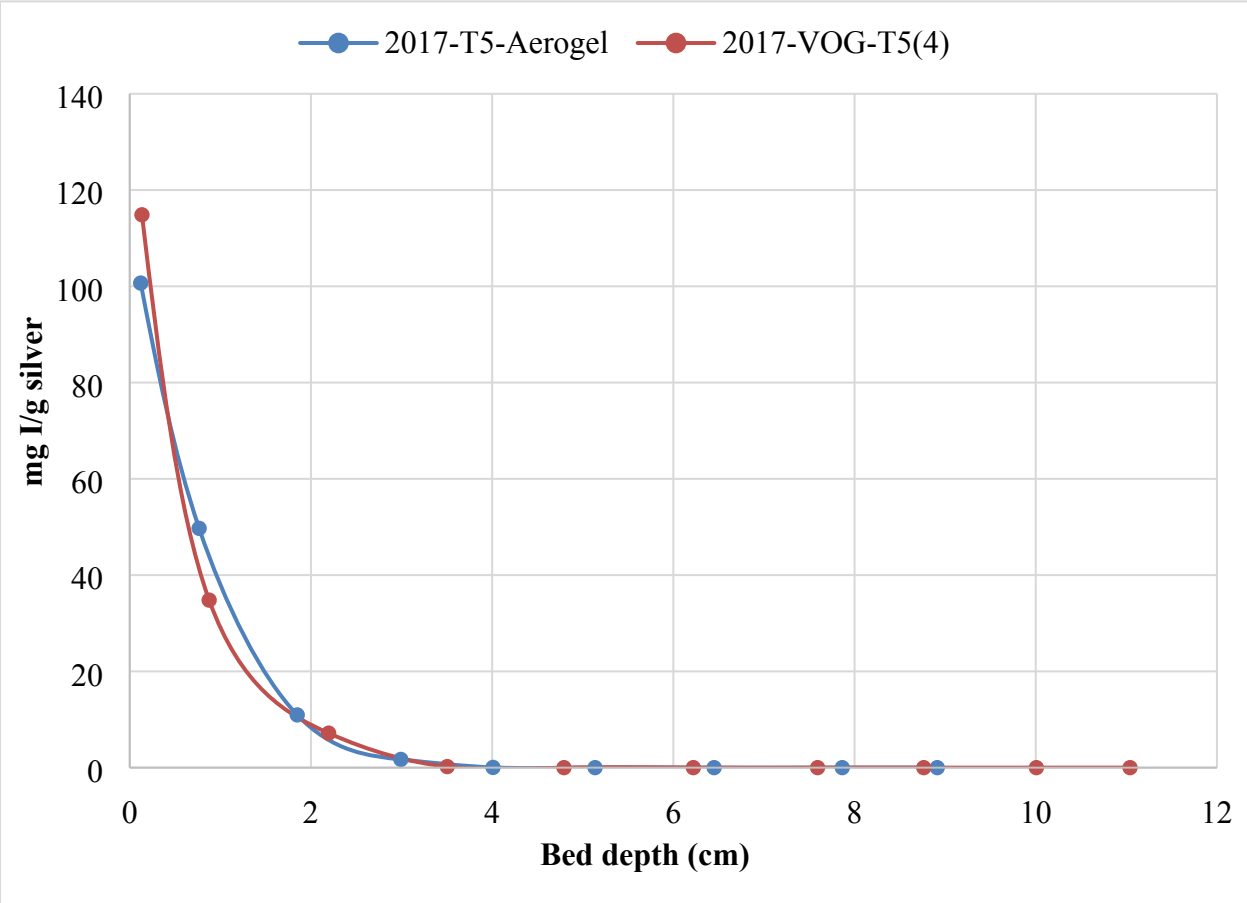

Figure 32. Adsorption of 400 ppb CH_3I on Ag^0Z and AgAerogel shown with iodine loading per mass silver contained in the sorbent (Test ID for AgAerogel: 2017 T5-Aerogel; and for Ag^0Z: 2017-VOG-T5(4)).

A comparison of these graphs readily shows that any differences in the total loading of the material are not a function of the sorbent matrix itself but rather the silver content of the sorbent. In the case of the two tests at 400 ppb CH_3I, the maximum observed loadings of each sorbent are equivalent once adjusted for silver content.

Figures 33 through 36 compare both I_2 and CH_3I adsorption on Ag^0Z and AgAerogel normalized for sorbent silver content for each selected concentration. In the case of CH_3I, concentrations examined, there are no measurable differences following normalization. The exception is 40 ppb CH_3I onto Ag^0Z and AgAerogel (Figure 33.) There appears to be a higher loading on the initial bed. The initial data point for the AgAerogel and the second and third data points exhibit an odd behavior that may reflect a sampling or analysis anomaly. In the case of I_2 adsorption onto Ag^0Z and AgAerogel, the penetration curves for the 7 ppb concentration do not overlay, with both different maximum sorbent loadings and penetration depths (see Figure 35). This can be attributed to the variation in the material balances between these two runs. In the case of Ag^0Z, the iodine material balance was 84%, whereas the AgAerogel had a material balance of 165%. Although both runs should have been fed the same amount of I_2, the AgAerogel appeared to recover more than was fed, which could account for the much higher apparent iodine loading on the initial bed. In the case of the 500 ppb I_2 testing (Figure 36) , the maximum sorbent loading is similar following normalization to sorbent silver content, but the total iodine loading and depth of I_2 penetration is different for the two sorbents. In the case of the AgAerogel, the iodine material balance is only 67%, whereas it is

99% for the Ag^0Z. This lower recovery of I_2 on the AgAerogel could account for the downward shift in the loading profile.

Figure 33. Adsorption of 40 ppb CH_3I onto Ag^0Z and AgAerogel, normalized to sorbent silver content (Test ID for AgAerogel: 2016-VOG-T3; and for Ag^0Z: 2015-VOG2).

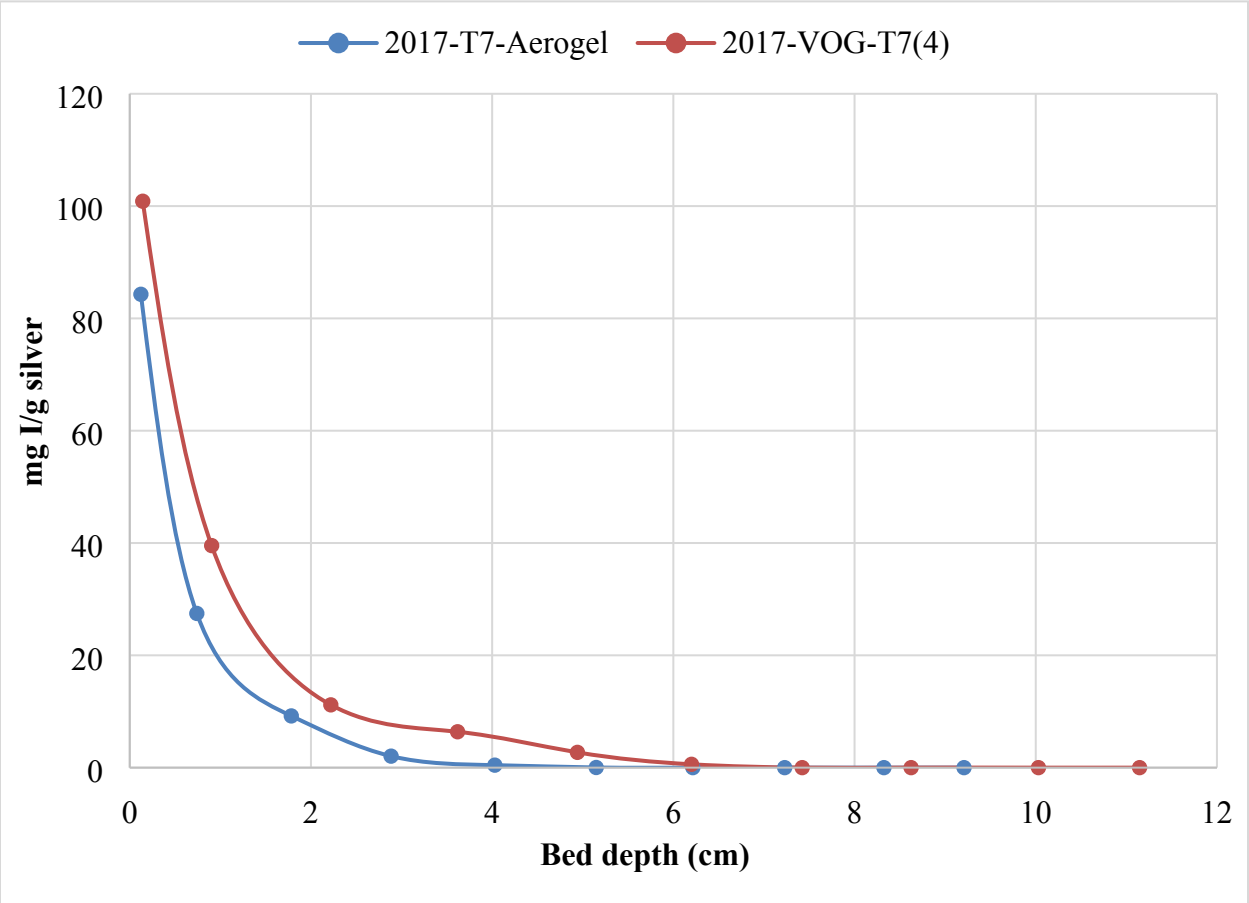

Figure 34. Adsorption of 1,000 ppb CH_3I onto Ag^0Z and AgAerogel, normalized to sorbent silver content (Test ID for AgAerogel: 2017 T7-Aerogel; and for Ag^0Z: 2017-VOG-T7(4)).

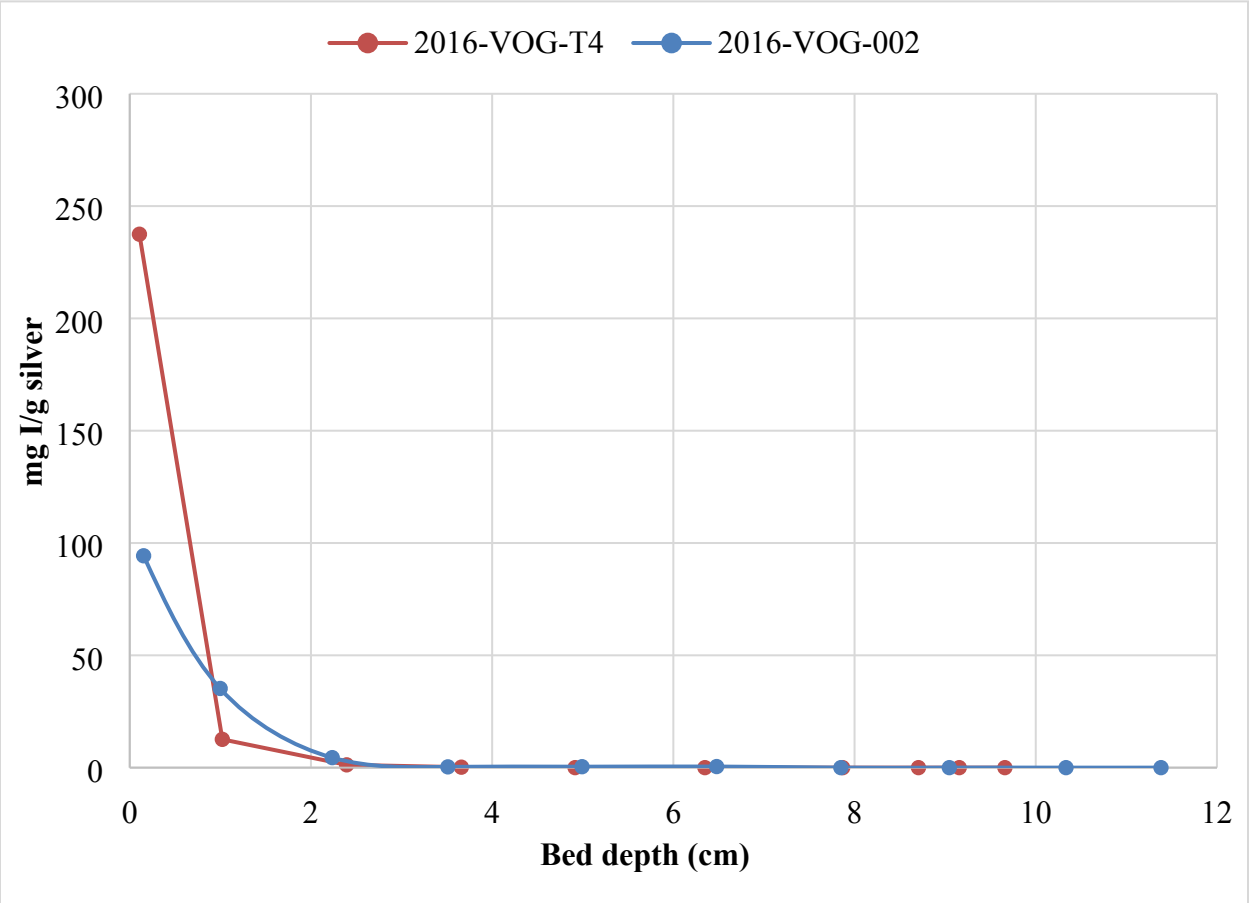

Figure 35. Adsorption of 7 ppb I_2 onto Ag^0Z and AgAerogel, normalized to sorbent silver content (Test ID for AgAerogel: 2016 VOG-T4; and for Ag^0Z: 2016-VOG-002).

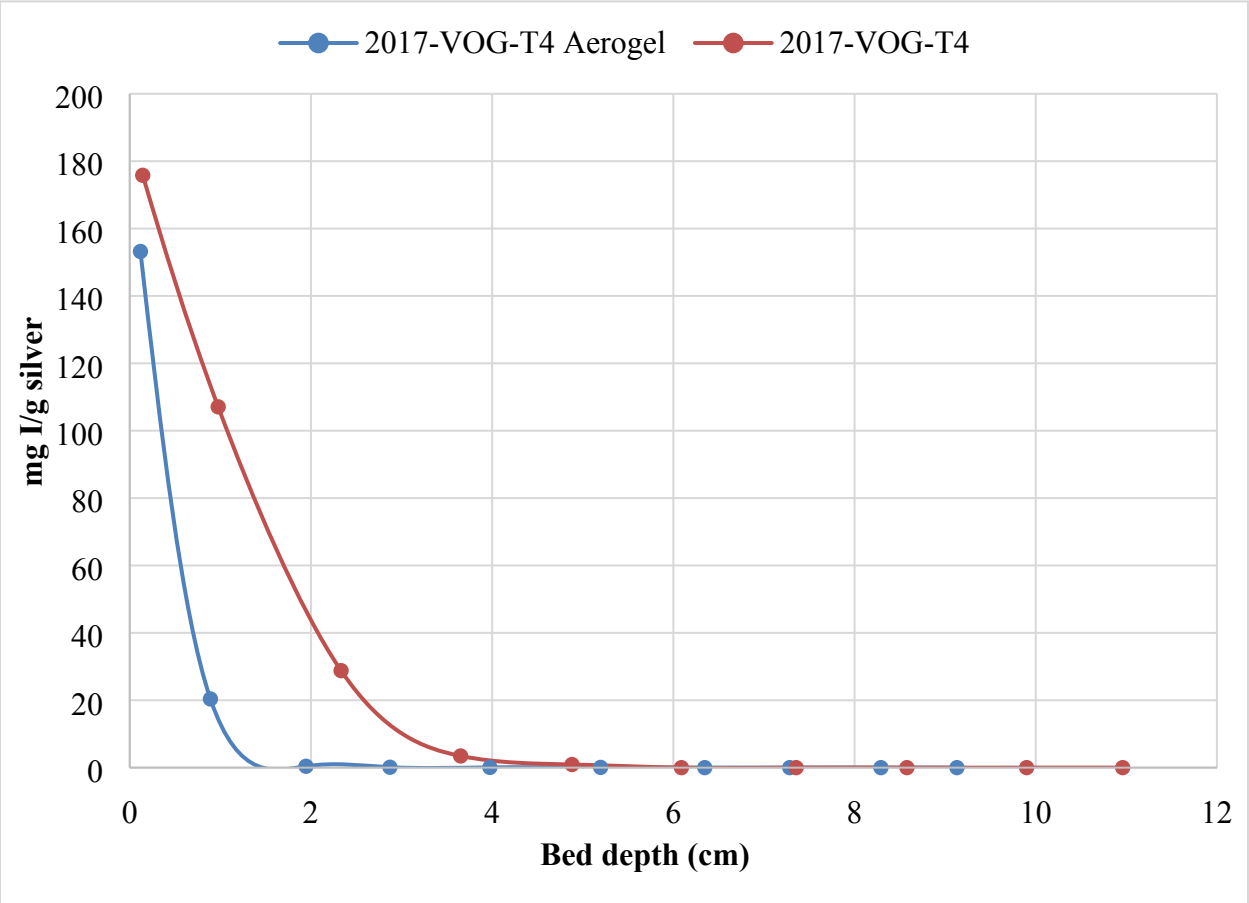

Figure 36. Adsorption of 500 ppb I_2 onto Ag^0Z and AgAerogel, normalized to sorbent silver content (Test ID for AgAerogel: 2017 T4-Aerogel; and for Ag^0Z: 2017-VOG-T4).

Figure 37 combines the data shown in Figures 32, 33, and 35 and recasts the data shown in Figure 29 by normalizing to the amount of silver contained in the sorbent. If the data is examined in this manner it appears that the amount of CH_3I captured per amount of silver in the sorbent from either 400 or 1,000 ppb feed streams is the same for both sorbents.

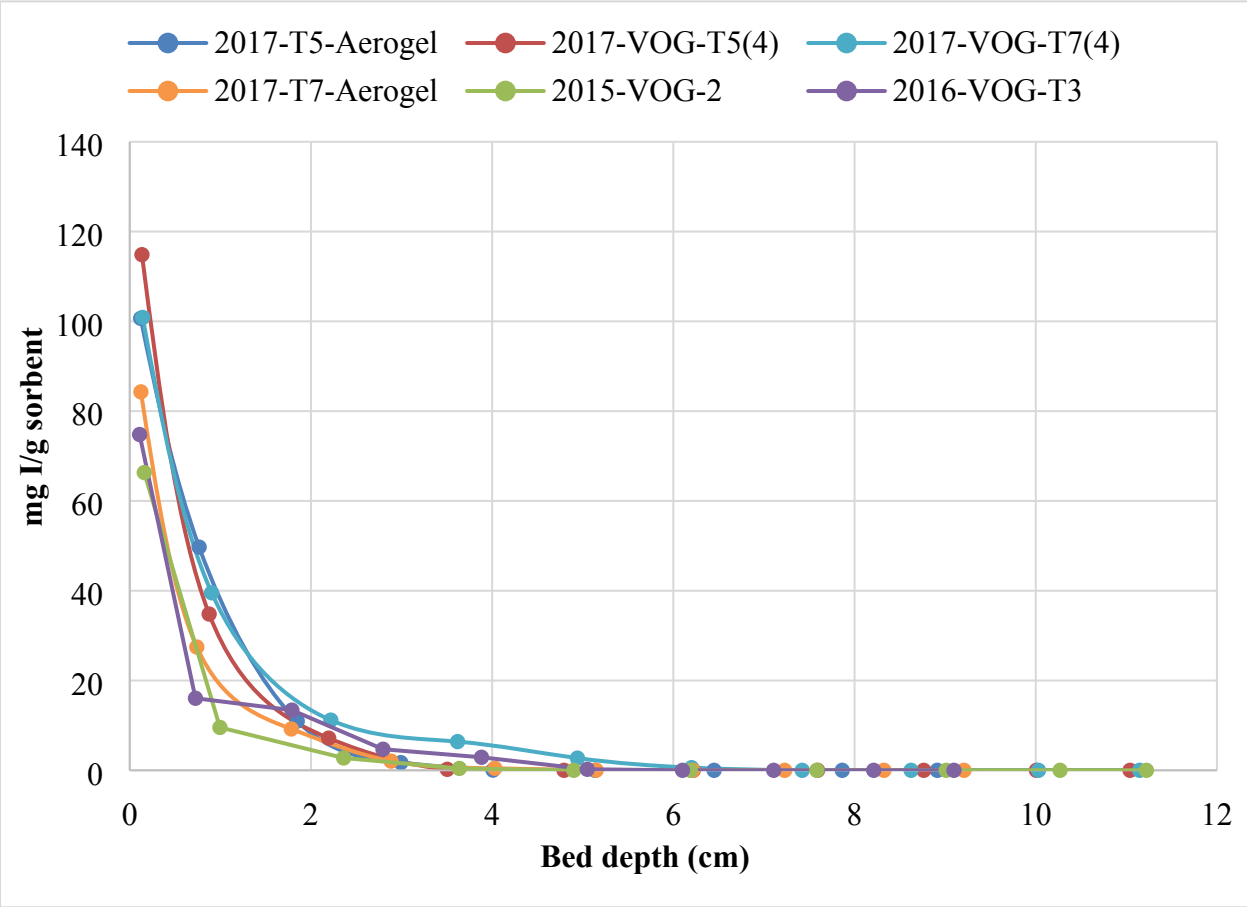

Figure 37. Comparison of CH_3I loading onto Ag^0Z and AgAerogel sorbent beds normalized for silver content of the sorbent. (Test ID for AgAerogel: 2016-VOG-T3, 40 ppb CH_3I; 2017 T5-Aerogel, 400 ppb CH_3I; 2017 T7-Aerogel, 1,000 ppb CH_3I; and for Ag^0Z: 2015-VOG2, 40 ppb CH_3I; 2017-VOG-T5(4), 400 ppb CH_3I; 2017-VOG-T7(4), 1,000 ppb CH_3I).

6. CONCLUSIONS

A test program was executed to characterize the adsorption of both I_2 and CH_3I onto Ag^0Z and AgAerogel silver-based sorbents. Each sorbent was exposed to either I_2 or CH_3I independently at one of several selected concentrations. Because of the length of time required to complete a single test, each test was only performed once, which is a recognized limitation on the data. Several replicate tests are in progress and will provide confirmation of the reported results.

The main aims of the testing described in this report were to (1) determine the effect of concentration on CH_3I adsorption by Ag^0Z and (2) compare the performance of Ag^0Z and AgAerogel sorbents in VOG conditions. Results presented in Section 4 show that the concentration of CH_3I within the range studied (40–1000 ppb CH_3I) does not affect either the maximum observed iodine loading for the sorbent or the penetration of CH_3I into the sorbent bed. Similar testing performed on the adsorption of CH_3I by AgAerogel at 40, 400, and 1,000 ppb CH_3I concentrations showed the same lack of dependence on CH_3I feed concentration.

Lack of dependence on feed concentration can provide a technical basis for the type of accelerated testing presented in this report. Early testing on the adsorption of iodine under VOG conditions was performed through extended duration testing using very low iodine feed concentrations (7–40 ppb). The tests were

required to run for 3–4 months to obtain an iodine adsorption profile through the sorbent deep bed. Testing at iodine concentrations of 400–1,000 ppb only required 1–3 weeks to complete. Because no concentration dependence is observed, there is potential for extrapolating results from accelerated testing at high concentrations to true VOG conditions. It is also possible that the depth of the mass transfer zone, an engineering parameter required for refinement of engineering designs based on this process, could be determined without test durations of 12–36 months, as was previously estimated based on very low concentration testing. At a minimum, the amount of data that can be obtained in a given time period is substantially increased if inlet iodine concentrations are in the range of 0.5–1 ppm.

An examination of the penetration depth for each test indicates that CH_3I does not necessarily penetrate the sorbent bed to a depth greater than that of I_2, which had been assumed to date. The penetrations for each test condition are summarized in Table 11. However, a visual examination of the curves reveals a tailing in the CH_3I. The percent of iodine retained in the first 2 cm of sorbent within the test system showed an inverse relationship to the penetration depth in the AgAerogel. This expected trend was not consistently observed for Ag^0Z.

Table 11. Penetration depths for all testing

Designation	Species	Concentration (ppb)	Penetration depth (cm)	Adsorbed iodine retained in first 2 cm (%)
Ag^0Z				
2016-VOG-002	I_2	7	2.8	96.4
2017-VOG-T4	I_2	500	5.5	85.8
2015-VOG2	CH_3I	40	4.2	84.4
2017-VOG-T5(4)	CH_3I	400	4.1	91.9
2017-VOG-T7(4)	CH_3I	1000	6.8	77.9
AgAerogel				
2016-VOG-T4	I_2	7	4.4	98
2017 T4-Aerogel	I_2	500	2.4	99.8
2016-VOG-T3	CH_3I	40	5.6	77
2017 T5-Aerogel	CH_3I	400	4.4	92.8
2017 T7-Aerogel	CH_3I	1000	5.7	90.1

Upon completion of testing at higher concentrations, some questions remained outstanding. This portion of the work was originally designed to provide insight into a discrepancy between the amount of iodine delivered to the sorbent bed and recovered on the sorbent bed. It was postulated that the sorbent may become less effective as the iodine feed concentration decreases. This hypothesis has been disproved and questions still remain about the iodine mass balances for the VOG testing reported in this document. A potential cause of the imbalance may be that physisorption of iodine on the bed leads to iodine loss during vacuum removal of bed segments. Preliminary testing has not disproved this hypothesis, and further testing is recommended to assess the effect of vacuum removal on measured iodine loadings. It is recognized that the time under vacuum is small and that the decrease in pressure is also small. If the iodine is removed in this manner, exposure to iodine-free air should have a similar effect.

The second aim of this report was to compare the performance of Ag^0Z and AgAerogel in VOG conditions. Ag^0Z and AgAerogel iodine adsorption performance was examined for two I_2 concentrations

(7 and 500 ppb) and three CH_3I concentrations (40, 400, and 1,000). The most notable difference between the two sorbents is that in all cases for both sorbates, the maximum observed iodine loadings are higher for AgAerogel. This has also been observed in thin-bed testing performed at higher concentrations. However, if the iodine loading data is normalized to account for the higher silver content in the AgAerogel then no clearly discernable differences exist between the two sorbents.

The penetration curves for each test condition were normalized for the two sorbents as a function of sorbent silver content. In most cases, this normalization removed the marked differences between the penetration curves and the maximum iodine loadings of each sorbent. This may indicate that the sorbent matrix itself is less important than the simple silver content of the sorbent per mass or volume. It is recommended that the data from replicate testing be analyzed prior to finalizing conclusions on the effect of sorbent matrix and silver content on the adsorption of iodine under VOG conditions.

While the loading data are similar, the mechanical performance for the two sorbents is notably different. Little or no mechanical degradation is observed for the Ag^0Z. During the course of each test a notable amount of fines are created from the AgAerogel material. Density measurements performed show that the post-run density of the AgAerogel is ~15% greater than for the initial material, while the total weight of the bed was virtually unchanged. This increase in bulk density can be attributed to the breakdown of the larger aerogel structure into finer particles resulting in bed compaction.

It was also found that for the same amount of I_2 delivered to the bed, it penetrates AgAerogel beds to a lesser extent than observed for Ag^0Z beds. For CH_3I, there were no observed differences in penetration depth between the two sorbents. In most cases, iodine loadings of the sorbent segments were found to be below detection by 6 cm into the bed.

Future work in this area should be focused on resolving the outstanding questions regarding the closure of the material balance. The first step here will be to determine the extent of physisorption under the CH_3I conditions and the extent that this is easily removed. The second objective should be the determination of the length of the mass transfer zone and saturation loadings under VOG conditions. This avenue of research appears more promising based on the data on concentration effects and the potential to conduct accelerated testing. However, the accelerated tests must also be balanced with the potential detrimental aging effects that may inadvertently be reduced by shortening the test duration.

7. REFERENCES

1. Jubin, RT, NR Soelberg, DM Strachan, and G Ilas. 2012. Fuel Age Impacts on Gaseous Fission Product Capture During Separations. Report No. FCRD-SWF-2012-000089, Oak Ridge National Laboratory, Oak Ridge, TN.
2. Jubin, RT, DM Strachan, and NR Soelberg, and G Ilas. 2013. Iodine Pathways and Off-Gas Stream Characteristics for Aqueous Reprocessing Plants—A Literature Survey and Assessment. Report No. FCRD-SWF-2013-000308, Oak Ridge National Laboratory, Oak Ridge, TN.
3. Bruffey, SH, RT Jubin, DM Strachan, BB Spencer, and BJ Riley. 2015. Literature Survey to Identify Potentially Problematic Volatile Iodine-bearing Species Present in Off-gas Streams. Report No. ORNL/SPR-2015/290, Oak Ridge National Laboratory, Oak Ridge, TN. June.
4. Bruffey, SH, and RT Jubin. 2015. Initial Evaluation of Effects of NO_x on Iodine and Methyl Iodide Loading of AgZ and Aerogels. Report No. FCRD-MRWFD-2015-000426, US Department of Energy Separations and Waste Forms Campaign, March 31.
5. Nenoff, TM, MA Rodriguez, NR Soelberg, and KW Chapman. 2014. "Silver-Mordenite for Radiologic Gas Capture from Complex Streams: Dual Catalytic CH_3I Decomposition and I Confinement." *Microporous Mesoporous Materials* 200: 297–303.
6. Sakurai, T, Y Komaki, A Takahashi, and M Izumo. 1983. "Application of Zeolites to Remove Iodine from Dissolver Off-Gas. III. Adsorption of Methyl-Iodide (CH_3I*) on Zeolite 13X." *Journal of Nuclear Science and Technology* 20(12): 1046–47.
7. Scheele, RD et al. 1983. Methyl Iodide Sorption by Reduced Silver Mordenite, Report No. PNL-4489, UC-70, Pacific Northwest National Laboratory, Richland, WA.
8. Jubin, RT, SH Bruffey, and BB Spencer. 2015. Performance of Silver-exchanged Mordenite for Iodine Capture under Vessel Off-gas Conditions. Proceedings of Global 2015. September.
9. Jubin, RT. 2011. Report of the FY11 Activities of the Off-Gas Sigma Team, FCR&D-SWF-2011-000306, US Department of Energy Separations and Waste Forms Campaign, September.
10. Anderson, KK, SH Bruffey, DL Lee, RT Jubin, and JF Walker. 2012. Iodine Loading of Partially Reduced Silver Mordenite. Report No. FCRD-SWF-2013-000079, ORNL/LTR-2012/624, Oak Ridge National Laboratory, Oak Ridge, TN, December 28.
11. Bruffey, SH et al. 2013. Complete Studies of Iodine Loading on NOx Aged AgZ. ORNL/LTR-2013/351. Oak Ridge, TN..

This page is intentionally left blank.

Appendix A

A.1. Data for Test 2016-VOG-002

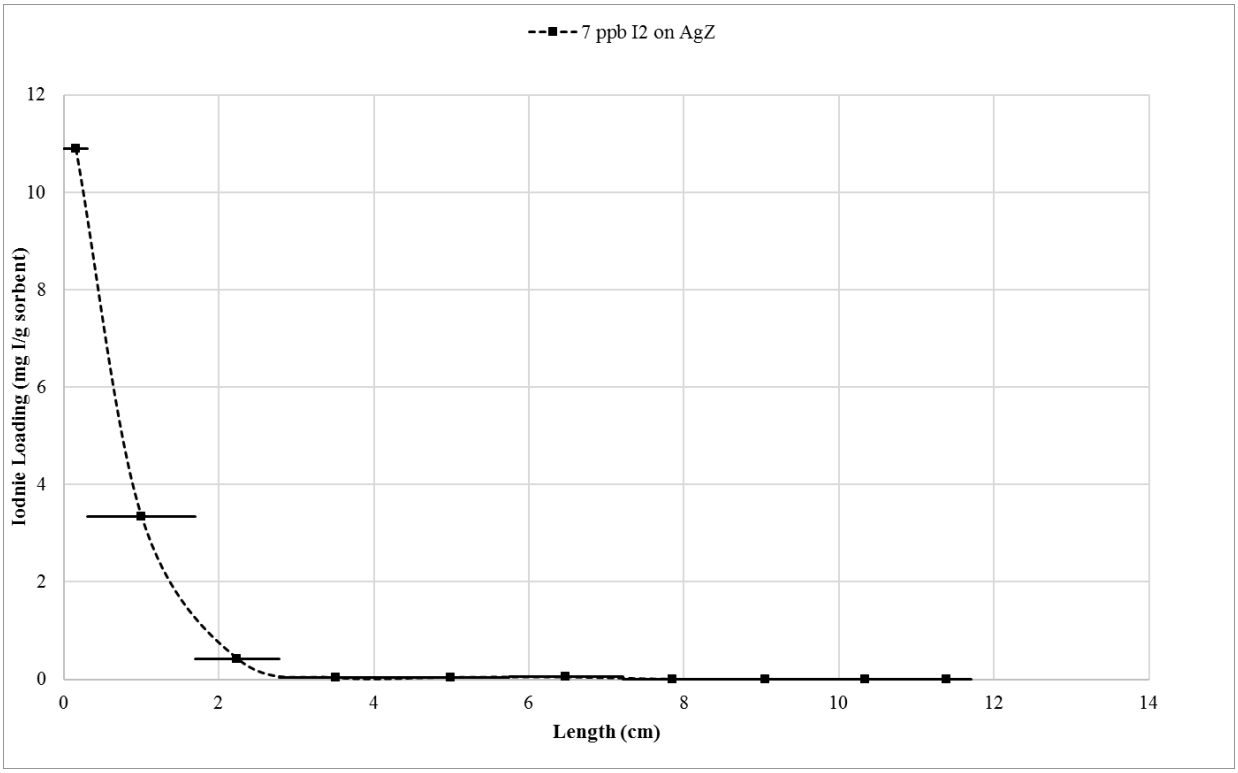

Figure A.1. Iodine loading profile on Ag^0Z with a feed of 7 ppb I_2 (Test ID: 2016-VOG-002).

Table A.1. Data obtained for Ag^0Z with a feed of 7 ppb I_2 (Test ID: 2016-VOG-002)

Sample	Online time (weeks)	Sample weight (g)	Length of segment (cm)	Cumulative length (cm)	Iodine collected (mg I/g sorbent)
I_2-Q1-1	1.14	0.5887			1.58
I_2-Q2-1	4	0.6275			5.36+
I_2-Q3-1	8.29	0.5810			8.36
I_2-Q4-1	16.28	0.5958	0.304	0.304	10.89
I_2-Q1-2	15.1	0.6307			11.18
I_2-Q2-2	12.28	0.5755			9.80
I_2-Q3-2	7.99	0.6087			6.98+
I2-Bed2A	16.28	10.8315	1.384	1.688	3.349
I2-Bed2B	16.28	8.5225	1.089	2.777	0.423
I2-Bed2C	16.28	11.4525	1.464	4.241	Below detection*
I2-Bed2D	16.28	11.7200	1.498	5.739	Below detection*
I2-Bed2E	16.28	11.5303	1.474	7.212	Below detection*
I2-Bed2F	16.28	9.9199	1.268	8.480	Below detection*
I2-Bed2G	16.28	8.8146	1.127	9.607	Below detection*
I2-Bed2H	16.28	11.3391	1.449	11.056	Below detection*
I2-Bed3A	4.00	5.0688	0.648	11.704	Below detection*
I2-Bed3B	4.29	5.0474			Below detection*
I2-Bed3C	3.86	4.9891			Below detection*
I2-Bed3D	1.86	4.9429			Below detection*
I2-Bed3E	2.29	5.1255			Below detection*

*The average minimum detectable activity that was reported for these analyses corresponds to a sorbent loading of 0.0038 mg/I/g sorbent.

+Estimated (sample lost)

Note: The bulk density of the sorbent is 0.83697 g/cm^3. The silver content of the sorbent is 11.9 wt%.

A.2. Data for Test 2017-VOG-T4

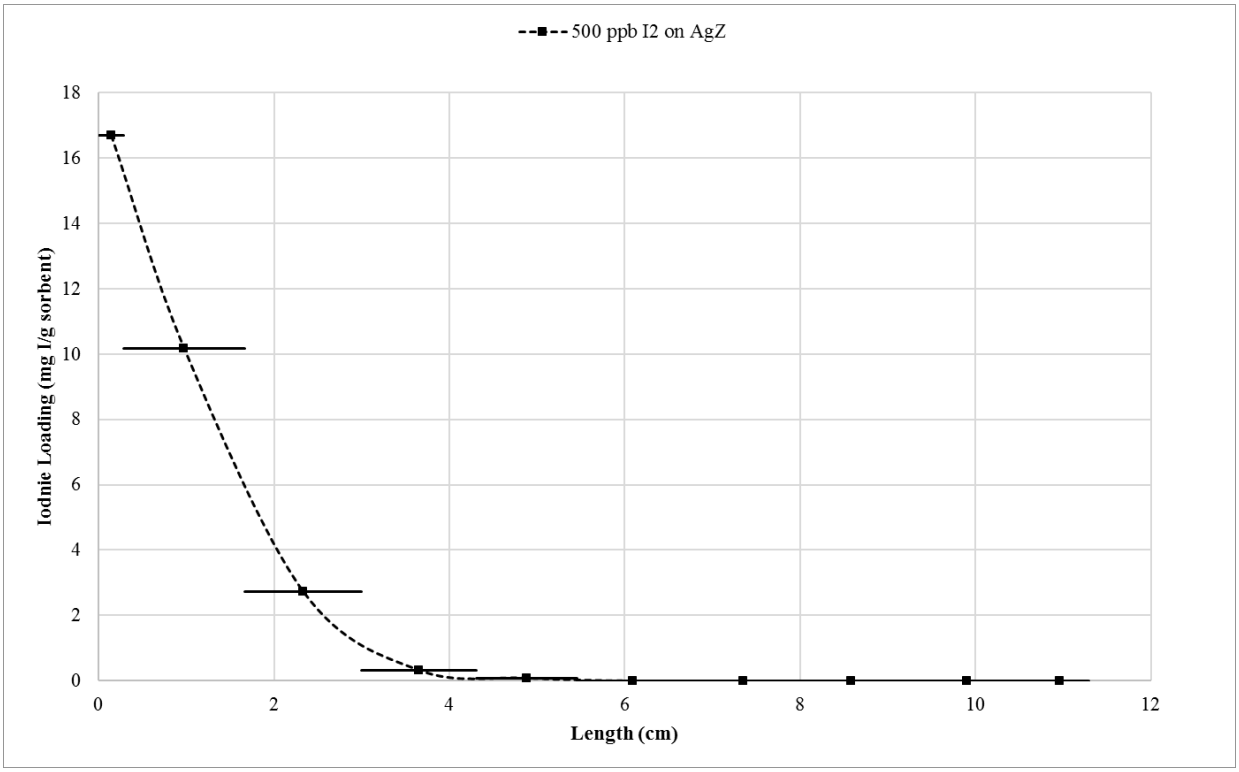

Figure A.2. Iodine loading profile on Ag^0Z with a feed of 500 ppb I_2 (Test ID: 2017-VOG-T4).

Table A.2. Data obtained for Ag^0Z with a feed of 500 ppb I_2 (Test ID: 2017-VOG-T4)

Sample	Online time (days)	Sample weight (g)	Length of segment (cm)	Cumulative length (cm)	Iodine collected (mg I/g sorbent)
VOG17-T4-Q1	9.985	0.5735			17.52207
VOG17-T4-Q2	9.985	0.5308			17.28376
VOG17-T4-Q3	9.985	0.5363			16.8599
VOG17-T4-Q4	9.985	0.6025	0.287	0.287	15.1408
VOG17-T4-Bed2A	9.985	10.7864	1.379	1.665	10.173
VOG17-T4-Bed2B	9.985	10.4405	1.334	3.000	2.735
VOG17-T4-Bed2C	9.985	10.2094	1.305	4.305	0.329
VOG17-T4-Bed2D	9.985	9.0242	1.153	5.458	0.088
VOG17-T4-Bed2E	9.985	9.8711	1.262	6.720	Below detection*
VOG17-T4-Bed2F	9.985	9.9472	1.271	7.991	Below detection*
VOG17-T4-Bed2G	9.985	9.1862	1.174	9.165	Below detection*
VOG17-T4-Bed2H	9.985	11.4864	1.468	10.633	Below detection*
VOG17-T4-Bed3	9.985	5.1137	0.654	11.287	Below detection*

*The average minimum detectable activity that was reported for these analyses corresponds to a sorbent loading of 0.0038 mg/I/g sorbent.

Note: The bulk density of the sorbent is 0.83697 g/cm^3. The silver content of the sorbent is 11.9 wt%.

A.3. Data for Test 2015-VOG2

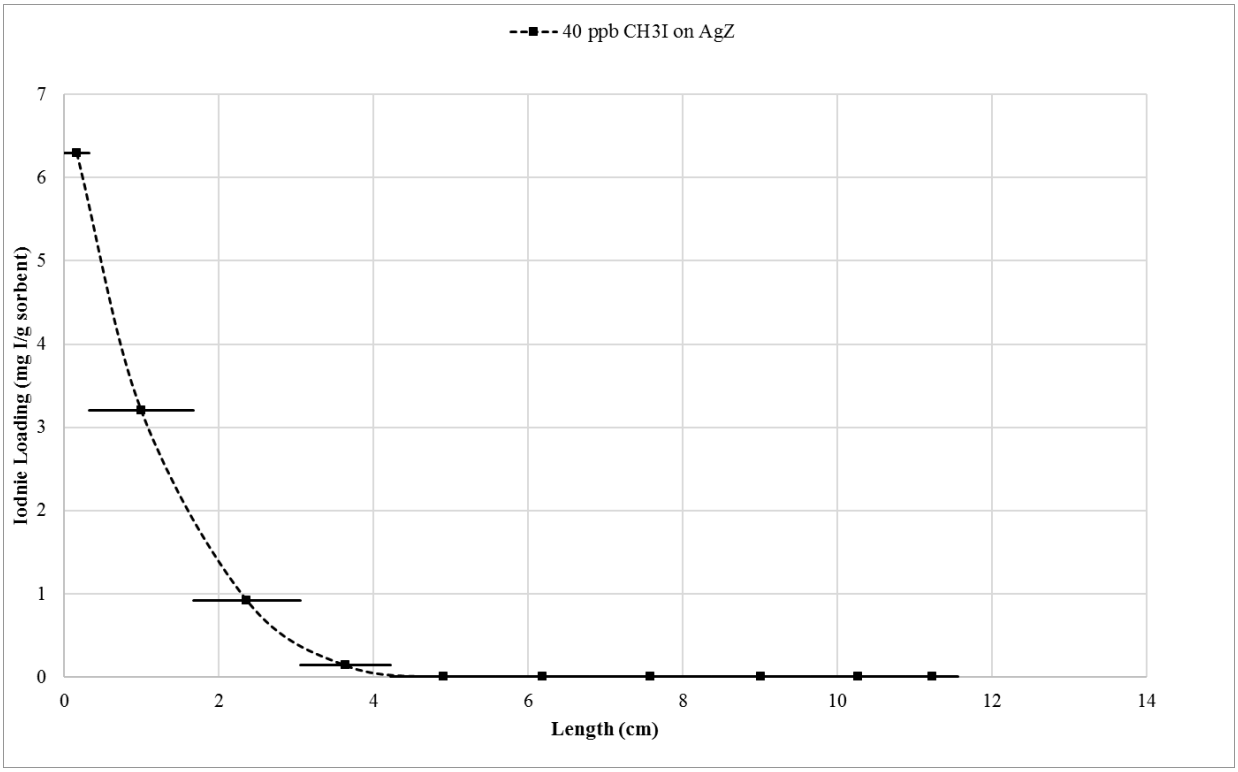

Figure A.3. Iodine loading profile on Ag^0Z with a feed of 40 ppb CH_3I (Test ID: 2015-VOG2).

Table A.3. Data obtained for Ag^0Z with a feed of 40 ppb CH_3I (Test ID: 2015-VOG2)

Sample	Online time (weeks)	Sample weight (g)	Length of segment (cm)	Cumulative length (cm)	Iodine collected (mg I/g sorbent)
CH_3I-Q1-1	0.71	0.6433			0.22
CH_3I -Q2-1	3.42	0.6041			0.34
CH_3I -Q3-1	7.71	0.6486			3.7
CH_3I -Q4-1	13.42	0.6094	0.320	0.320	5.3
CH_3I -Q1-2	12.70	0.6061			6.3
CH_3I -Q2-2	9.99	0.6370			6.5
CH_3I -Q3-2	5.71	0.6286			2.9
CH_3I -Bed2A	13.42	10.5659	1.350	1.670	3.2
CH_3I -Bed2B	13.42	10.7974	1.380	3.050	0.92
CH_3I -Bed2C	13.42	9.1888	1.174	4.225	0.14
CH_3I -Bed2D	13.42	10.5793	1.352	5.577	Below detection*
CH_3I -Bed2E	13.42	9.5393	1.219	6.796	Below detection*
CH_3I -Bed2F	13.42	12.3171	1.574	8.370	Below detection*
CH_3I -Bed2G	13.42	10.0365	1.283	9.653	Below detection*
CH_3I -Bed2H	13.42	9.6251	1.230	10.883	Below detection*
CH_3I -Bed3A	3.42	5.2955	0.676	11.559	Below detection*
CH_3I -Bed3B	4.00	5.9529			Below detection*
CH_3I -Bed3C	3.00	5.0529			Below detection*
CH_3I -Bed3D	2.42	5.1290			Below detection*
CH_3I -Bed3E	0.57	5.0317			Below detection*

*The average minimum detectable activity that was reported for these analyses corresponds to a sorbent loading of 0.0038 mg/I/g sorbent.

Note: The bulk density of the sorbent is 0.83697 g/cm^3. The silver content of the sorbent is 9.5 wt%.

A.4. Data for Test 2017-VOG-T5(4)

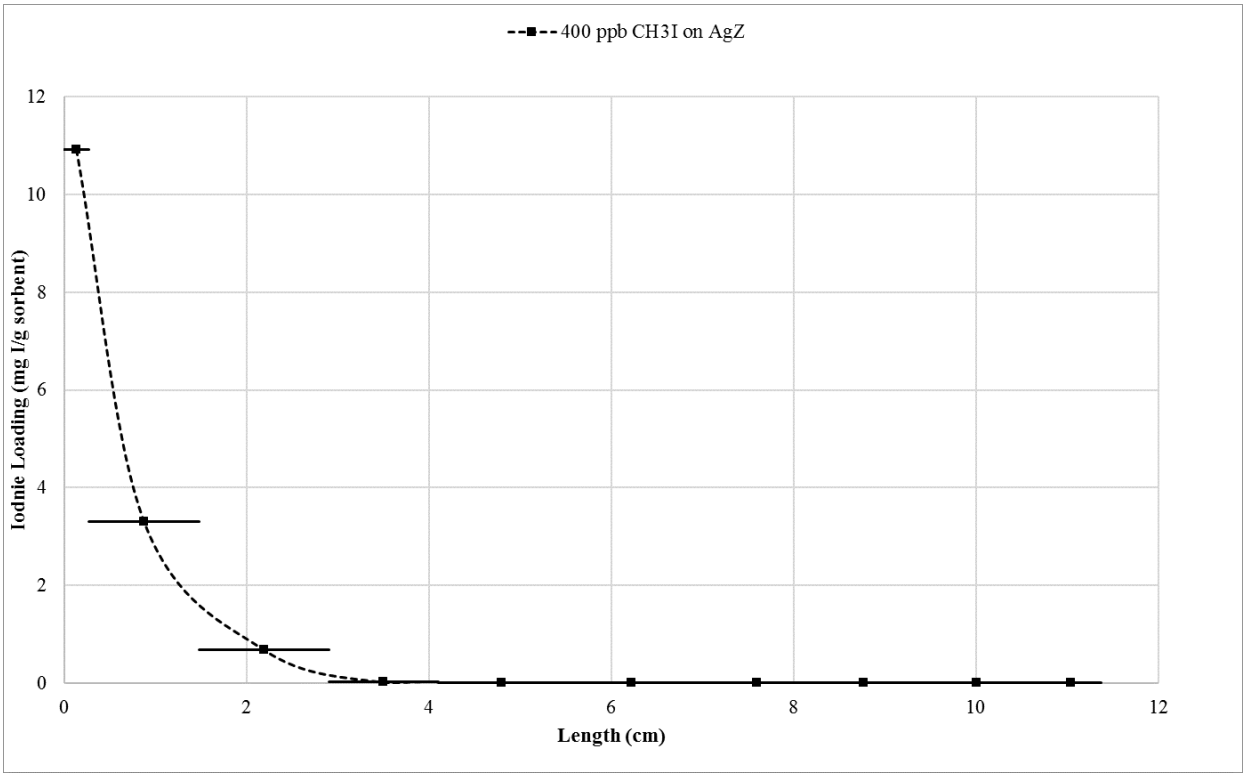

Figure A.4. Iodine loading profile on Ag^0Z with a feed of 400 ppb CH_3I (Test ID: 2017-VOG-T5(4)).

Table A.4. Data obtained for Ag^0Z with a feed of 400 ppb CH_3I (Test ID: 2017-VOG-T5(4))

Sample	Online time (days)	Sample weight (g)	Length of segment (cm)	Cumulative length (cm)	Iodine collected (mg I/g sorbent)
VOG17-T5(4)-Q1	1.858	0.5241			4.291
VOG17-T5(4)-Q2	6.146	0.525			6.650+
VOG17-T5(4)-Q3	8.096	0.547			8.454
VOG17-T5(4)-Q4	9.985	0.5115	0.270	0.270	9.132
VOG17-T5(4)-Q1-2	8.126	0.5202			8.295
VOG17-T5(4)-Q2-2	3.842	0.5297			4.360
VOG17-T5(4)-Q3-2	1.889	0.5413			2.590
VOG17-T5(4)-Bed2a	9.985	9.4969	1.214	0.270	9.132
VOG17-T5(4)-Bed2b	9.985	11.149	1.425	1.484	3.307
VOG17-T5(4)-Bed2c	9.985	9.3297	1.192	2.909	0.681
VOG17-T5(4)-Bed2d	9.985	10.8309	1.384	4.101	0.021
VOG17-T5(4)-Bed2e	9.985	11.5094	1.471	5.486	Below detection*
VOG17-T5(4)-Bed2f	9.985	9.9589	1.273	6.957	Below detection*
VOG17-T5(4)-Bed2g	9.985	8.3757	1.070	8.229	Below detection*
VOG17-T5(4)-Bed2h	9.985	11.0715	1.415	9.300	Below detection*
VOG17-T5(4)-Bed3	9.985	5.1085	0.653	10.715	Below detection*

*The average minimum detectable activity that was reported for these analyses corresponds to a sorbent loading of 0.0038 mg/I/g sorbent.

Note: The bulk density of the sorbent is 0.83697 g/cm^3. The silver content of the sorbent is 9.5 wt%.

A.5. Data for Test 2017-VOG-T7(4)

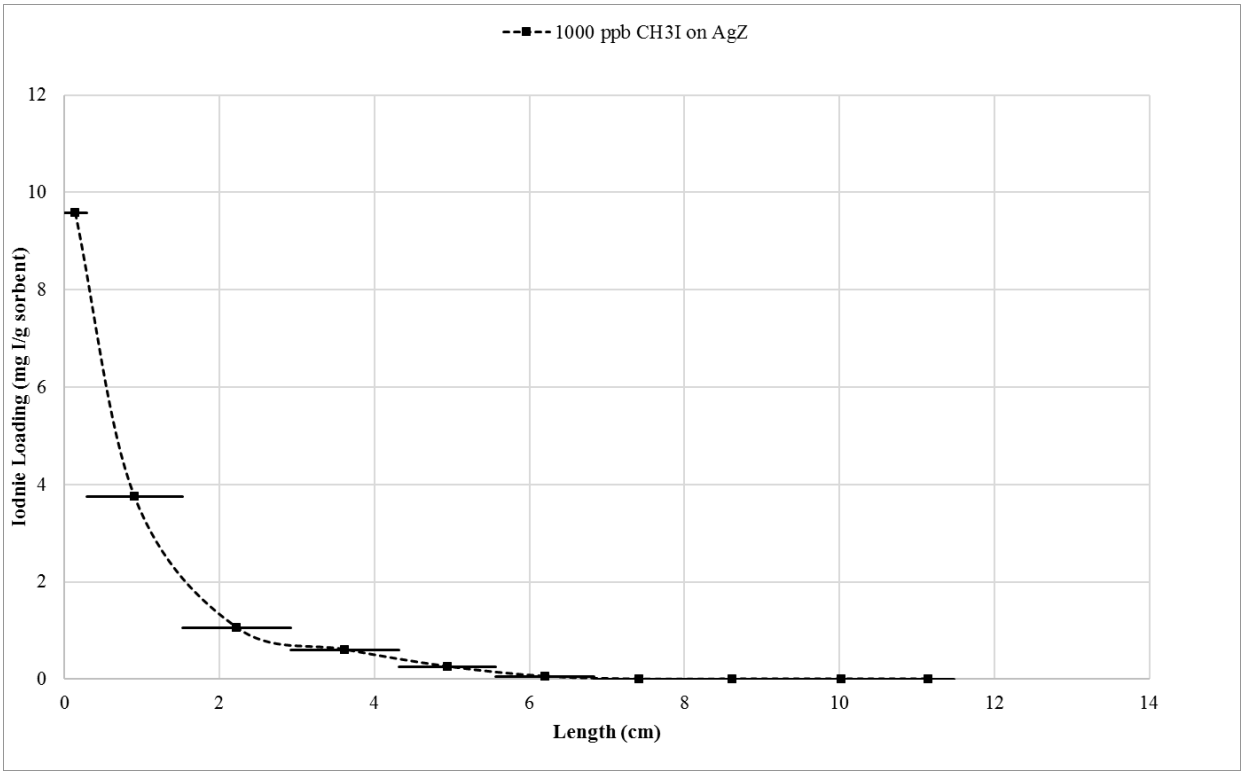

Figure A.5. Iodine loading profile on Ag^0Z with a feed of 1,000 ppb CH_3I (Test ID: 2017-VOG-T7(4)).

Table A.5. Data obtained for Ag^0Z with a feed of 1,000 ppb CH_3I (Test ID: 2017-VOG-T7(4))

Sample	Online time (days)	Sample weight (g)	Length of segment (cm)	Cumulative length (cm)	Iodine collected (mg I/g sorbent)
VOG17-T7(4)-Q1	0.816	0.5411			2.160
VOG17-T7(4)-Q2	2.026	0.5828			5.145
VOG17-T7(4)-Q3	3.020	0.5546			6.510
VOG17-T7(4)-Q4	3.980	0.5646	0.279	0.279	8.473
VOG17-T7(4)-Q1-2	3.164	0.5298			8.386
VOG17-T7(4)-Q2-2	1.953	0.519			5.142
VOG17-T7(4)-Q3-2	0.960	0.5216			2.399
VOG17-T7(4)-Bed2a	3.980	10.8315	1.235	1.514	3.757
VOG17-T7(4)-Bed2b	3.980	8.5225	1.396	2.910	1.062
VOG17-T7(4)-Bed2c	3.980	11.4525	1.403	4.312	0.607
VOG17-T7(4)-Bed2d	3.980	11.7200	1.242	5.555	0.258
VOG17-T7(4)-Bed2e	3.980	11.5303	1.277	6.831	0.056
VOG17-T7(4)-Bed2f	3.980	9.9199	1.166	7.998	Below detection*
VOG17-T7(4)-Bed2g	3.980	8.8146	1.238	9.235	Below detection*
VOG17-T7(4)-Bed2h	3.980	11.3391	1.574	10.809	Below detection*
VOG17-T7(4)-Bed3a	3.980	5.0688	0.659	11.468	Below detection*
VOG17-T7(4)-Bed3b	4.29	5.0474			Below detection*
VOG17-T7(4)-Bed3c	3.86	4.9891			Below detection*

*The average minimum detectable activity that was reported for these analyses corresponds to a sorbent loading of 0.0038 mg/I/g sorbent.

Note: The bulk density of the sorbent is 0.83697 g/cm^3. The silver content of the sorbent is 9.5 wt%.

A.6. Data for Test 2016-VOG-T4

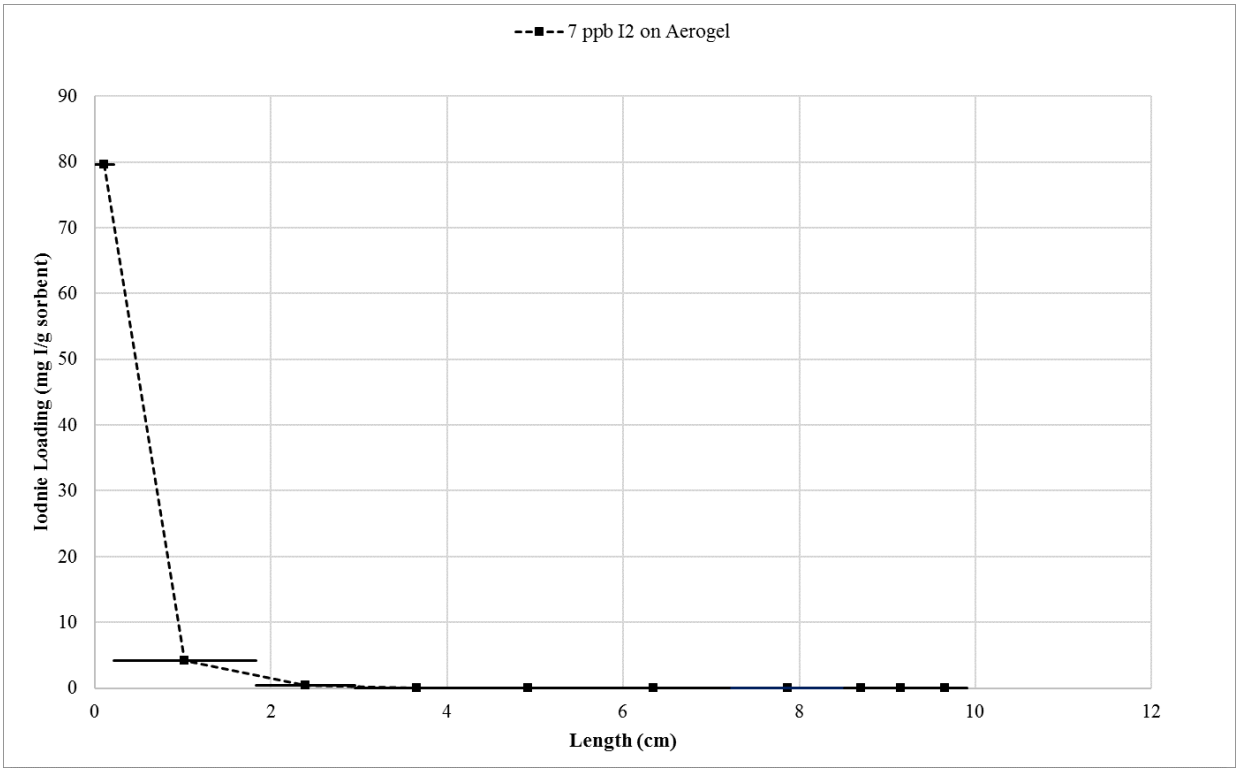

Figure A.6. Iodine loading profile on AgAerogel with a feed of 7 ppb I_2 (Test ID: 2016-VOG-T4).

Table A.6. Data obtained for AgAerogel with a feed of 7 ppb I_2 (Test ID: 2016-VOG-T4)

Sample	Online time (weeks)	Sample weight (g)	Length of segment (cm)	Cumulative length (cm)	Iodine collected (mg I/g sorbent)
VOG-T4-Q1	1	0.2392			4.516
VOG-T4-Q2	4	0.3194			14.400
VOG-T4-Q3	8.14	0.2484			36.590
VOGT4-Q4-1	16.14	0.3224	0.215	0.215	73.192
VOGT4-Q1-2	15.14	0.4175			58.436
VOGT4-Q2-2	12.14	0.3583			63.953
VOGT4-Q3-2	8	0.2584			49.062
VOGT4-Bed-2A	16.14	9.2785	1.617	1.832	4.219
VOGT4-Bed-2B	16.14	6.4738	1.128	2.960	0.416
VOGT4-Bed-2C	16.14	8.0542	1.403	4.364	0.070
VOGT4-Bed-2D	16.14	6.3526	1.107	5.471	Below detection*
VOGT4-Bed-2E	16.14	10.0962	1.759	7.230	Below detection*
VOGT4-Bed-2F	16.14	7.3573	1.282	8.512	Below detection*
VOG-T4-Bed3a	4	2.2437	0.391	8.903	Below detection*
VOG-T4-Bed3b	4.14	2.922	0.509	9.412	Below detection*
VOGT4-Bed-3c	3.86	2.8603	0.498	9.911	Below detection*
VOGT4-Bed-3E	2	2.1362	1.617	1.832	Below detection*

*The average minimum detectable activity that was reported for these analyses corresponds to a sorbent loading of 0.0038 mg/I/g sorbent.

[+] Estimated (sample lost)

Note: The bulk density of the sorbent is 0.61389 g/cm^3. The silver content of the sorbent is 33.5 wt%.

A.7. Data for Test 2017 T4-Aerogel

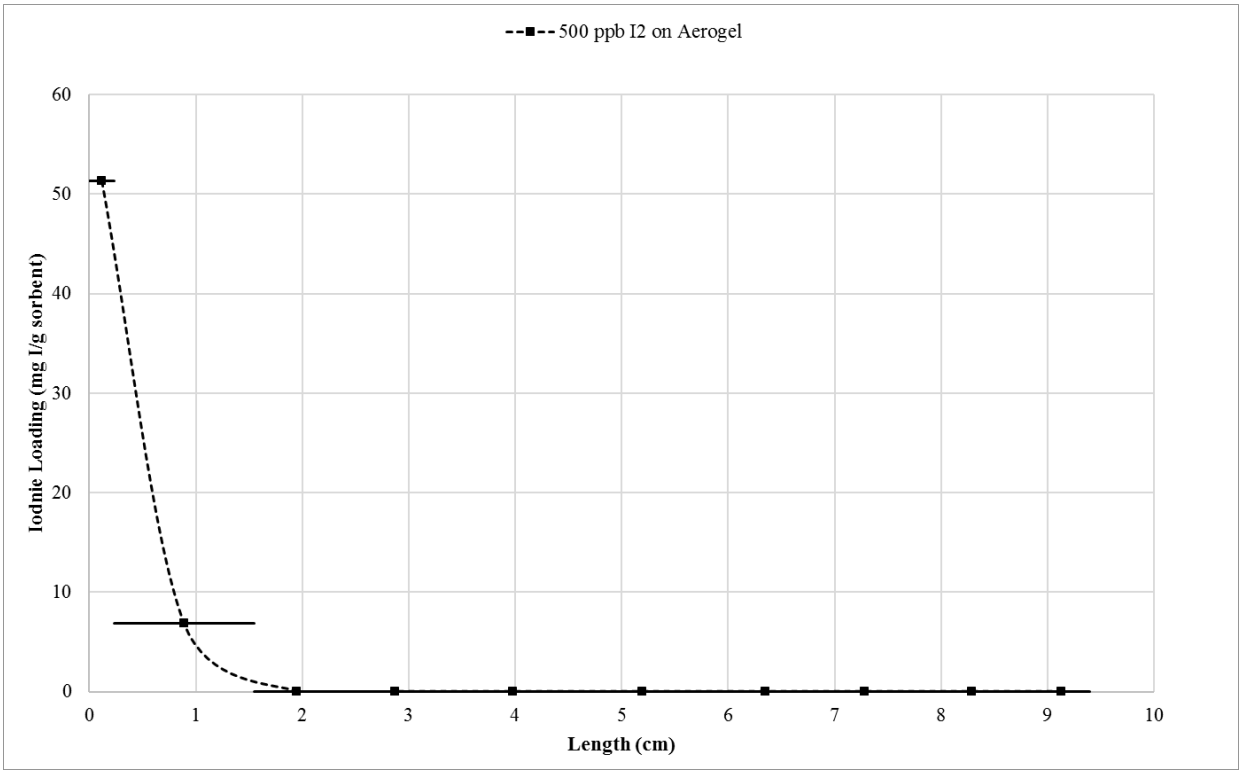

Figure A.7. Iodine loading profile on AgAerogel with a feed of 500 ppb I_2 (Test ID: 2017 T4-Aerogel).

Table A.7. Data obtained for AgAerogel with a feed of 500 ppb I_2 (Test ID: 2017 T4-Aerogel)

Sample	Online time (days)	Sample weight (g)	Length of segment (cm)	Cumulative length (cm)	Iodine collected (mg I/g sorbent)
FY17-T4-Aerogel-Q1	3.84	0.3627			13.50
FY17-T4-Aerogel-Q2	7.89	0.3339			20.72
FY17-T4-Aerogel-Q3	9.44	0.3184			28.59
FY17-T4-Aerogel-Q4	9.44	0.3388	0.225	0.225	62.70
FY17-T4-Aerogel-Q1b	9.19	0.3182			38.96
FY17-T4-Aerogel-Q2b	9.66	0.2944			27.65
FY17-T4-Aerogel-Q3b	9.36	0.2917			12.09
FY17-T4-Aerogel-Bed 2a	9.23	7.5109	1.309	1.534	6.829
FY17-T4-Aerogel-Bed 2b	9.40	4.5992	0.801	2.335	0.039
FY17-T4-Aerogel-Bed 2c	9.30	6.0328	1.051	3.386	Below detection*
FY17-T4-Aerogel-Bed 2d	10.16	6.6289	1.155	4.541	Below detection*
FY17-T4-Aerogel-Bed 2e	9.48	7.3967	1.289	5.830	Below detection*
FY17-T4-Aerogel-Bed 2f	9.29	5.7981	1.010	6.841	Below detection*
FY17-T4-Aerogel-Bed 2g	9.44	4.9662	0.865	7.706	Below detection*
FY17-T4-Aerogel-Bed 2h	9.10	6.5879	1.148	8.854	Below detection*
FY17-T4-Aerogel-Bed 3	9.12	3.042	0.530	9.384	Below detection*

*The average minimum detectable activity that was reported for these analyses corresponds to a sorbent loading of 0.0038 mg/I/g sorbent.

Note: The bulk density of the sorbent is 0.61389 g/cm^3. The silver content of the sorbent is 33.5 wt%.

A.8. Data for Test 2016-VOG-T3

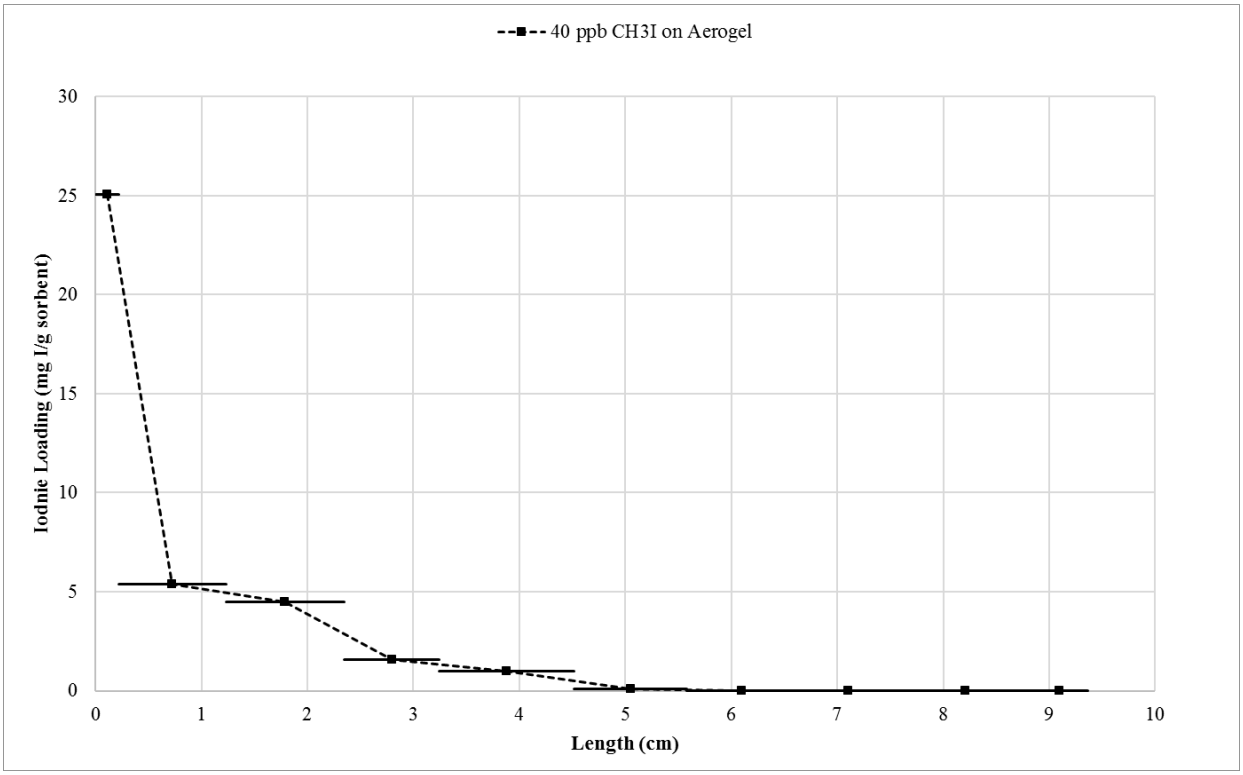

Figure A.8. Iodine loading profile on AgAerogel with a feed of 40 ppb CH_3I (Test ID: 2016-VOG-T3).

Table A.8. Data obtained for AgAerogel with a feed of 40 ppb CH_3I (Test ID: 2016-VOG-T3)

Sample	Online time (days)	Sample weight (g)	Length of segment (cm)	Cumulative length (cm)	Iodine collected (mg I/g sorbent)
VOG2-Q1	1.00	0.3135			3.88
VOG-T2-Q2	4.00	0.3119			12.06
VOG-T2-Q3	8.00	0.3157			17.35
VOG-T2-Q4f	16.00	0.3047	0.219	0.219	21.55
VOG-T2-Q1f	15.00	0.3146			19.75
VOG-T2-Q2f	12.00	0.3007			18.56
VOG-T2-Q3f	8.00	0.3346			7.83
VOG-T2-Bed2a	16.00	5.8311	1.016	1.235	5.38
VOG-T2-Bed2b	16.00	6.3866	1.113	2.348	4.49
VOG-T2-Bed2c	16.00	5.1578	0.899	3.246	1.57
VOG-T2-Bed2d	16.00	7.3175	1.275	4.521	0.97
VOG-T2-Bed2e	16.00	6.085	1.060	5.582	0.08
VOG-T2-Bed2f	16.00	5.9788	1.042	6.624	Below detection*
VOG-T2-Bed2g	16.00	5.5711	0.971	7.594	Below detection*
VOG-T2-Bed2h	16.00	7.0988	1.237	8.831	Below detection*
VOG-T2-Bed3a	4	3.0306			Below detection*
VOG-T2-Bed3b	4	3.0521			Below detection*
VOG-T2-Bed3c	4	3.1835			Below detection*
VOG-T2-Bed3d	2	3.0249			Below detection*
VOG-T2-Bed3e	2	3.0499			Below detection*

*The average minimum detectable activity that was reported for these analyses corresponds to a sorbent loading of 0.0038 mg/I/g sorbent.

Note: The bulk density of the sorbent is 0.61389 g/cm^3. The silver content of the sorbent is 33.5 wt%.

A.9. Data for Test 2017 T5-Aerogel

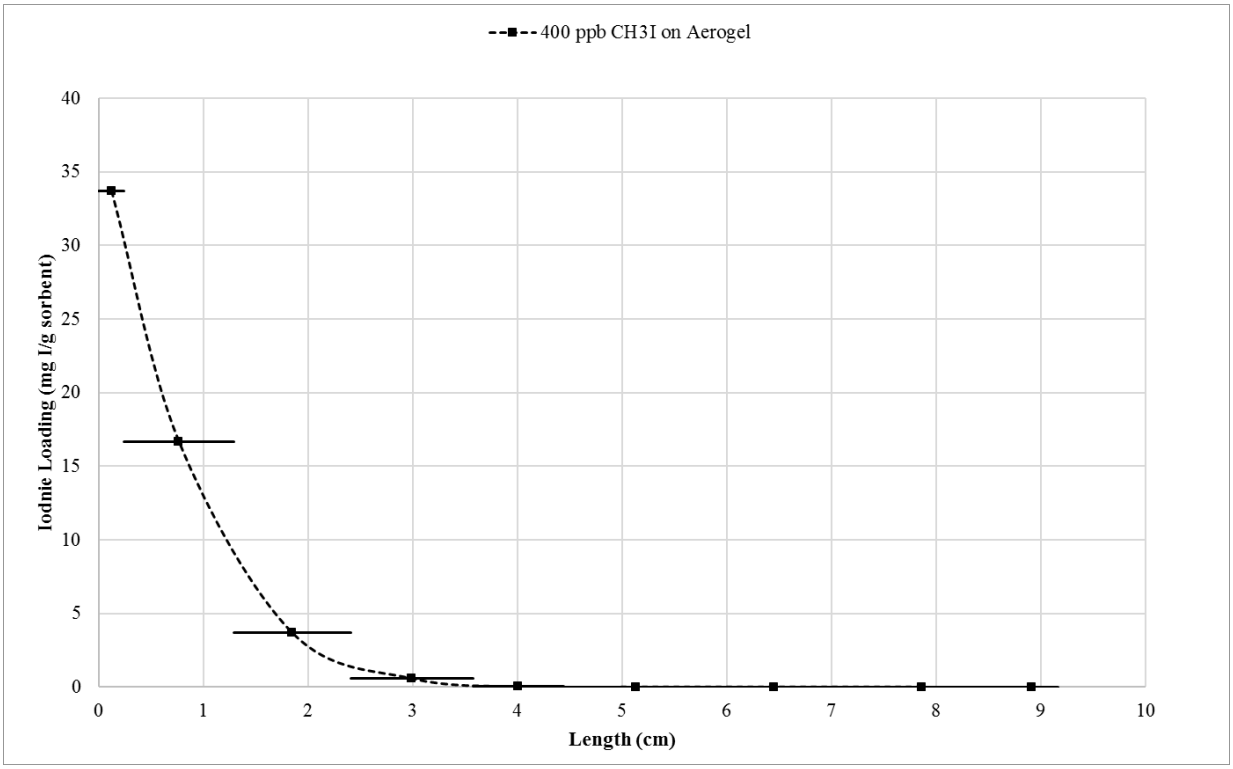

Figure A.9. Iodine loading profile on AgAerogel with a feed of 400 ppb CH_3I (Test ID: 2017 T5-Aerogel).

Table A.9. Data obtained for AgAerogel with a feed of 400 ppb CH_3I (Test ID: 2017 T5-Aerogel).

Sample	Online time (days)	Sample weight (g)	Length of segment (cm)	Cumulative length (cm)	Iodine collected (mg I/g sorbent)
VOG17-T5-Aerogel-Q1	1.979	0.3385			7.27
VOG17-T5-Aerogel-Q2	5.742	0.3477			20.06
VOG17-T5-Aerogel-Q3	7.862	0.3565			23.61
VOG17-T5-Aerogel-Q4	9.744	0.3435	0.236	0.236	29.75
VOG17-T5-Aerogel-Q1b	7.765	0.3373			30.16
VOG17-T5-Aerogel-Q2b	4.001	0.3037			14.72
VOG17-T5-Aerogel-Q3b	1.881	0.3428			8.62
VOG17-T5-Aerogel-Bed2a	9.744	6.0183	1.049	1.285	16.65
VOG17-T5-Aerogel-Bed2b	9.744	6.4086	1.117	2.401	3.67
VOG17-T5-Aerogel-Bed2c	9.744	6.7176	1.171	3.572	0.57
VOG17-T5-Aerogel-Bed2d	9.744	4.9562	0.864	4.436	0.02
VOG17-T5-Aerogel-Bed2e	9.744	7.9724	1.389	5.825	Below detection*
VOG17-T5-Aerogel-Bed2f	9.744	7.1104	1.239	7.064	Below detection*
VOG17-T5-Aerogel-Bed2g	9.744	9.1226	1.590	8.653	Below detection*
VOG17-T5-Aerogel-Bed3	9.744	2.9146	0.508	9.161	Below detection*

*The average minimum detectable activity that was reported for these analyses corresponds to a sorbent loading of 0.0038 mg/I/g sorbent.

Note: The bulk density of the sorbent is 0.61389 g/cm^3. The silver content of the sorbent is 33.5 wt%.

A.10. Data for Test 2017 T7-Aerogel

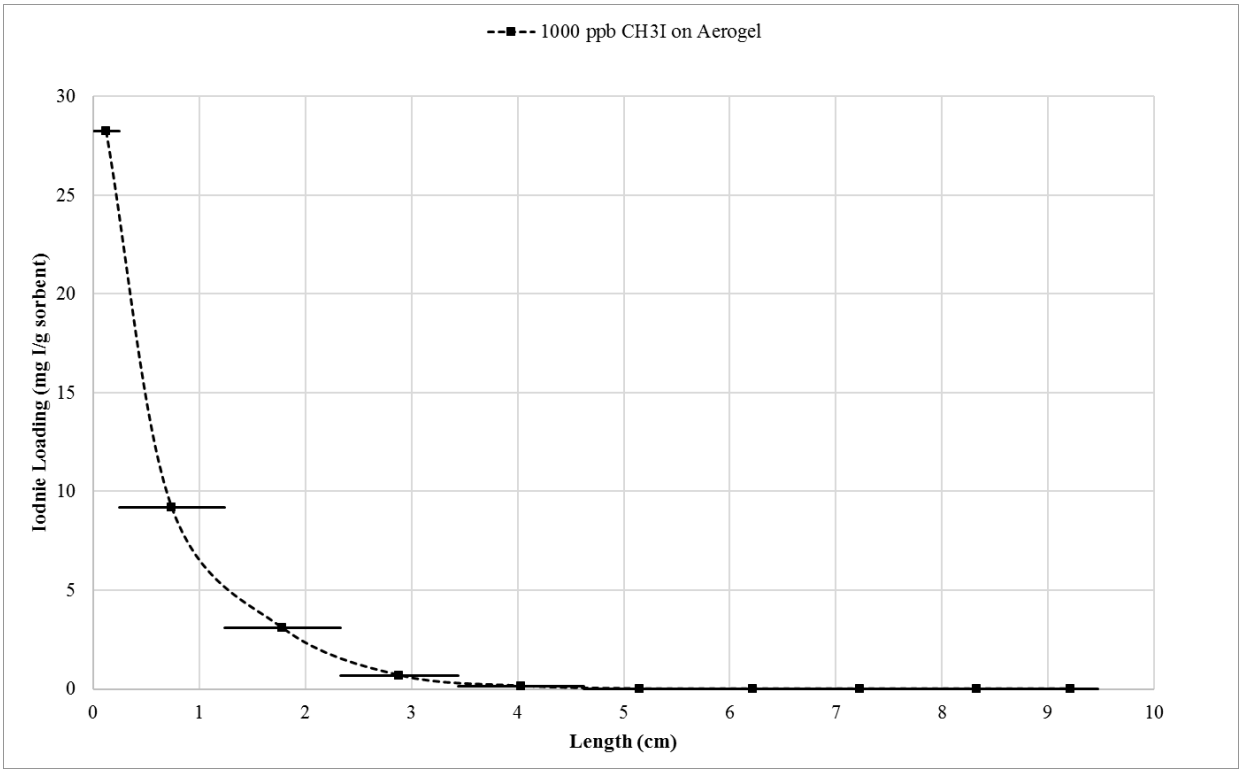

Figure A.10. Iodine loading profile on AgAerogel with a feed of 1,000 ppb CH_3I (Test ID: 2017 T7-Aerogel).

Table A.10. Data obtained for AgAerogel with a feed of 1,000 ppb CH_3I (Test ID: 2017 T7-Aerogel)

Sample	Online time (days)	Sample weight (g)	Length of segment (cm)	Cumulative length (cm)	Iodine collected (mg I/g sorbent)
FY17-T7-Aerogel-Q1	0.92	0.3672			7.94
FY17-T7-Aerogel-Q2	1.88	0.3317			15.50
FY17-T7-Aerogel-Q3	2.89	0.3334			21.90
FY17-T7-Aerogel-Q4	3.68	0.38	0.304	0.304	24.21
FY17-T7-Aerogel-Q1b	2.77	0.3039			19.92
FY17-T7-Aerogel-Q2b	1.81	0.3091			14.36
FY17-T7-Aerogel-Q3b	0.80	0.2888			7.92
FY17-T7-Aerogel-Bed 2a	3.68	5.6719	1.384	1.688	9.20
FY17-T7-Aerogel-Bed 2b	3.68	6.2974	1.089	2.777	3.09
FY17-T7-Aerogel-Bed 2c	3.68	6.3435	1.464	4.241	0.69
FY17-T7-Aerogel-Bed 2d	3.68	6.7985	1.498	5.739	0.15
FY17-T7-Aerogel-Bed 2e	3.68	6.0442	1.474	7.212	Below detection*
FY17-T7-Aerogel-Bed 2f	3.68	6.1968	1.268	8.480	Below detection*
FY17-T7-Aerogel-Bed 2g	3.68	5.4403	1.127	9.607	Below detection*
FY17-T7-Aerogel-Bed 2h	3.68	7.1326	1.449	11.056	Below detection*
FY17-T7-Aerogel-Bed 3	3.68	3.0137	0.648	11.704	Below detection*

*The average minimum detectable activity that was reported for these analyses corresponds to a sorbent loading of 0.0038 mg/I/g sorbent.

Note: The bulk density of the sorbent is 0.61389 g/cm^3. The silver content of the sorbent is 33.5 wt%.

Table A.11. Summary of VOG test conditions

Run ID	Start Date	Duration (days)	Sorbent	Sorbate	Concentration (ppb)	Iodine source
2016-VOG-002	12/29/2015	114.0	Ag^0Z	I_2	7	Certified permeation tubes
2017-VOG-T4	12/1/2016	4.6	Ag^0Z	I_2	500	Crystal iodine generator
2015-VOG2	4/24/2015	93.9	Ag^0Z	CH_3I	40	CH_3I cylinder
2017-VOG-T5(4)	4/11/2017	10.0	Ag^0Z	CH_3I	400	Certified permeation tubes
2017-VOG-T7(4)	4/24/2017	4.0	Ag^0Z	CH_3I	1,000	Certified permeation tubes
2016-VOG-T4	7/6/2016	113.0	AgAerogel	I_2	7	Certified permeation tubes
2017 T4-Aerogel	7/24/2017	3.7	AgAerogel	I_2	500	Crystal iodine generator
2016-VOG-T3	2/1/2016	112.0	AgAerogel	CH_3I	40	CH_3I cylinder
2017 T5-Aerogel	7/11/2017	9.7	AgAerogel	CH_3I	400	Certified permeation tubes
2017 T7-Aerogel	7/24/2017	3.7	AgAerogel	CH_3I	1,000	Certified permeation tubes

Table A.12. Summary of VOG test results

Run ID	Sorbent	Sorbate	Concentration (ppb)	Total sorbate fed (g iodine)	Total iodine recovered (g)	Material Balance based on recovered I/calculated feed (%)	Maximum iodine loading (mg/g sorbent)	Iodine retained in Bed 1 (%)	Iodine retained in first 2 cm (%)	Penetration depth (cm)
2016-VOG-002	Ag^0Z	I_2	7	0.08599	0.0725	84.3	11	45.0	96.4	2.8
2017-VOG-T4	Ag^0Z	I_2	500	0.18134	0.1806	99.6	17	20.8	85.8	5.5
2015-VOG2	Ag^0Z	CH_3I	40	0.18003	0.0608	33.8	6	25.9	84.4	4.2
2017-VOG-T5(4)	Ag^0Z	CH_3I	400	0.15538	0.0609	39.2	9	35.0	91.9	4.1
2017-VOG-T7(4)	Ag^0Z	CH_3I	1,000	0.15509	0.0785	50.6	8	26.6	77.9	6.8
2016-VOG-T4	AgAerogel	I_2	7	0.08525	0.1408	165.1	73	69.9	98	4.4
2017 T4-Aerogel	AgAerogel	I_2	500	0.17651	0.1177	66.7	63	56.1	99.8	2.4
2016-VOG-T3	AgAerogel	CH_3I	40	0.21450	0.1073	50.0	21	26.6	77	5.6
2017 T5-Aerogel	AgAerogel	CH_3I	400	0.15161	0.1734	114.3	30	31.3	92.8	4.4
2017 T7-Aerogel	AgAerogel	CH_3I	1,000	0.14370	0.1144	79.6	24	32.7	90.1	5.7